# Pricing FX-TARN Under Lévy Processes Using Numerical Methods

Valentin Bandelier

*June 22, 2017*
Version: 1.5

École Polytechnique Fédérale de Lausanne - EPFL

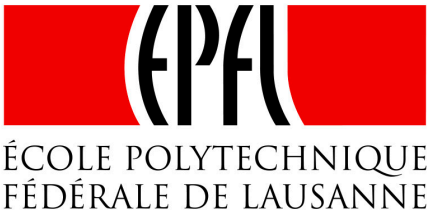

ÉCOLE POLYTECHNIQUE
FÉDÉRALE DE LAUSANNE

School of Basic Sciences - SB
Institute of Mathematics - MATH

Master Thesis

# Pricing FX-TARN Under Lévy Processes Using Numerical Methods

Valentin Bandelier

*Supervisors* Fabio Nobile
EPFL
Institute of Mathematics - MATH

Julien Hugonnier
EPFL
Swiss Finance Institute - SFI

*Co-supervisor* Francesco Statti
EPFL
Institute of Mathematics - MATH

June 22, 2017

**Valentin Bandelier**

*Pricing FX-TARN Under Lévy Processes*
*Using Numerical Methods*
Master Thesis, June 22, 2017
Supervisors: Fabio Nobile and Julien Hugonnier
Co-supervisor: Francesco Statti

**École Polytechnique Fédérale de Lausanne - EPFL**
Institute of Mathematics - MATH
School of Basic Sciences - SB
Route Cantonale
1015 Lausanne

# Abstract

The FX Target Accrual Redemption Notes (FX-TARN) are financial products on currency pairs. These are speculative products of a very risky nature, which makes them very popular in Asia.

This thesis presents different numerical methods for pricing FX-TARN under Lévy processes. The main goal is to go beyond the famous Black-Scholes model, which does not perform good with respect to the market structure. Thus, Lévy processes including jumps are more adapted to the market observations.

In general, options with path dependents payoff, such as this product, are evaluated by Monte Carlo simulations. We will describe two other methods based respectively on Finite Difference (FD) and Fast Fourier Transform (FFT) in order to boost the performances of our pricing engine. At the end of this project, we will be able to propose a fast and accurate method, which is not available in the literature, to price FX-TARN. This method is a combination of the methods proposed by Luo and Shevchenko (2015) [LS15] and Lord et al. (2008) [Lor+08].

The main advantage of the method, proposed in this work, is that it is easy to implement and allows us to extend it to all Lévy processes with closed form characteristic function.

# Résumé

Les FX Target Accrual Redemption Notes (FX-TARN) sont des produits financier sur des paires de devises. Ce sont des produits de spéculation à caractère très risqué, ce qui les rend très populaires en Asie.

Cette thèse présente différentes méthodes numériques pour l'évaluation du prix d'un FX-TARN à l'aide de processus de Lévy. L'objectif principal est d'aller au-delà du célèbre modèle de Black-Scholes, qui ne performe pas bien par rapport à la structure du marché. Ainsi, les processus Lévy avec sauts sont plus adaptés aux observations du marché.

En général, les options avec un profit fortement dépendant de l'évolution du cours de la monnaie, comme ce produit, sont évaluées avec des simulations de Monte Carlo. Nous allons décrire deux autres méthodes basées respectivement sur les Différences Finies (FD) et les Transformées de Fourier (FFT) dans le but d'améliorer les perfomances de notre outil d'évaluation. A la fin de ce projet, nous serons en mesure de proposer une méthode rapide et précise, qui n'existe pas dans la litérature, pour évaluer les FX-TARN. Cette méthode est une combinaison des méthodes proposées par Luo and Shevchenko (2015) [LS15] et Lord et al. (2008) [Lor+08].

Le principal avantage de la méthode proposée dans ce travail, est qu'elle est facile à implémenter et nous permet de l'étendre à tous les modèles de Lévy avec une fonction caractéristique sous forme close.

# Remerciements

J'ai choisi ma langue natale pour faire mes remerciements afin que toutes celles et ceux qui m'ont soutenu dans mon parcours puissent recevoir ma gratitude à sa juste valeur.

Je tiens, pour commencer, à remercier Christophe Ansermoz, Emmanuel Duterme et Gregory Chevalley de la banque Pictet pour avoir cru en moi et m'avoir fait confiance pour exercer l'art, que j'ai particulièrement apprécié développer, de l'évaluation de produits financiers.

Il s'ensuit naturellement les remerciements les plus sincères envers mes professeurs Fabio Nobile et Julien Hugonnier pour avoir accepté de superviser ce projet qui m'est cher. En plus de leur aide, je suis très reconnaissant de la collaboration précieuse que j'ai entretenue avec mon assistant, co-superviseur, Francesco Statti.

Mais au delà de ce projet de master, c'est un parcours académique très rude qui s'achève, et c'est pourquoi je tiens à réserver tout particulièrement le mot de la fin à ma compagne, Maria Pacios, qui m'a soutenu, encouragé et surtout permis de surpasser toutes les difficultés que j'ai pu rencontrer. Je ne pourrais jamais être assez reconnaissant pour tout ce qu'elle a pu m'apporter durant cette aventure, qui a aussi, je l'admets, été éprouvante pour elle. J'espère que cette place d'honneur puisse remplacer tous les mots nécessaires pour exprimer ma reconnaissance infinie.

Finalement, si des collègues, des amis, des proches, mes parents ou mes beaux-parents sont amenés à lire ce projet, je ne les oublie pas et tiens également à les remercier pour avoir partagé cette période de vie à l'EPFL ou même une partie avec moi.

Bonne lecture!

*Je dédie ce travail à* ***@****baboOu__*

Valentin Bandelier

# Contents


**1 Introduction** **1**

1.1 Motivation . . . 1
1.2 FX-TARN Description . . . 2
1.3 Example of Term Sheet . . . 6
1.4 Overview of the Thesis . . . 8

**2 Lévy Processes** **11**

2.1 Definitions and properties . . . 11
2.2 Lévy-Khinchine formula and Lévy-Itô decomposition . . . 14
2.3 Lévy measure and path properties . . . 17
2.4 Exponential Lévy processes and Equivalent martingale measure . . . 19
2.4.1 Esscher transform method . . . 19
2.4.2 Mean-correction method . . . 21

**3 Financial Mathematic Models** **23**

3.1 Black-Scholes Model . . . 23
3.2 Jump-diffusion Models . . . 25
3.2.1 Merton Model . . . 26
3.2.2 Kou Model . . . 27
3.3 Pure jump Models . . . 29
3.3.1 Normal Inverse Gaussian Model . . . 29
3.3.2 Variance Gamma Model . . . 32
3.4 Summary . . . 36

**4 Numerical Methods** **39**

4.1 Monte Carlo Method . . . 39
4.1.1 Simulations under Black-Scholes model . . . 40
4.1.2 Simulations under Jump-diffusion models . . . 41
4.1.3 Simulations under Pure jump models . . . 44
4.1.4 Pricing FX-TARN with Monte Carlo . . . 46
4.2 Finite Difference Method . . . 47
4.2.1 Black-Scholes world . . . 47
4.2.2 Jump-diffusion models . . . 52
4.2.3 Pure jump models . . . 58

4.3 The Convolution Method . . . . . 60
4.3.1 Description of the method . . . . . 61
4.3.2 Implementation of the method . . . . . 62
4.3.3 Criticism . . . . . 64
4.4 Summary . . . . . 65

**5 Calibration** **67**
5.1 Calibration inputs . . . . . 67
5.2 Calibration method . . . . . 69
5.3 Results of calibrations . . . . . 70
5.4 Analysis of the calibration . . . . . 71

**6 Numerical Results** **75**
6.1 Experimental setup . . . . . 75
6.2 Results . . . . . 76
6.2.1 Settings . . . . . 77
6.2.2 Results tables . . . . . 78
6.3 Speed, Accuracy and Convergence analysis . . . . . 78
6.3.1 Monte Carlo method analysis . . . . . 78
6.3.2 Convergence analysis . . . . . 79
6.3.3 Speed and accuracy analysis . . . . . 80
6.4 Value of the term sheet example . . . . . 81

**7 Conclusion** **85**
7.1 Review of main findings . . . . . 85
7.2 Further works . . . . . 86

**Bibliography** **87**

# 1 Introduction

> *Finance is the art of passing currency from hand to hand until it finally disappears.*
>
> — **Robert W. Sarnoff**
> (1918-1997)

This introductory chapter starts, in Section 1.1, with the motivation on the option pricing, that have been the starting point for this work. We will briefly discuss about the existing works we used to develop this project. Then, in Section 1.2, the FX-TARN product is presented. In Section 1.3, an example of term sheet illustrates this exotic product. Finally, the chapter concludes with an overview of the thesis in Section 1.4.

## 1.1 Motivation

This project was born during my internship in market risk management at Pictet, a Swiss private bank. In fact, I had to reprice FX-TARN to evaluate the risk on this product. The first approach was to price it with Monte Carlo simulations. However, the computational cost was very expensive. Some literature research brought me to the paper of Luo and Shevchenko (2015) [LS15], in which they develop a Finite Difference (FD) method for Black-Scholes model.

It is well known that the assumptions under Black-Scholes model are too restrictive with respect to the market. Indeed, the log-normality of the returns and the path continuity are contradicted by the analysis of the financial data. We can clearly identify jumps in financial time series. In addition, the implied volatility presents in general a negative skew which means that the returns distribution is more leptokurtic (fat tails) than the normal one. This can be due effectively to the jumps in the market prices, accentuated during the economic crises.

To go beyond the Black-Scholes model and avoid inconsistencies with the markets, we can model stock price with exponential Lévy processes. There are two different classes of Lévy models used in this thesis, the jump-diffusion (finite activity) models

which are extension of Black-Scholes model including jumps, and pure jump (infinite activity) models which model the asset price by infinitely many small jumps. The advantage of these models is that they capture the volatility smile structure.

The first part of the study was thus to enlarge the Finite Difference (FD) method proposed by Luo and Shevchenko to the Lévy processes with jumps. This generalization involves the Lévy measure characterizing the jumps. This leads to large complexities in the implementation of the method and then the computational time grows up with the complexity. Therefore the question was how to boost the pricing engine. The Computational Finance lesson given by the Prof. Nobile [Nob15] in collaboration with Prof. Pulido and Kressner from the Swiss Institute of Technology Lausanne (EPFL), gave me the idea to solve the problem with Fast Fourier Transform (FFT). At the end, the solution was found in the Convolution method proposed by Lord et al. (2008) [Lor+08], where they apply a FFT based method to the early exercised option like Bermudan or American options. Then, the combination of the methods of Luo and Shevchenko and Lord et al. allow us to develop our own method to price FX-TARN with the FFT approach.

To achieve this project, it was natural to call Prof. Fabio Nobile, who is a specialist of numerical analysis in partial differential equations (PDE), and Prof. Julien Hugonnier, who taught me the pricing of financial derivatives. Thank's to them for their useful supervision.

## 1.2 FX-TARN Description

First of all, the foreign exchange market, also called Forex, FX, or currency market, is an over-the-counter OTC market (trading directly between two parties without supervision) for the trading of the currencies. This is the largest financial market in the world in term of trading volume, with trillions of dollars worth of transactions each day.

Thus, an FX Target Accrual Redemption Note (FX-TARN) is an exotic financial product on a currency pair (e.g. USD/CHF) very popular in Asia. It allows an investor to accumulate, over a predefined period of time, an amount of cash until a certain *target accrual level* $U$ is reached. More precisely, the contract between the bank and the client imposes positive and negative cash flows on scheduled dates (called *fixing dates*). These cash flows can take the form of Call or Put option payoffs. For example, in a so called FX-TARN Accumulator, a positive cash flow is a Call option payoff and a negative cash flow is a Put option payoff multiplied by a gear factor $g$ that penalizes

the client versus the bank. In the case of an FX-TARN Decumulator, the roles of the Call options and Put options are inverted.

Hence, we can replicate this exotic option with a series of FX call options (resp. FX put options) with strike $K$, that the bank sells to a client, and at the same time a series of FX put options (resp. FX call options) with the same strike $K$, that the bank buys from the client. The scheduling is defined by a number of fixing dates $t_1, t_2, \ldots, t_N$ that correspond to the options expiry dates.

Finally, a redemption condition is done on the accumulated positive amount. In fact, the product knocks-out if the total sum of the positive cash flows exceeds the given target $U$. We will study three types of knock-out when the target $U$ is breached:

- **No Gain :** the last payment is disallowed when the target $U$ is breached,
- **Part Gain :** only a part of the payment is allowed such that only the target is paid,
- **Full Gain :** the last payment is allowed when the target $U$ is breached.

This pure speculative financial product is very risky and enjoys the Chinese. Investing in such derivative is like playing in a casino where the casino has a bounded risk while the client can lose a lot. Indeed, the knock-out condition cuts the loss of the bank when the client wins too much money.

### Payoff Definition

We will use the following notation:

- $S(t)$ : FX rate at time $t$,
- $K$ : strike(s) (could be different for each fixing dates),
- $t_0$ : today's date,
- $t_1, t_2, \ldots, t_N$ : fixing dates,
- $U$ : target accrual level,
- $A(t)$ : accumulated amount of positive cash-flow at time $t$,
- $N_f$ : notional amount per fixing date.

In order to understand a bit more the running of the FX-TARN, we will explain in more detail the payoff.

On each fixing date $t_n, n = 1, \ldots, N$, if the target level $U$ is not breached by the accumulated amount $A(t_n)$, we can define the positive payoff per unit of notional foreign amount by

$$\tilde{C}_n^{\text{pos}} \equiv \tilde{C}^{\text{pos}}(t_n) = \max(\beta(S(t_n) - K), 0),$$

and the negative payoff by

$$\tilde{C}_n^{\text{neg}} \equiv \tilde{C}^{\text{neg}}(t_n) = -g \times \max(\beta(K - S(t_n)), 0),$$

where $\beta$ is the investor strategy, i.e. with $\beta = 1$ he buys Call options, and with $\beta = -1$ he buys Put options. If he buys Call options, we say that he accumulates the domestic currency and in the other case, if he buys Put options, we say that he decumulates. This gives the respective name of FX-TARN Accumulator or Decumulator.

Let $A^+(t_n) = \sum_{j=1}^{n} \tilde{C}_n^{\text{pos}} = A^+(t_{n-1}) + \tilde{C}_n^{\text{pos}}$ be the accumulated positive cash flow at time $t_n$.

Denote $t_{\tilde{N}}$ the first fixing date before maturity $T$ on which the target level $U$ is breached by the total accumulated positive cash flow $A^+(t_n), n = 1, \ldots, N$, (without decumulating with negative cash flows!). In other words,

$$\tilde{N} = \min\{n : A^+(t_n) \geq U\}, \qquad n = 1, 2, \ldots, N.$$

If the target $U$ is not breached, we set $\tilde{N} = N$.

The three different knockout conditions, No Gain, Part Gain and Full Gain mean that if the accumulated amount breaches the target $U$ in the No Gain case, the last cash flow is not payed, while in the Full Gain case it is payed and then the product is killed. In the Part Gain case, the last cash flow completes the target amount and then the deal is over.

Hence, the actual accumulated cash flow is:

For $t_n < t_{\tilde{N}}$:

$$A(t_n) = A(t_{n-1}) + \tilde{C}_n^{\text{pos}} = A^+(t_n).$$

For $t_n = t_{\tilde{N}}$:

$$A(t_n) = \begin{cases} A(t_{n-1}), & \text{No Gain,} \\ U, & \text{Part Gain,} \\ A(t_{n-1}) + \tilde{C}_n^{\text{pos}}, & \text{Full Gain.} \end{cases}$$

For $t_n > t_{\tilde{N}}$:

$$A(t_n) = A(t_{\tilde{N}}).$$

Then for $t_n \leq t_{\tilde{N}}$ we can write the positive cash flow on $t_n$ as

$$C^{\text{pos}}(S(t_n), A(t_{n-1})) = \tilde{C}_n^{\text{pos}} \times \left( \mathbf{1}_{\left\{A(t_{n-1})+\tilde{C}_n^{\text{pos}} < U\right\}} + W_n \times \mathbf{1}_{\left\{A(t_{n-1})+\tilde{C}_n^{\text{pos}} \geq U\right\}} \right), \tag{1.1}$$

where

$$W_n = \begin{cases} 0, & \text{for No Gain,} \\ \frac{U - A(t_{n-1})}{\beta \times (S(t_n) - K)}, & \text{for Part Gain,} \\ 1, & \text{for Full Gain.} \end{cases}$$

The negative cash flow does not count in the knock-out condition but will also knock-out by the same redemption event. Therefore we have that

$$C^{\text{neg}}(S(t_n), A(t_{n-1})) = \tilde{C}_n^{\text{neg}} \times \left( \mathbf{1}_{\left\{A(t_{n-1}))+\tilde{C}_n^{\text{pos}} < U\right\}} + W_n \times \mathbf{1}_{\left\{A(t_{n-1})+\tilde{C}_n^{\text{pos}} \geq U\right\}} \right) \tag{1.2}$$

In Figure 1.1, we can see the plot of the positive cash flow $C^{\text{pos}}(S(t), A(t^-)) = C^{\text{pos}}(S, A)$ that counts in the accumulated amount and produces jumps in the price on each fixing date.

Let us finally introduce the stopping time condition in the definitions of $C^{\text{pos}}$ and $C^{\text{neg}}$, which gives us

$$\hat{C}^{\text{pos}} = C^{\text{pos}} \times \mathbf{1}_{\{t_n \leq t_{\tilde{N}}\}},$$
$$\hat{C}^{\text{neg}} = C^{\text{neg}} \times \mathbf{1}_{\{t_n \leq t_{\tilde{N}}\}}.$$

Hence, the net present value of FX-TARN in domestic currency for FX rate realization $\mathbf{S} = (S(t_1), S(t_2), \ldots, S(t_N))$ is

$$P(\mathbf{S}) = N_f \times \sum_{n=1}^{N} \frac{\hat{C}^{\text{tot}}(S(t_n), A(t_{n-1}))}{B_d(t_0, t_n)}, \qquad A(t_0) = 0, \tag{1.3}$$

where $B_d(t_0, t_n)^{-1}$ is the domestic discounting factor from $t_n$ to $t_0$ and

$$\hat{C}^{\text{tot}} = \hat{C}^{\text{pos}}(S(t_n), A(t_{n-1})) + \hat{C}^{\text{neg}}(S(t_n), A(t_{n-1}))$$

is the total cash flow at time $t_n$. Remark that a positive cash flow can not appears in the same time of a negative cash flow. Then the total cash flow is either positive or negative.

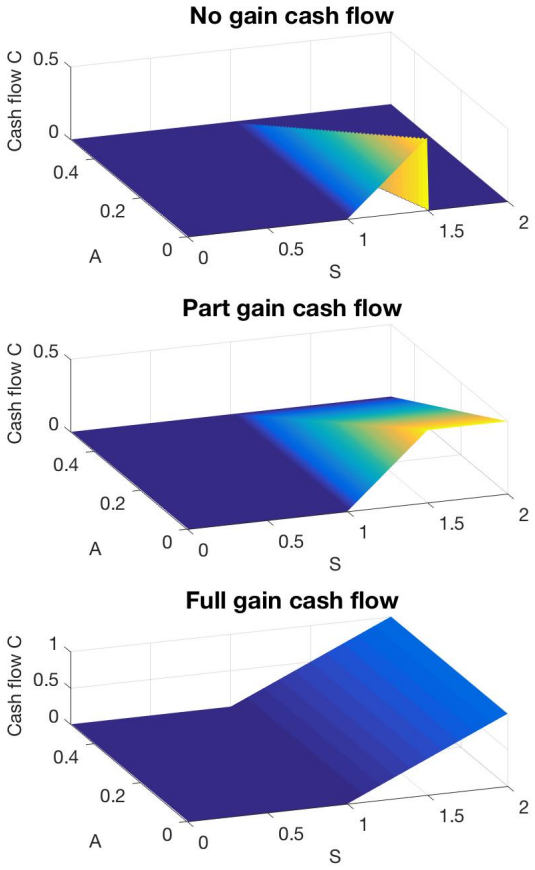


**Fig. 1.1:** Positive cash flow that produces jump on a fixing date for different type of knock-out.

## 1.3 Example of Term Sheet

In this section, we will give an example of a particular TARN called "*Leveraged Foreign Exchange Target Accrual Redemption Note with Full Settlement*", i.e. Full Gain FX-TARN with gear factor. The term sheet has the following form.

| **USD/CHF FX-TARN** | **Key Characteristics of the Transaction** |
|---|---|
| Instrument Type | Leverage FX Target Accrual Redemption Note (TARN) |
| Trade Date | 23 May 2017 |
| Buyer of CHF | The Bank |
| Buyer of USD | The Client |
| Underlying | USD/CHF Foreign Exchange rate |
| Notional Amount | USD 2'080'000.00<br>(versus maximum notional amount USD 4'160'000.00) |
| Accrual Amount | USD 40'000.00 |

| | |
|---|---|
| (Notional per fixing) | (versus Leveraged Accrual Amount USD 80'000.00) |
| Leverage factor | 2 |
| Initial Spot Price | 0.9730 CHF per 1 USD |
| Strike Price | As per date schedule below |
| Target Redemption Level | 0.4 CHF per 1 USD |
| Weekly Gains | On each Fixing Date,<br>• If USD/CHF > Strike Price :<br>Weekly Gains = USD/CHF - Strike Price<br>• Otherwise :<br>Weekly Gains = 0 CHF |
| Cumulated Gains | In respect of any Fixing Date, the Weekly Gains on that Fixing Date plus the sum of all Weekly Gains in respect of all previous Fixing Dates. |
| Redemption Event | A Redemption Event is deemed to have occurred if the Cumulated Gains (including the present fixing) is greater than or equal to the Target Redemption Level on any Fixing Date. |
| Expiration Date | 22 May 2018 |
| Fixing Reference | Weekly (Business Days) |
| Fixing Dates | 52 Fixings (see Schedule below) |
| Profile on Fixing Date | In respect of each Fixing Date :<br>**1)** If no Redemption Event occurs and the Fixing Price is :<br>• At or above the Strike Price, the Client will buy from the Bank the Accrual Amount at the strike price :<br>**Strike Price x Accrual Amount**<br>Or<br>• Below the Strike Price, the Client will buy from the Bank the Leveraged Accrual Amount at the Strike Price:<br>**Leveraged Factor x Strike Price x Accrual Amount**<br>**2)** If a Redemption Event occurs :<br>• The Client will buy from the Bank the Accrual Amount at the Strike Price for the Fixing Date that Redemption Event is deemed to have occurred :<br>**Strike Price x Accrual Amount**<br>• The product is then knocked out for all remaining subsequent Fixings. There will be no further obligations between the Client and the Bank. |
| Schedule | |

| Fixing | Fixing Date | Strike Level |
|---|---|---|
| 1 | 30 May 2017 | 0.9275 |
| 2 | 6 June 2017 | 0.9275 |
| 3 | 13 June 2017 | 0.9350 |
| 4 | 20 June 2017 | 0.9350 |
| 5 | 27 June 2017 | 0.9350 |
| 6 | 4 July 2017 | 0.9420 |
| 7 | 18 July 2017 | 0.9420 |
| 8 | 25 July 2017 | 0.9420 |
| ⋮ | ⋮ | ⋮ |
| 50 | 8 May 2018 | 0.9420 |
| 51 | 15 May 2018 | 0.9420 |
| 52 | 22 May 2018 | 0.9420 |

(Pay intention about the strike that is increasing in time.)

**Tab. 1.1:** FX-TARN Term Sheet example.

## 1.4 Overview of the Thesis

To be able to price such a product, we first have to model the FX rate in mathematical terms. Then after studying its properties we can develop numerical methods to evaluate the fair value at the trade date. Thus this thesis is organized as follow. In the Chapter 2, we introduce the Lévy processes used to model the FX rate.

In the Chapter 3, we deal with the financial models such as jump-diffusion and pure jump models. We will see in particular the finite activity models of Merton and Kou. Then we will devote some time to the Normal Inverse Gaussian (NIG) and Variance Gamma (VG) models, that are special cases of infinite activity models. The tools characterizing the Lévy processes such as the Lévy densities and characteristic functions will be very useful in the Finite Difference method and the Convolution method respectively.

In the Chapter 4, we expose the three numerical methods to price exotic options, which are the Monte Carlo method, the Finite Difference method and the Convolution method.

In the Chapter 5, we calibrate all the models with respect to the market data such that the price of our FX-TARN corresponds to the reality of the market.

The Chapter 6 is devoted to the results of experimental options. This allows us to analyze the performances of the three different methods. Then, this chapter ends with the pricing of our real case example.

Finally, the Chapter 7 concludes this thesis with an overview of possible future works.

# 2 Lévy Processes

> *Paul Lévy was a painter in the probabilistic world.*
>
> — **Michel Loève**
> (1907-1979)

Lévy processes play a central role in mathematical finance. They can describe the reality of financial markets in a more accurate way than models based on the geometric Brownian motion used in particular in Black-Scholes model. Indeed we can observe in the real world that the asset price processes have some jumps. Moreover, the log returns of the underlying have empirical distributions with fat tails and skewness which deviate from normality supposed by Black and Scholes. We begin this chapter, in Section 2.1, with the definition of a Lévy process and expose its fundamental properties. Next, in section 2.2, we present two main results about Lévy processes, namely the Lévy-Khinchine formula and the Lévy-Itô decomposition. In Section 2.3, the Lévy measure and path properties of a Lévy process are exposed. Finally, Section 2.4 presents the class of exponential Lévy processes and the equivalent martingale measure used to describe the asset price in financial modeling.

## 2.1 Definitions and properties

Lévy processes are continuous time stochastic processes used as the main ingredients for building continuous-time stochastic models. The simplest Lévy process is the linear drift. The Wiener process, Poisson process, and compound Poisson process are the most famous examples of Lévy processes. We will see later in this chapter that the sum of a linear drift, a Wiener process, and a compound Poisson process is again a Lévy process. It is called a *Lévy jump-diffusion* process.

**Definition 2.1 (*Wiener Process*)**

*A stochastic process $W = \{W_t, t \geq 0\}$, with $W_0 = 0$, is a **Wiener process**, also called a standard Brownian motion, on a probability space $(\Omega, \mathcal{F}, \mathbb{P})$ if:*

1. *$W$ has independent increments, i.e. $(W_{t+s} - W_t)$ is independent of $\mathcal{F}_t$ for any $s > 0$.*
2. *$W$ has stationary increments, i.e. the distribution of $(W_{t+s} - W_t)$ does not depend on $t$.*
3. *$W$ has Gaussian increments, i.e. $(W_{t+s} - W_t) \sim \mathcal{N}(0, s)$.*
4. *$W$ is stochastically continuous, i.e.*

$$\forall \epsilon > 0 : \lim_{s \to t} \mathbb{P}(|W_t - W_s| > \epsilon) = 0.$$

This motion was discovered by Brown in 1827 and taken back by Bachelier (1900) [Bac00] to model the stock market prices. Only in 1923 the Brownian motion was defined and constructed rigorously by R. Wiener.

**Definition 2.2 (*Poisson process*)**

*Let $(\tau_i)_{i \geq 1}$ be a sequence of independent exponential random variables with parameter $\lambda$ and $T_n = \sum_{i=1}^{n} \tau_i$. The process $N = \{N_t, t \geq 0\}$, with $N_0 = 0$, defined by*

$$N_t = \sum_{n \geq 1} \mathbf{1}_{\{t \geq T_n\}}$$

*is called **Poisson process** with intensity $\lambda$.*
*This process has the following properties:*

1. *$N$ has independent increments, i.e. $(N_{t+s} - N_t)$ is independent of $\mathcal{F}_t$ for any $s > 0$.*
2. *$N$ has stationary increments, i.e. the distribution of $(N_{t+s} - N_t)$ does not depend on $t$.*
3. *$N$ has Poisson increments, i.e. $(N_{t+s} - N_t)$ has a Poisson distribution with parameter $\lambda s$.*
4. *$N$ is stochastically continuous, i.e.*

$$\forall \epsilon > 0 : \lim_{s \to 0} \mathbb{P}(|N_{t+s} - N_t| > \epsilon) = 0.$$

*When the process is characterized by a constant intensity parameter $\lambda$, we say that the process is homogeneous. If the intensity parameter varies with time $t$ as $\lambda(t)$, the process is said to be non-homogeneous.*

The Poisson process, which bears the name of the French physicist and mathematician Siméon Denis Poisson, defines a counting process. It counts the number of random times $(T_n)$ which occur in $[0, t]$. Therefore, this is an increasing pure jump process. The jumps of size 1 occur at times $T_n$ and the intervals between two jumps are exponentially distributed. If we compare definitions 2.1 and 2.2, we can see that only the third property differs between the two processes, only the distribution changes. The main idea of a Lévy process is to ignore the distribution of increments.

**Definition 2.3 (*Lévy process*)**

*A cadlag stochastic process $X = \{X_t, t \geq 0\}$ on $(\Omega, \mathcal{F}, \mathbb{P})$ with real values is called a **Lévy process** if it has the following properties:*

1. *$X$ has independent increments, i.e. $(X_{t+s} - X_t)$ is independent of $\mathcal{F}_t$ for any $s > 0$.*
2. *$X$ has stationary increments, i.e. the distribution of $(X_{t+s} - X_t)$ does not depend on $t$.*
3. *$X$ is stochastically continuous, i.e.*

$$\forall \epsilon > 0 : \lim_{s \to 0} \mathbb{P}(|X_{t+s} - X_t| < \epsilon) = 0.$$

The third condition does not imply that the sample paths are continuous. In fact, the Brownian motion is the only (non-deterministic) Lévy process with continuous sample paths. This condition serves to exclude jumps at non-random times. In other words, for a given $t$, the probability of seeing a jump at $t$ is zero, discontinuities occur at random time. The compound Poisson process is a good example of a Lévy process.

**Definition 2.4 (*Compound Poisson process*)**

*A **compound Poisson process** with intensity $\lambda > 0$ and jump size distribution $f$ is a stochastic process $X = \{X_t, t \geq 0\}$ defined as*

$$X_t = \sum_{i=1}^{N_t} Y_i,$$

*where jumps size $Y_i$ are i.i.d. with the density function $f$ and $N = \{N_t, t \geq 0\}$ is a Poisson process with intensity $\lambda$, independent from $(Y_i)_{i \geq 1}$.*

We can easily deduce the following properties from this definition:

1. The sample paths of $X$ are cadlag piecewise constant functions.

2. The jump times $(T_i)_{i\geq 1}$ have the same law as the jump times of the Poisson process $N_t$. They can be expressed as partial sums of an independent exponential random variable with parameter $\lambda$.
3. The jump sizes $(Y_i)_{i\geq 1}$ are i.i.d. with law $f$.

We can also see that the Poisson process itself can be seen as a compound Poisson process with $Y_i \equiv 1$. This explains the origin of the name of the definition. Finally, the compound Poisson process allows us to work with jump sizes which have an arbitrary distribution.

## 2.2 Lévy-Khinchine formula and Lévy-Itô decomposition

We will now present in this section two main results about Lévy processes: the *Lévy-Khinchine formula* and the *Lévy-Itô decomposition*. Let's start with the relationship between infinitely divisible distributions and Lévy process.

**Definition 2.5 (*Infinite divisibility*)**

*A probability distribution $F$ is said to be **infinitely divisible** if for any integer $n \geq 2$, there exists $n$ i.i.d. random variables $Y_1, \dots, Y_n$ such that $Y_1 + \cdots + Y_n$ has distribution $F$.*

If $X$ is a Lévy process, for any $t > 0$ the distribution of $X_t$ is infinitely divisible. This comes from the fact that for any $n \geq 1$,

$$X_t = X_{t/n} + (X_{2t/n} - X_{t/n}) + \cdots + (X_t - X_{(n-1)t/n}) = nX_{t/n}, \tag{2.1}$$

and the property of stationary and independent increments. Let us define now the characteristic function and characteristic exponent of $X_t$.

**Definition 2.6 (*Characteristic function and exponent*)**

*The* ***characteristic function*** $\Phi_t$ *of a random variable* $X_t$ *with cumulative distribution* $F_t$ *is given by*

$$\Phi_t(u) = \mathbb{E}\left[e^{iuX_t}\right] = \int_{-\infty}^{\infty} e^{iux} dF_t(x).$$

*Its* ***characteristic exponent*** *is given by*

$$\Psi_t(u) = \log\left(\mathbb{E}\left[e^{iuX_t}\right]\right),$$

*for* $u \in \mathbb{R}$ *and* $t > 0$.

Then using twice equation (2.1) we obtain for any positive integers $m, n$ that

$$m\Psi_1(u) = \Psi_m(u) = n\Psi_{m/n}(u).$$

Hence for any rational $t = \frac{m}{n} > 0$ we have

$$\Psi_t(u) = t\Psi_1(u).$$

We can generalize this relation for all $t > 0$ with the help of the almost sure continuity of $X$ and a sequence of rational $\{t_n, n \geq 1\}$ such that $t_n \downarrow t$.

In conclusion, any Lévy process has the property that for all $t > 0$

$$\mathbb{E}\left[e^{iuX_t}\right] = e^{t\Psi(u)},$$

where $\Psi(u) = \Psi_1(u)$ is the characteristic exponent of $X_1$.

Then it is clear that each Lévy process has an infinitely divisible distribution. This allows us to apply the celebrated Lévy-Khinchine formula.

**Theorem 2.7 (*Lévy-Khintchine formula*)**

*Each Lévy process can be characterized by a triplet* $(\gamma, \sigma, \nu)$ *with* $\gamma \in \mathbb{R}, \sigma \geq 0$ *and* $\nu$ *a measure satisfying* $\nu(\{0\}) = 0$ *and*

$$\int_{\mathbb{R}} \min\{1, |x|^2\}\nu(dx) < \infty.$$

*In term of this triplet the characteristic function of the Lévy process equals:*

$$\begin{aligned}\Phi_t(u) &= \mathbb{E}\left[\exp(iuX_t)\right] \\ &= \exp\left(t\left(i\gamma u - \frac{1}{2}\sigma^2 u^2 + \int_{\mathbb{R}}\left(e^{iux} - 1 - iux\mathbf{1}_{\{|x|<1\}}\right)\nu(dx)\right)\right).\end{aligned} \tag{2.2}$$

(The proof can be find in Tankov and Cont (2003) [TC03])

The triplet $(\gamma, \sigma, \nu)$ is called the *Lévy* or *characteristic triplet*. Moreover, $\gamma$ is called the *drift term*, $\sigma$ the *Gaussian* or *diffusion coefficient* and $\nu(dx)$ is the *Lévy measure*, being the intensity of jumps of size $x$. This brings us to the following great result which is the Lévy-Itô decomposition.

**Theorem 2.8 (*Lévy-Itô decomposition*)**

*Consider a triplet* $(\gamma, \sigma, \nu)$ *where* $\gamma \in \mathbb{R}$, $\sigma \geq 0$ *and* $\nu$ *is a measure satisfying* $\nu(\{0\}) = 0$ *and*

$$\int_{\mathbb{R}} \min\{1, |x|^2\}\nu(dx) < \infty.$$

*Then, there exists a probability space* $(\Omega, \mathcal{F}, \mathbb{P})$ *on which four independent Lévy processes exist,* $X^{(1)}, X^{(2)}, X^{(3)}$ *and* $X^{(4)}$*, where* $X^{(1)}$ *is a constant drift,* $X^{(2)}$ *is a Wiener process,* $X^{(3)}$ *is a compound Poisson process and* $X^{(4)}$ *is a square integrable (pure jump) martingale with an a.s. countable number of jumps of magnitude less than 1 on each finite time interval. Taking* $X = X^{(1)} + X^{(2)} + X^{(3)} + X^{(4)}$*, we have that there exists a probability space on which a Lévy process* $X = \{X_t, 0 \leq t \leq T\}$ *with characteristic exponent*

$$\Psi(u) = i\gamma u - \frac{1}{2}\sigma^2 u^2 + \int_{\mathbb{R}}\left(e^{iux} - 1 - iux\mathbf{1}_{\{|x|<1\}}\right)\nu(dx),$$

*for all* $u \in \mathbb{R}$*, is defined.*

(See Kyprianou (2006) [Kyp06] for the proof)

The Lévy process is characterized by its triplet $(\gamma, \sigma, \nu)$. The simplest Lévy process is the linear *drift* with the triplet $(\gamma, 0, 0)$. Adding a *diffusion* component we get the

triplet $(\gamma, \sigma, 0)$ which is the case of the Black-Scholes model. A *pure jump* process will be identified by the triplet $(0, 0, \nu)$ and finally a *Lévy jump-diffusion* process will have the complete triplet $(\gamma, \sigma, \nu)$. The figure 2.1 illustrates some examples of Lévy processes.

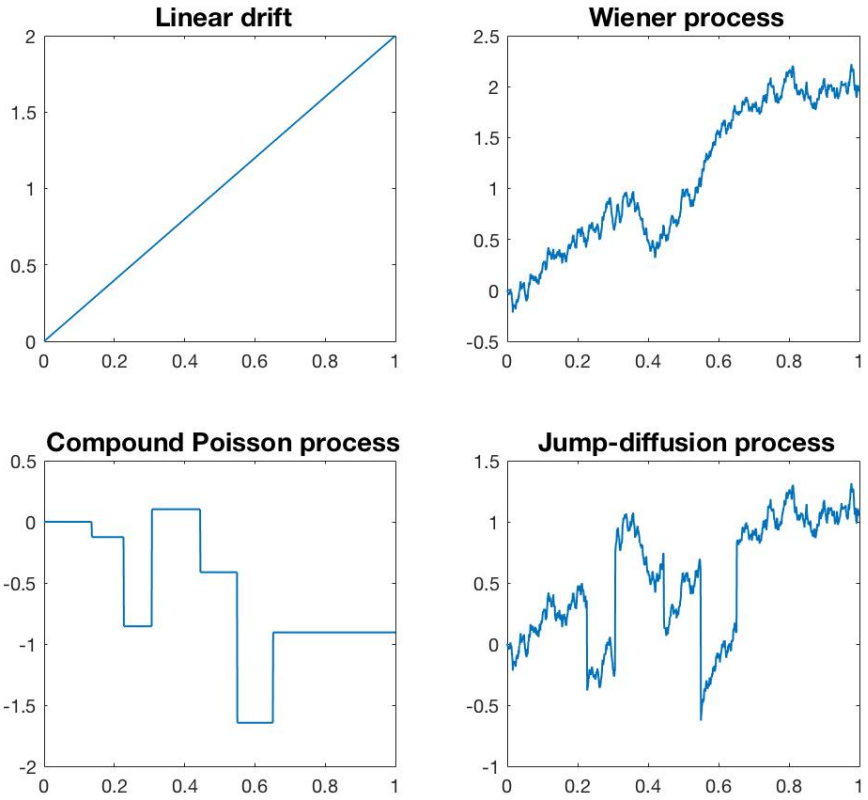


**Fig. 2.1:** Examples of Lévy processes: a linear drift with Lévy triplet $(2, 0, 0)$, a Wiener process with Lévy triplet $(2, 1, 0)$, a compound Poisson process with Lévy triplet $(0, 0, \lambda \cdot f_J)$, where $\lambda = 5$, and $f_J \sim \mathcal{N}(0, 1)$ and finally a jump-diffusion process with Lévy triplet $(2, 1, \lambda \cdot f_J)$.

## 2.3 Lévy measure and path properties

The *Lévy measure* dictates the behavior of the jumps.

**Definition 2.9 (*Lévy measure*)**

*Let $X = \{X_t, t \geq 0\}$ be a Lévy process on $\mathbb{R}$. The measure $\nu$ on $\mathbb{R}$ defined by*

$$\nu(A) = \mathbb{E}\left[\#\{t \in [0,1] : \Delta X_t = X_t - X_{t^-} \neq 0, \Delta X_t \in A\}\right],$$

*is called the **Lévy measure** of $X$: $\nu(A)$ is the expected number, per unit time, of jumps whose size belongs to $A$.*

For example, the Lévy measure of a compound Poisson process is given by $\nu(dx) = \lambda f_J(x)dx$, where $f_J(x)$ is called the Lévy density. In other words, the expected number of jumps, in a time interval of length 1, is $\lambda$, and the jump size is distributed according to $f_J$.

More generally, if $\nu$ is a finite measure, that is $\lambda = \nu(\mathbb{R}) = \int_{\mathbb{R}} \nu(dx) < \infty$, then we can defined $f(dx) = \frac{\nu(dx)}{\lambda}$, which is a probability measure. Then, $\lambda$ is the expected number of jumps and $f(dx)$ is the distribution of the jump size $x$. If $\nu(\mathbb{R}) = \infty$, an infinite number of (small) jumps is expected.

**Proposition 2.10 (*Finite and infinite activity*)**

*Let $X = \{X_t, t \geq 0\}$ be a Lévy process with triplet $(\gamma, \sigma, \nu)$.*

1. *If $\nu(\mathbb{R}) < \infty$ then almost all paths of $X$ have a finite number of jumps on every compact interval. In that case, the Lévy process has **finite activity**.*
2. *If $\nu(\mathbb{R}) = \infty$ then almost all paths of $X$ have a infinite number of jumps on every compact interval. In that case, the Lévy process has **infinite activity**.*

(See Theorem 21.3 in Sato (1999) [Sat99] for the proof)

Then the Lévy jump models can be classified into two categories from their Lévy measure: jump-diffusion or pure jump models. The jump-diffusions models are modeled by a Gaussian part (Wiener process) combined with a jump part (compound Poisson process), that has finitely many jumps in every time interval, i.e. finite activity models. The second category consists of models with an infinite number of jumps in every interval, i.e. infinite activity models. In these models, there is no need of Gaussian part because the dynamics of jumps is already rich enough to generate nontrivial small time behavior. Merton model and Variance Gamma model are good examples of jump-diffusion and pure jump models respectively. In Figure 2.2 are represented their respective Lévy densities. In Variance Gamma model, the density explodes at the origin. This means that the model allows infinitely many very small jumps. Since the Lévy density of Merton model is continuous, there is finite number of jumps on every time interval.

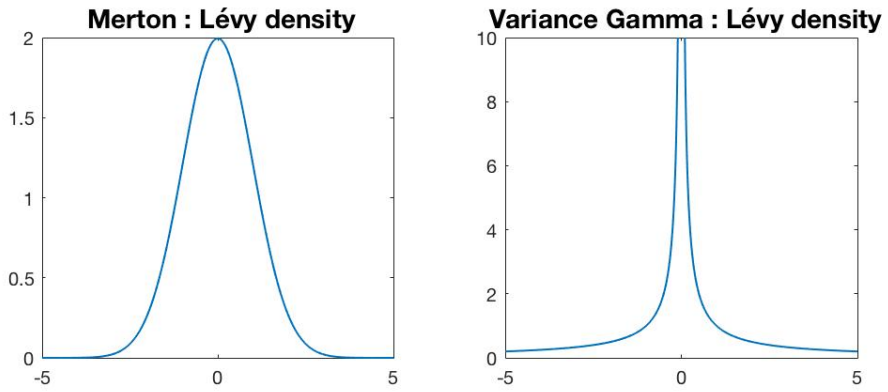


**Fig. 2.2:** The density of Lévy measure in the Merton model (left) and the Variance Gamma model (right).

## 2.4 Exponential Lévy processes and Equivalent martingale measure

In finance, it is common to model the stock price process as the exponential of a Lévy process:

$$S_t = S_0 e^{X_t}, \qquad \text{with } X_0 = 0.$$

The advantage of this representation is that the stock prices process is nonnegative and the log returns $\log(S_{t+s}/S_t)$, for $s, t > 0$, follow the distribution of increments of length $s$ dictated by the Lévy process $X = \{X_t, t \geq 0\}$. Thus they have independent and stationary increments.

In order to avoid an arbitrage opportunity, the discounted and reinvested process $\hat{S} = \{\hat{S}_t = e^{-(r-q)t} S_t, t \geq 0\}$ has to be a martingale under an *equivalent martingale measure* (EMM) $\mathbb{Q}$, called the *risk-neutral measure*. Recall that $r$ is the *(domestic) risk-free rate* and $q$ is the *continuous dividend yield (or foreign interest rate in the FX market)* of the asset. In other words, we are looking for a measure $\mathbb{Q}$ such that

$$\mathbb{E}^{\mathbb{Q}}\left[\hat{S}_T | \mathcal{F}_t\right] = \hat{S}_t.$$

Since the market is not complete under Lévy processes, there exists several ways to find a risk-neutral measure. We will see two different methods to determine this probability measure.

### 2.4.1 Esscher transform method

The first approach to find an EMM $\mathbb{Q}$ is proposed by Gerber, Shiu, et al. (1994) [G+94] using the Esscher transform. Suppose that the Lévy process $X = \{X_t, t \geq 0\}$

has a density function $f(x;t)$. Now multiply this density by an exponential factor $e^{\theta t}$ to get a new density function:

$$f(x;t,\theta) = \frac{e^{\theta x} f(x;t)}{\int_{\mathbb{R}} e^{\theta y} f(y;t) dy}.$$

Note that the denominator ensures the properties of $f(x;t,\theta)$ to be a density function, i.e.

$$\int_{\mathbb{R}} f(y;t,\theta) dy = 1.$$

With this transformation we obtain a new probability function defined by

$$d\mathbb{P}_t^\theta = \frac{e^{\theta x} d\mathbb{P}_t}{\int_{\mathbb{R}} e^{\theta y} d\mathbb{P}_t} = \frac{e^{\theta x} d\mathbb{P}_t}{M(\theta;t)},$$

where $M(\theta;t)$ is the moment-generating function and $\mathbb{P}$ is the real world probability measure. The goal is to determine the parameter $\theta$ such that $\mathbb{P}^\theta$ is an EEM. Take a look at the moment-generating function of $X_t$ under $\mathbb{P}$,

$$M(u;t) = \mathbb{E}\left[e^{uX_t}\right] = \Phi_t(-iu),$$

and the moment-generating function of $X_t$ under $\mathbb{P}^\theta$,

$$\begin{aligned} M(u;t,\theta) &= \int_{\mathbb{R}} e^{ux} f(x;t,\theta) dx \\ &= \frac{\int_{\mathbb{R}} e^{(u+\theta)x} f(x;t) dx}{\int_{\mathbb{R}} e^{\theta y} f(y;t) dy} \\ &= \frac{M(u+\theta;t)}{M(\theta;t)} \\ &= \frac{\Phi_t(-i(u+\theta))}{\Phi_t(-i\theta)}. \end{aligned} \tag{2.3}$$

The martingale condition on $\hat{S} = \{\hat{S}_t = S_0 e^{-(r-q)t+X_t}, t \geq 0\}$ gives us the following relation:

$$S_0 = e^{-(r-q)t}\mathbb{E}^{\mathbb{P}^\theta}[S_t] = e^{-(r-q)t} S_0 \underbrace{\mathbb{E}^{\mathbb{P}^\theta}\left[e^{X_t}\right]}_{=M(u;t,\theta)} = e^{-(r-q)t} S_0 \frac{\Phi_t(-i(u+\theta))}{\Phi_t(-i\theta)}.$$

Therefore, $\theta$ is given by the explicit equation

$$e^{(r-q)t} = \frac{\Phi_t(-i(1+\theta))}{\Phi_t(-i\theta)}.$$

Thus the solution $\theta^*$ of this equation gives us the Esscher transform martingale measure and we have $\mathbb{Q} \equiv \mathbb{P}^{\theta^*}$.

#### Characterization of the risk-neutral Lévy process

With the help of equation (2.3) we have that

$$\Phi_t^\theta(-iu) = \frac{\Phi_t(-i(u+\theta))}{\Phi_t(-i\theta)} \Longleftrightarrow \Phi_t^\theta(z) = \frac{\Phi_t(z-i\theta))}{\Phi_t(-i\theta)}.$$

We can also add that the new Lévy process is characterized by the triplet $(\gamma^\theta, \sigma^\theta, \nu^\theta(dx))$, and with the Lévy-Khintchine formula 2.7 combined to the definition (2.6) of the characteristic exponent, we can recover

$$\begin{aligned}\gamma^\theta &= \gamma + \sigma^2\theta + \int_{-1}^{1}\left(e^{\theta x}-1\right)\nu(dx),\\ \sigma^\theta &= \sigma,\\ \nu^\theta(dx) &= e^{\theta x}\nu(dx).\end{aligned}$$

### 2.4.2 Mean-correction method

The second way to obtain an equivalent martingale measure $\mathbb{Q}$ is to correct the mean of the exponential Lévy process to satisfy the martingale condition of the discounted stock price process $\hat{S} = \{\hat{S}_t = e^{-(r-q)t}S_t, t \geq 0\}$. The idea is to add a drift to the Lévy process to kill the drift of the discounted asset price process. Therefore we obtain a new Lévy process $\tilde{X} = \left\{\tilde{X}_t = X_t + \omega t, t \geq 0\right\}$ and consequently

$$\begin{aligned}S_0 &= \mathbb{E}^{\mathbb{Q}}\left[e^{-(r-q)t}S_t\right]\\ &= S_0 e^{-(r-q)t}\mathbb{E}^{\mathbb{Q}}\left[e^{\tilde{X}_t}\right]\\ &= S_0 e^{-(r-q)t}\mathbb{E}^{\mathbb{Q}}\left[e^{X_t+\omega t}\right]\\ &= S_0 e^{[\omega-(r-q))+\Psi(-i)]t}\end{aligned}$$

Hence we have that $\omega$ have to be equal to $[(r-q)-\Psi(-i)]$, where $\Psi$ is the characteristic exponent of $X_1$. Moreover we have that the new risk-neutral Lévy process $\tilde{X}$ is characterized by the triplet $(\gamma^*, \sigma, \nu)$ with

$$\gamma^* = \gamma + (r-q) - \Psi(-i). \tag{2.4}$$

The mean-correction method is simpler than the Esscher transform method and this is the method we will use throughout this thesis. There are several other measures that can be found in the book of Miyahara (2011) [Miy11].

# 3 Financial Mathematic Models

> *Essentially, all models are wrong, but some are useful.*
>
> **— George E. P. Box**
> (1919-2013)

In this chapter, we will take a look on some popular models in financial mathematics. To begin, in Section 3.1 we will describe the Black-Scholes model (1973) [BS73] and compute its risk-neutral characteristic function. In Section 3.2 we will talk about *jump-diffusion models*. These models evolve with a diffusion process, punctuated by jumps at random intervals. We can model this behavior with a Wiener process and a compound Poisson process to characterize the jumps with size distribution $f_J$. We will discuss, in particular, two examples: the Merton model (1976) [Mer76] and the Kou model (2002) [Kou02]. Finally, Section 3.3 is devoted to *pure jump models*. This category of models is characterized by infinite number of jumps in any time interval, called *infinite activity* models. These particular models do not need a Brownian part because the dynamics of the process is already modeled by an infinity of small jumps. However, we will see that it is possible to construct these models by a Brownian subordination, which is called a time-changed Brownian motion. We will discuss two examples: the Normal Inverse Gaussian (NIG) model, proposed by Barndorff-Nielsen (1997) [Bar97b] and the Variance Gamma (VG) model, proposed by Madan et al. (1998) [MCC98].

## 3.1 Black-Scholes Model

Samuelson (1965) was the first one to introduce Brownian motion to model asset prices. Then his work was taken over by Black and Scholes (1973) to create the most famous model, the Black-Scholes model. In this model, the stock price $S = \{S_t, t \geq 0\}$ follows a geometric Brownian motion, i.e.

$$dS_t = \mu S_t dt + \sigma S_t dW_t,$$

where $\mu$ and $\sigma$ are respectively the drift and the volatility of the process. This stochastic differential equation has a unique solution which is

$$S_t = S_0 e^{\left(\mu - \frac{1}{2}\sigma^2\right)t + \sigma W_t}.$$

In fact this model is based on an exponential Lévy process $X = \{X_t, t \geq 0\}$ defined by

$$X_t = \left(\mu - \frac{1}{2}\sigma^2\right) t + \sigma W_t.$$

Hence his characteristic triplet is $\left(\mu - \frac{1}{2}\sigma^2, \sigma, 0\right)$.

### Risk-neutral Characteristic Function

Recall that $X_t$ in this model is described by the characteristic triplet $(\gamma, \sigma, 0)$ with $\gamma = \left(\mu - \frac{1}{2}\sigma^2\right)$. Thus the Lévy-Khintchine formula 2.7 gives us the characteristic function of $X_t$

$$\Phi_t(u) = \exp\left\{t\left(\left(\mu - \frac{1}{2}\sigma^2\right) iu - \frac{1}{2}\sigma^2 u^2\right)\right\}.$$

Hence the characteristic exponent of $X_1$ evaluated at $-i$ is

$$\Psi(-i) = \mu - \frac{1}{2}\sigma^2 + \frac{1}{2}\sigma^2 = \mu.$$

With equation (2.4), we obtain the risk-neutral drift

$$\gamma^* = r - q - \frac{1}{2}\sigma^2,$$

and the risk-neutral characteristic function is given by

$$\Phi_t^{\text{RN}}(u) = \exp\left\{t\left(i\gamma^* u - \frac{1}{2}\sigma^2 u^2\right)\right\}.$$

Finally the risk-neutral stock price process is defined by

$$\begin{aligned} S_t &= S_0 \exp\left\{\left(r - q - \frac{1}{2}\sigma^2\right) t + \sigma W_t\right\} \\ &= S_0 \exp\left\{X_t^{\text{BS}}(r, q, \sigma)\right\} \end{aligned}$$

## 3.2 Jump-diffusion Models

Consider now the Lévy jump-diffusion process $X = \{X_t, t \geq 0\}$. It is modeled by a drifted Brownian motion and a compound Poisson process. Therefore we can write it in the form

$$X_t = \gamma t + \sigma W_t + \sum_{i=1}^{N_t} Y_i,$$

with $\gamma \in \mathbb{R}, \sigma \in \mathbb{R}_+, W = \{W_t, t \geq 0\}$ is a Wiener process, $N = \{N_t, t \geq 0\}$ is a Poisson process with parameter $\lambda$ and $Y = \{Y_t, t \geq 0\}$ is an i.i.d sequence of random variables with density $f_J$.

The characteristic function of $X_t$ is given by

$$\begin{aligned}
\Phi_t(u) &= \mathbb{E}\left[e^{iuX_t}\right] \\
&= \mathbb{E}\left[\exp\left\{iu\left(\gamma t + \sigma W_t + \sum_{i=1}^{N_t} Y_i\right)\right\}\right] \\
&= \exp\{iu\gamma t\}\,\mathbb{E}\left[\exp\{iu\sigma W_t\}\right]\mathbb{E}\left[\exp\left\{iu\sum_{i=1}^{N_t} Y_i\right\}\right],
\end{aligned}$$

by independence of $W_t$ and $N_t$. Since $W_t \sim \mathcal{N}(0, \sigma^2 t)$ and $N_t \sim \text{Poisson}(\lambda t)$, we have

$$\begin{aligned}
\mathbb{E}\left[e^{iu\sigma W_t}\right] &= e^{-\frac{1}{2}\sigma^2 u^2 t}, \\
\mathbb{E}\left[e^{iu\sum_{i=1}^{N_t} Y_i}\right] &= \sum_{n=0}^{\infty} \mathbb{E}\left[e^{iuY}\right]^n \mathbb{P}(N_t = n) \\
&= \sum_{n=0}^{\infty} \Phi_Y(u)^n \frac{(\lambda t)^n}{n!} e^{-\lambda t} \\
&= e^{\lambda t(\Phi_Y(u)-1)} \\
&= e^{\lambda t \int_{\mathbb{R}} \left(e^{iuy}-1\right) f_J(y)dy}.
\end{aligned}$$

Hence we get

$$\begin{aligned}
\Phi_t(u) &= \exp\{iu\gamma t\}\exp\left\{-\frac{1}{2}\sigma^2 u^2 t\right\}\exp\left\{\lambda t\int_{\mathbb{R}}\left(e^{iuy}-1\right) f_J(y)dy\right\} \\
&= \exp\left\{t\left(iu\gamma - \frac{1}{2}\sigma^2 u^2 + \int_{\mathbb{R}}\left(e^{iuy}-1\right)\lambda f_J(y)dy\right)\right\}. \qquad (3.1)
\end{aligned}$$

Then we have a characterization of a Lévy jump-diffusion process by its characteristic triplet $(\gamma, \sigma, \lambda \cdot f_J)$.

### 3.2.1 Merton Model

Under the Black-Scholes model, the stock price is supposed to be continuous. Unfortunately this is not the case in reality. Merton (1976) [Mer76] is the first to use the notion of discontinuous price process to model asset returns. In his model, Merton uses a Normal distribution to model the jump size, i.e. $Y_i$ are independent and identically distributed with a Normal distribution $\mathcal{N}(\alpha, \delta^2)$. Then the Lévy process is

$$X_t = \gamma t + \sigma W_t + \sum_{i=0}^{N_t} Y_i,$$

with $Y_i \sim \mathcal{N}(\alpha, \delta^2)$. Hence, the density function of the jump size is

$$f_J(x) = \frac{1}{\sqrt{2\pi}\delta} e^{-\frac{(x-\alpha)^2}{2\delta^2}},$$

and the Lévy density is

$$\nu^{\text{Mer}}(dx) = \lambda f_J(x)dx = \frac{\lambda}{\sqrt{2\pi}\delta} e^{-\frac{(x-\alpha)^2}{2\delta^2}} dx.$$

Then there are four parameters in the Merton model excluding the drift parameter $\mu$:

- $\sigma$ - the diffusion volatility,
- $\lambda$ - the jump intensity,
- $\alpha$ - the mean of jump size,
- $\delta$ - the standard deviation of jump size.

#### Risk-neutral Characteristic Function

With the help of equation 3.1, we obtain the characteristic function of the model under the real world measure $\mathbb{P}$:

$$\begin{aligned}
\Phi_t(u) &= \exp\left\{t\left(iu\gamma - \frac{1}{2}\sigma^2u^2 + \int_{\mathbb{R}}\left(e^{iuy}-1\right)\lambda f_J(ydy)\right)\right\} \\
&= \exp\left\{t\left(iu\gamma - \frac{1}{2}\sigma^2u^2 + \lambda\left(\Phi_Y(u)-1\right)\right)\right\} \\
&= \exp\left\{t\left(iu\gamma - \frac{1}{2}\sigma^2u^2 + \lambda\left(e^{iu\alpha-\frac{1}{2}\delta^2u^2}-1\right)\right)\right\},
\end{aligned}$$

where $\Phi_Y$ is the characteristic function of a jump $Y$. Hence the model is characterized by the triplet $(\gamma, \sigma, \lambda \cdot f_J)$.

We can now compute the characteristic exponent in order to apply the mean-correction and get the risk-neutral process.

$$\Psi(-i) = \gamma + \frac{1}{2}\sigma^2 + \lambda\left(e^{\alpha+\frac{1}{2}\delta^2} - 1\right).$$

Applying equation (2.4), we obtain the risk-neutral drift

$$\gamma^* = (r-q) - \frac{1}{2}\sigma^2 - \lambda\left(e^{\alpha+\frac{1}{2}\delta^2} - 1\right),$$

and the risk-neutral characteristic function of the Merton jump-diffusion model is given by

$$\Phi_t^{\text{RN}}(u) = \exp\left\{t\left(i\gamma^* u - \frac{1}{2}\sigma^2 u^2 + \lambda\left(e^{i\alpha u - \frac{1}{2}\delta^2 u^2} - 1\right)\right)\right\}.$$

The risk-neutral stock price process is finally

$$S_t = S_0 \exp\left\{X_t^{\text{Mer}}(r, q, \sigma, \lambda, \alpha, \delta)\right\},$$

where $X^{\text{Mer}}$ is the Lévy jump-diffusion process characterized by the triplet $(\gamma^*, \sigma, \lambda \cdot f_J)$.

### 3.2.2 Kou Model

The Kou model (2002) is very similar to Merton's one. The only difference is in the distribution of the jump size, which is double-exponential. Then the Lévy process under Kou model is

$$X_t = \gamma t + \sigma W_t + \sum_{i=0}^{N_t} Y_i,$$

with $Y_i \sim \text{DoubleExp}(p, \eta_1, \eta_2)$. In other words, jump size has the density

$$f_J(x) = \begin{cases} p \cdot \eta_1 e^{-\eta_1 x}, & \text{if } x \geq 0, \\ (1-p) \cdot \eta_2 e^{\eta_2 x}, & \text{if } x < 0. \end{cases}$$

The probability $p$ represents the probability of an upward jump and $(1-p)$ the probability of a downward jump. Thus the Lévy density is given by

$$\nu(dx) = \lambda\left(p \cdot \eta_1 e^{-\eta_1 x}\mathbf{1}_{x\geq 0} + (1-p) \cdot \eta_2 e^{\eta_2 x}\mathbf{1}_{x<0}\right) dx.$$

Then there are five parameters in the Kou model excluding the drift parameter $\gamma$:

- $\sigma$ - the diffusion volatility,
- $\lambda$ - the jump intensity,

- $p$ - the probability of an upward jump,
- $\eta_1, \eta_2$ - control the decay of the tails in the distribution.

Note that the mean and the variance of positive or negative jumps are given by $\eta_1^{-1}, \eta_2^{-1}$ and $\eta_1^{-2}, \eta_2^{-2}$ respectively.

### Risk-neutral Characteristic Function

A preliminary computation of the characteristic function of a double exponential random variable $Y$ is needed.

$$\begin{aligned}\Phi_Y(u) &= \int_{\mathbb{R}} e^{iuy} f_J(y) dy \\ &= \int_0^{\infty} e^{iuy} p \cdot \eta_1 e^{-\eta_1 y} dy + \int_{-\infty}^{0} e^{iuy}(1-p) \cdot \eta_2 e^{\eta_2 y} dy \\ &= p \cdot \eta_1 \left[ \frac{e^{(iu-\eta_1)y}}{iu - \eta_1} \right]_0^{\infty} + (1-p) \cdot \eta_2 \left[ \frac{e^{(iu+\eta_2)y}}{iu + \eta_2} \right]_{-\infty}^{0} \\ &= \frac{p \cdot \eta_1}{\eta_1 - iu} + \frac{(1-p) \cdot \eta_2}{\eta_2 + iu}\end{aligned}$$

Now as for Merton model, the equation (3.1) gives us the characteristic function of $X_t$

$$\begin{aligned}\Phi_t(u) &= \exp\left\{ t \left( iu\gamma - \frac{1}{2}\sigma^2 u^2 + \lambda \left( \Phi_Y(u) - 1 \right) \right) \right\} \\ &= \exp\left\{ t \left( iu\gamma - \frac{1}{2}\sigma^2 u^2 + \lambda \left( \frac{p \cdot \eta_1}{\eta_1 - iu} + \frac{(1-p) \cdot \eta_2}{\eta_2 + iu} - 1 \right) \right) \right\}.\end{aligned}$$

Hence the model is characterized by the triplet $(\gamma, \sigma, \lambda \cdot f_J)$.

The characteristic exponent of this process gives us

$$\Psi(-i) = \gamma + \frac{1}{2}\sigma^2 + \lambda \left( \frac{p \cdot \eta_1}{\eta_1 - 1} + \frac{(1-p) \cdot \eta_2}{\eta_2 + 1} - 1 \right).$$

Consequently we obtain the risk-neutral drift

$$\gamma^* = (r - q) - \frac{1}{2}\sigma^2 - \lambda \left( \frac{p \cdot \eta_1}{\eta_1 - 1} + \frac{(1-p) \cdot \eta_2}{\eta_2 + 1} - 1 \right),$$

and the risk-neutral characteristic function of the Double Exponential Kou jump-diffusion model

$$\Phi_t^{\text{RN}}(u) = \exp\left\{ t \left( i\gamma^* u - \frac{1}{2}\sigma^2 u^2 + \lambda \left( \frac{p \cdot \eta_1}{\eta_1 + iu} + \frac{(1-p) \cdot \eta_2}{\eta_2 + iu} - 1 \right) \right) \right\}.$$

Therefore we can model the risk-neutral stock price process by

$$S_t = S_0 \exp\left\{X_t^{\text{Kou}}(r, q, \sigma, \lambda, p, \eta_1, \eta_2)\right\},$$

where $X_t^{\text{Kou}}$ is the Lévy jump-diffusion process characterized by the triplet $(\gamma^*, \sigma, \lambda \cdot f_J)$.

## 3.3 Pure jump Models

To go beyond the jump-diffusion process, initially proposed by Merton in 1976, infinite activity models have been proposed. There exist a lot of papers about these kind of Lévy processes. We will see two different models which are the *Normal Inverse Gaussian* (NIG) model, proposed by Barndorff-Nielsen in 1997, and the *Variance Gamma* (VG) model, proposed by Madan et al. in 1998. They are both particular cases of the Generalized Hyperbolic model, developed by Eberlein and Prause (1998).

These two models can be described as a Brownian motion $W = \{W_t, t \geq 0\}$ with constant drift $\theta$ and volatility $\sigma$ evaluated at a random time $T = \{T_t, t \geq 0\}$,

$$X_t = \theta T_t + \sigma W_{T_t}.$$

This process is called *time changed Brownian motion* with constant drift. Moreover, the process $T$ is called the *subordinator* process, which is an increasing Lévy process. The subordinating processes in the NIG and VG models are respectively an *Inverse Gaussian* process and a *Gamma* process.

### 3.3.1 Normal Inverse Gaussian Model

First of all, we will present the subordinating Inverse Gaussian process which is used to construct the Normal Inverse Gaussian (NIG) process.

#### Inverse Gaussian Process

Let $T \sim \text{IG}(a, b)$ be an inverse Gaussian random variable. This is in fact the first time that a Brownian motion with drift $b > 0$ reaches the level $a > 0$ Its density function is given by

$$f_{\text{IG}}(x; a, b) = \frac{ae^{ab}}{\sqrt{2\pi}} x^{-\frac{3}{2}} \exp\left\{-\frac{1}{2}\left(\frac{a^2}{x} + b^2 x\right)\right\}, \qquad x > 0,$$

and its characteristic function is

$$\Phi_{\text{IG}}(u; a, b) = \exp\left\{-a\left(\sqrt{-2iu + b^2} - b\right)\right\}.$$

Note that if $X_1, \ldots, X_n$ are independent IG random variables with parameters $(a/n, b)$, then $X_1 + \cdots + X_n \sim \text{IG}(a, b)$. Thus this distribution is infinitely divisible and we are able to define an IG process $X^{\text{IG}} = \{X_t^{\text{IG}}, t \geq 0\}$ as a process that starts at $0$ and has independent and stationary increments such that $X_t^{\text{IG}} \sim \text{IG}(at, b)$. Hence it has the following characteristic function

$$\begin{aligned}\Phi_t^{\text{IG}}(u; at, b) &= \mathbb{E}\left[e^{iuX_t^{\text{IG}}}\right] \\ &= \exp\left\{-at\left(\sqrt{-2iu + b^2} - b\right)\right\}\end{aligned}$$

Now let's verify the non-decreasing condition for a subordinator. We have that

$$\begin{aligned}\mathbb{P}\left(X_{t+\Delta t}^{\text{IG}} < X_t^{\text{IG}}\right) &= \mathbb{P}\left(X_{t+\Delta t}^{\text{IG}} - X_t^{\text{IG}} < 0\right) \\ &= \mathbb{P}\left(X_{\Delta t}^{\text{IG}} < 0\right) = 0,\end{aligned}$$

since an IG random variable takes only positive values. Thus it is a good candidate as subordinator.

### Normal Inverse Gaussian Process

As mention by Geman (2002), we can represent the NIG process by a time-changed Brownian motion with an IG process as subordinator. Let $W = \{W_t, t \geq 0\}$ be a standard Brownian motion and $T = \{T_t, t \geq 0\}$ be an IG process with parameters $a = 1$ and $b$. Then the NIG process is given by

$$X_t = \theta T_t + \sigma W_{T_t}.$$

Thus its characteristic function is

$$\begin{aligned}
\Phi_t^{\text{NIG}}(u;\theta,\sigma) &= \mathbb{E}\left[e^{iuX_t}\right] \\
&= \mathbb{E}\left[e^{\left(iu\theta-\frac{\sigma^2u^2}{2}\right)T_t}\right] \\
&= \Phi_t^{\text{IG}}\left(u\theta + i\frac{\sigma^2u^2}{2}\right) \\
&= \exp\left\{-t\left(\sqrt{-2i\left(u\theta+i\frac{\sigma^2u^2}{2}\right)+b^2}-b\right)\right\} \\
&= \exp\left\{-t\left(\sqrt{b^2-2iu\theta+\sigma^2u^2}-b\right)\right\} \\
&= \exp\left\{-t\sigma\left(\sqrt{\frac{b^2}{\sigma^2}+\frac{\theta^2}{\sigma^4}-\left(\frac{\theta}{\sigma^2}+iu\right)^2}-\frac{b}{\sigma}\right)\right\}.
\end{aligned}$$

To simplify the notation, we can set

$$\begin{aligned}
\alpha^2 &= \frac{b^2}{\sigma^2}+\frac{\theta^2}{\sigma^4}, \\
\beta &= \frac{\theta}{\sigma^2}, \\
\delta &= \sigma.
\end{aligned}$$

Then the subordinator $T_t \sim \text{IG}\left(t, \delta\sqrt{\alpha^2-\beta^2}\right)$ and the NIG process becomes

$$X_t^{\text{NIG}} = \beta\delta^2 T_t + \delta W_{T_t},$$

and we get the characteristic function given by Barndorff-Nielsen (1997) in the form

$$\Phi_t^{\text{NIG}}(u;\alpha,\beta,\delta) = \exp\left\{t\delta\left(\sqrt{\alpha^2-\beta^2}-\sqrt{\alpha^2-(\beta+iu)^2}\right)\right\}.$$

Then the NIG model has three parameters to control the shape of the distribution:

- $\alpha$ - tail heaviest of steepness,
- $\beta$ - symmetry,
- $\delta$ - scale.

Note that the parameters have to satisfy the conditions $\alpha, \delta > 0$ and $-\alpha < \beta < \alpha$.

### Risk-neutral Characteristic Function

Here, since the characteristic triplet $(\gamma, 0, \nu)$ is not trivial, we will find a risk-neutral characteristic function using the following form of the stock price

$$S_t = S_0 e^{(r-q)t+\omega t+X_t^{\text{NIG}}}.$$

Hence we have that

$$\begin{aligned} S_0 &= \mathbb{E}^{\mathbb{Q}}\left[e^{-(r-q)t}S_t\right] \\ &= S_0\mathbb{E}^{\mathbb{Q}}\left[e^{\omega t+X_t^{\text{NIG}}}\right] \\ &= S_0 e^{\omega t}\Phi_t^{\text{NIG}}(-i). \end{aligned}$$

Therefore we must have $e^{\omega t}\Phi_t^{\text{NIG}}(-i) = 1$ or equivalently

$$\omega = -\delta\left(\sqrt{\alpha^2-\beta^2} - \sqrt{\alpha^2-(\beta+1)^2}\right).$$

This gives us the risk-neutral drift

$$\gamma^* = (r-q) - \delta\left(\sqrt{\alpha^2-\beta^2} - \sqrt{\alpha^2-(\beta+1)^2}\right),$$

and the risk-neutral characteristic function is

$$\Phi_t^{RN}(u) = \exp\left\{t\left(i\gamma^* u + \delta\left(\sqrt{\alpha^2-\beta^2} - \sqrt{\alpha^2-(\beta+iu)^2}\right)\right)\right\}.$$

Finally, the risk-neutral stock price process is in the form

$$S_t = S_0 \exp\{\gamma^* t + X_t^{\text{NIG}}(\alpha, \beta, \delta)\},$$

where $X_t^{\text{NIG}}$ is the Normal Inverse Gaussian process characterized by the Lévy triplet $(\gamma^*, 0, \nu^{\text{NIG}})$, with

$$\nu^{\text{NIG}}(dx) = \frac{\delta\alpha}{\pi}\frac{\exp(\beta x)K_1(\alpha|x|)}{|x|}dx,$$

where $K_\lambda$ is the modified Bessel of the second king with index $\lambda$.

## 3.3.2 Variance Gamma Model

Madan et al. in 1998 had the same approach as the previous Normal Inverse Gaussian model. The difference is that the random time in the Brownian motion is Gamma distributed. In a second time, since this process has also finite variation, it can be represent by the difference of two increasing processes. The first one models the price increases while the second one reflects the price decreases. To begin, let us

introduce the subordinating Gamma process used to construct the Variance Gamma process.

### Gamma process

The Gamma density function $f_\Gamma(x; a, b)$ with parameters $a, b > 0$ is given by

$$f_\Gamma(x; a, b) = x^{a-1} \frac{b^a e^{-bx}}{\Gamma(a)},$$

where $\Gamma$ is the Euler gamma function. Then its characteristic function is

$$\Phi_\Gamma(u; a, b) = \left(1 - \frac{iu}{b}\right)^{-a}.$$

This distribution is also infinitely divible because if $X_1, \ldots, X_n \sim \text{Gamma}(a/n, b)$, we have that $X_1 + \cdots + X_n \sim \text{Gamma}(a, b)$. Therefore, we can define a Gamma process $X^{\text{Gam}} = \left\{X_t^{\text{Gam}}, t \geq 0\right\}$, which is a stochastic process that starts at 0 and has stationary and independent increments such that $X_t^{\text{Gamma}} \sim \Gamma(at, b)$. The corresponding characteristic function is given by

$$\begin{aligned}
\Phi_t^{\text{Gam}}(u; at, b) &= \mathbb{E}\left[e^{iuX_t^{\text{Gam}}}\right] \\
&= \left(1 - \frac{iu}{b}\right)^{-at} \\
&= \left(\frac{1}{1 - \frac{iu\nu}{\mu}}\right)^{\frac{\mu^2}{\nu}t},
\end{aligned}$$

where $\mu = \frac{a}{b}$ and $\nu = \frac{a}{b^2}$ are respectively the mean rate and the variance rate of the process.

### Variance Gamma process

As in the case of the Normal Inverse Gamma process, we can represent the Variance Gamma process as a time-changed Brownian motion

$$X_t = \theta T_t + \sigma W_{T_t},$$

with $T = \{T_t, t \geq 0\}$ a gamma process with mean rate $\mu = 1$ and variance rate $\nu$. Therefore the characteristic function of this process is

$$\begin{aligned}\Phi_t^{\text{VG}}(u;\theta,\sigma,\nu) &= \mathbb{E}\left[e^{iuX_t}\right] \\ &= \Phi_t^{\text{Gam}}\left(u\theta + i\frac{\sigma^2u^2}{2}\right) \\ &= \left(\frac{1}{1 - iu\theta\nu + \frac{\sigma^2\nu}{2}u^2}\right)^{\frac{t}{\nu}}. \end{aligned} \tag{3.2}$$

Then we have that the VG model has three parameters:

- $\theta$ - drift of the Brownian motion,
- $\sigma$ - volatility of the Brownian motion,
- $\nu$ - variance rate of the time change.

Madan et al. (1998) showed that the VG process has finite variation. Therefore we can represent this process by the difference of two independent and increasing gamma processes with mean rate $\mu_\pm$ variance rate $\nu_\pm$, i.e.

$$X_t = \gamma_t^+(\mu_+,\nu_+) - \gamma_t^-(\mu_-,\nu_-),$$

where $\gamma_t^+$ and $\gamma_t^-$ correspond respectively to the positive and negative shocks. Therefore the characteristic function of this representation is

$$\begin{aligned}\Phi_t^{\text{VG}}(u) &= \mathbb{E}\left[e^{iu(\gamma_t^+ - \gamma_t^-)}\right] \\ &= \Phi_{\gamma_t^+}(u)\Phi_{-\gamma_t^-}(u) \\ &= \left(\frac{1}{1 - \frac{iu\nu_+}{\mu_+}}\right)^{\frac{\mu_+^2}{\nu_+}t}\left(\frac{1}{1 + \frac{iu\nu_-}{\mu_-}}\right)^{\frac{\mu_-^2}{\nu_-}t}. \end{aligned} \tag{3.3}$$

Thus, comparing both characteristic functions (3.2) and (3.3), we get the following relations

$$\begin{aligned}\frac{\mu_+^2}{\nu_+} = \frac{\mu_-^2}{\nu_-} &= \frac{1}{\nu}, \\ \frac{\nu_+\nu_-}{\mu_+\mu_-} &= \frac{\sigma^2\nu}{2}, \\ \frac{\nu_+}{\mu_+} - \frac{\nu_-}{\mu_-} &= \theta\nu. \end{aligned}$$

Hence we have that

$$\begin{aligned}
\mu_+ &= \frac{1}{2}\sqrt{\theta^2 + \frac{2\sigma^2}{\nu}} + \frac{\theta}{2}, \\
\mu_- &= \frac{1}{2}\sqrt{\theta^2 + \frac{2\sigma^2}{\nu}} - \frac{\theta}{2}, \\
\nu_+ &= \left(\frac{1}{2}\sqrt{\theta^2 + \frac{2\sigma^2}{\nu}} + \frac{\theta}{2}\right)^2 \nu, \\
\nu_- &= \left(\frac{1}{2}\sqrt{\theta^2 + \frac{2\sigma^2}{\nu}} - \frac{\theta}{2}\right)^2 \nu.
\end{aligned}$$

Finally, the VG process is effectively the difference of two independent gamma processes.

### Risk-neutral Characteristic Function

Just recall that the characteristic function under real world probability $\mathbb{P}$ is given by

$$\begin{aligned}
\Phi_t^{\text{VG}}(u) &= \left(1 - iu\theta\nu + \frac{\sigma^2\nu}{2}u^2\right)^{-\frac{t}{\nu}} \\
&= \exp\left\{-\frac{t}{\nu}\ln\left(1 - iu\theta\nu + \frac{\sigma^2\nu}{2}u^2\right)\right\}.
\end{aligned}$$

In the same way as in the NIG model, we can construct the risk-neutral drift by considering

$$S_t = S_0 e^{(r-q)t + \omega t + X_t^{\text{VG}}}.$$

Then

$$\begin{aligned}
S_0 &= \mathbb{E}^{\mathbb{Q}}\left[e^{-(r-q)t}S_t\right] \\
&= S_0\mathbb{E}^{\mathbb{Q}}\left[e^{\omega t + X_t^{\text{VG}}}\right] \\
&= S_0 e^{\omega t}\Phi_t^{\text{VG}}(-i),
\end{aligned}$$

and we must have that $e^{\omega t}\Phi_t^{\text{VG}}(-i) = 1$ or in other words

$$\omega = \frac{1}{\nu}\ln\left(1 - \theta\nu - \frac{\sigma^2\nu}{2}\right).$$

At the end we obtain the risk-neutral drift

$$\gamma^* = (r-q) + \frac{1}{\nu}\ln\left(1 - \theta\nu - \frac{\sigma^2\nu}{2}\right),$$

and the risk-neutral characteristic function is given by

$$\Phi_t^{\text{RN}}(u) = \exp\left\{t\left(i\gamma^* u - \frac{1}{\nu}\ln\left(1 - iu\theta\nu + \frac{\sigma^2\nu}{2}u^2\right)\right)\right\}.$$

Finally, the risk-neutral stock price process is

$$S_t = S_0 \exp\left\{\gamma^* t + X_t^{\text{VG}}(\theta, \sigma, \nu)\right\},$$

where $X_t^{\text{VG}}$ is the Variance Gamma process characterized by the Lévy triplet $(\gamma^*, 0, \nu^{\text{VG}})$, with

$$\nu^{\text{VG}}(dx) = \begin{cases} \frac{C\exp(Gx)}{|x|}dx, & x < 0, \\ \frac{C\exp(-Mx)}{x}dx, & x > 0, \end{cases}$$

where

$$\begin{aligned} C &= \frac{1}{\nu} > 0, \\ G &= \left(\sqrt{\frac{1}{4}\theta^2\nu^2 + \frac{1}{2}\sigma^2\nu} - \frac{1}{2}\theta\nu\right)^{-1} > 0, \\ M &= \left(\sqrt{\frac{1}{4}\theta^2\nu^2 + \frac{1}{2}\sigma^2\nu} + \frac{1}{2}\theta\nu\right)^{-1} > 0. \end{aligned}$$

## 3.4 Summary

To summarize, we can see that in all models the risk-neutral stock price process can be written in the form:

$$S_t = S_0 \exp\left\{\gamma^* t + X_t\right\},$$

with the risk-neutral drift $\gamma^*$ and a Lévy process $X_t$. Moreover, the risk-neutral characteristic function is in the form:

$$\Phi_t^{\text{RN}}(u) = \exp\left\{t\left(i\gamma^* u + \Psi(u)\right)\right\},$$

where $\Psi$ is the characteristic exponent of $X_1$. Tables 3.1, 3.2, 3.3 and 3.4 illustrate respectively the drift-less Lévy process $X_t$, the risk-neutral drift $\gamma^*$, the Lévy measure $\nu(dx)$ and the characteristic exponent $\Psi(u)$ for all the models which we have just studied in this chapter.

| **Models** | **Lévy process $X_t$** | **Comments** |
|---|---|---|
| Black-Scholes | $\sigma W_t$ | |
| Merton | $\sigma W_t + \sum_{i=1}^{N_t} Y_i$ | $Y_i \sim \mathcal{N}(\alpha, \delta^2), N_t \sim \text{Poisson}(\lambda t)$ |
| Kou | $\sigma W_t + \sum_{i=1}^{N_t} Y_i$ | $Y_i \sim \text{DoubleExp}(p, \eta_1, \eta_2)$ |
| Normal Inverse Gaussian | $\beta\delta^2 T_t + \delta W_{T_t}$ | $T_t \sim \text{IG}\left(t, \delta\sqrt{\alpha^2-\beta^2}\right)$ |
| Variance Gamma | $\theta T_t + \sigma W_{T_t}$ | $T_t \sim \text{Gamma}\left(\frac{t}{\nu}, \frac{1}{\nu}\right)$ |

**Tab. 3.1:** Lévy processes $X_t$ for several models.

| **Models** | **Risk-neutral drift $\gamma^*$** |
|---|---|
| Black-Scholes | $r - q - \frac{1}{2}\sigma^2$ |
| Merton | $r - q - \frac{1}{2}\sigma^2 - \lambda\left(e^{\alpha+\frac{1}{2}\delta^2} - 1\right)$ |
| Kou | $r - q - \frac{1}{2}\sigma^2 - \lambda\left(\frac{p\cdot\eta_1}{\eta_1-1} + \frac{(1-p)\cdot\eta_2}{\eta_2+1} - 1\right)$ |
| Normal Inverse Gaussian | $r - q - \delta\left(\sqrt{\alpha^2-\beta^2} - \sqrt{\alpha^2-(\beta+1)^2}\right)$ |
| Variance Gamma | $r - q + \frac{1}{\nu}\ln\left(1 - \theta\nu - \frac{\sigma^2\nu}{2}\right)$ |

**Tab. 3.2:** Risk-neutral drifts $\gamma^*$ for several models.

| **Models** | **Lévy measure $\nu(dx)$** |
|---|---|
| Black-Scholes | $0$ |
| Merton | $\frac{\lambda}{\sqrt{2\pi\delta}} e^{-\frac{(x-\alpha)^2}{2\delta^2}} dx$ |
| Kou | $\lambda\left(p\cdot\eta_1 e^{-\eta_1 x}\mathbf{1}_{x\geq 0} + (1-p)\cdot\eta_2 e^{\eta_2 x}\mathbf{1}_{x<0}\right) dx$ |
| Normal Inverse Gaussian | $\frac{\delta\alpha}{\pi}\frac{\exp(\beta x)K_1(\alpha\lvert x\rvert)}{\lvert x\rvert} dx$ |
| Variance Gamma | $\left(\frac{C\exp(-Mx)}{x}\mathbf{1}_{x\geq 0} + \frac{C\exp(Gx)}{\lvert x\rvert}\mathbf{1}_{x<0}\right) dx$ |

**Tab. 3.3:** Lévy measure $\nu(dx)$ for several models.

| **Models** | **Characteristic exponent $\Psi(u)$** |
|---|---|
| Black-Scholes | $-\frac{1}{2}\sigma^2 u^2$ |
| Merton | $-\frac{1}{2}\sigma^2 u^2 + \lambda\left(e^{i\alpha u - \frac{1}{2}\delta^2 u^2} - 1\right)$ |
| Kou | $-\frac{1}{2}\sigma^2 u^2 + \lambda\left(\frac{p\cdot\eta_1}{\eta_1 - iu} + \frac{(1-p)\cdot\eta_2}{\eta_2+iu} - 1\right)$ |
| Normal Inverse Gaussian | $\delta\left(\sqrt{\alpha^2-\beta^2} - \sqrt{\alpha^2-(\beta+iu)^2}\right)$ |
| Variance Gamma | $-\frac{1}{\nu}\ln\left(1 - iu\theta\nu + \frac{\sigma^2\nu}{2}u^2\right)$ |

**Tab. 3.4:** Characteristic exponent $\Psi(u)$ for several models.

# 4 Numerical Methods

> *FFT is the most important numerical algorithm of our lifetime.*
>
> **— Gilbert Strang**
> (1934)

Several methods can be used to price an option under Lévy process. A method easy to implement and available for exotic options it the *Monte Carlo method*. In this method, we need to simulate a multitude of risk-neutral paths, and then discount the average value of all scenarios. However, this method is very expensive computationally, in particular for a large number of fixing dates that forces us to discretize more the paths. The section 4.1 is dedicated to this method.

A second way to price exotic options, is to derive the partial differential equation (PDE) or the partial integro differential equation (PIDE) in the case of jump processes. Then we can solve these PDE or PIDE with *Finite Difference method*, for example, to get the price of the option. This method invokes the Lévy density measure $\nu(dx)$ and could be very complex to implement. We will see that in section 4.2.

A third method, very useful since the density function is often not known in closed form, invokes the characteristic function of the Lévy process which is always in closed form for Lévy processes. Then we can use Fourier transform to price the option. Therefore, we will use in section 4.3 a method based on Fast Fourier Transform (FFT), which is called the *Convolution method*. This method is very well performing and can be efficiently computed using fast algorithms.

Finally, we will closed this chapter by summarizing the whole algorithm used to price the FX-TARN.

## 4.1 Monte Carlo Method

In this section we will briefly recall the principle of the Monte Carlo simulations and present algorithms to simulate the different processes that we have studied in the

last chapter. The idea in the Monte Carlo method is to simulate $M$ sample paths of the stock price process $\mathbf{S}_m, m = 1, \dots, M$, under the corresponding model and, for each path, compute the present value $P(\mathbf{S}_i)$ of the financial product. Then, by the law of the large numbers, we obtain the following proxy:

$$\hat{P}(\mathbf{S}) = \frac{1}{M} \sum_{m=1}^{M} P(\mathbf{S}_m) \xrightarrow{M \to \infty} P(\mathbf{S}),$$

where $\mathbf{S} = (S(t_1), \dots, S(t_N))$ is the realization of the stock price. The standard error of the estimate is given by

$$\text{SE} = \sqrt{\frac{1}{M-1} \sum_{i=1}^{M} \left( \hat{P}(\mathbf{S}) - P(\mathbf{S}_i) \right)^2}.$$

Remark that the standard error decreases with the square root of the number of sample paths $M$. By the central limit theorem, we can construct the following $95\%$ confidence interval for the real price $P(\mathbf{S})$

$$\left[ \hat{P}(\mathbf{S}) - 1.96 \frac{\text{SE}}{\sqrt{M}}, \hat{P}(\mathbf{S}) + 1.96 \frac{\text{SE}}{\sqrt{M}} \right]$$

Recall that in our case, the present value of the FX TARN is given by equation (1.3):

$$P(\mathbf{S}) = N_f \times \sum_{n=1}^{N} \frac{\hat{C}^{\text{pos}}(S(t_n), A(t_{n-1})) + \hat{C}^{\text{neg}}(S(t_n), A(t_{n-1}))}{B_d(t_0, t_n)}, \qquad A(t_0) = 0,$$

where $\hat{C}^{\text{pos}}$ and $\hat{C}^{\text{neg}}$ are respectively the gain and the loss on the $n^{\text{th}}$ fixing date given by equations (1.1) and (1.2). The variable $A(t_n)$ models the accumulated positive cash flow until the date $t_n$ and $B_d(t_0, t_n)^{-1} = e^{-r_d(t_n - t_0)}$ is the domestic discounting factor from $t_n$ to $t_0$. In the rest of the thesis, we will consider the present value per unit of notional $(N_f = 1)$.

### 4.1.1 Simulations under Black-Scholes model

We have seen that the Lévy process in the Black-Scholes model is given by

$$X_t^{\text{BS}} = \left( r - q - \frac{1}{2}\sigma^2 \right) t + \sigma W_t,$$

where $W_t$ is a Wiener process. Therefore, by discretization of time, we get

$$\Delta X_t^{\text{BS}} = \left( r - q - \frac{1}{2}\sigma^2 \right) \Delta t + \sigma \sqrt{\Delta t} Z,$$

with $Z \sim \mathcal{N}(0,1)$. Finally we easily have

$$\begin{aligned} S_{t+\Delta t} &= \exp\left\{X_t^{\text{BS}} + \left(r - q - \frac{1}{2}\sigma^2\right)\Delta t + \sigma\sqrt{\Delta t}Z\right\} \\ &= S_t \exp\left\{\left(r - q - \frac{1}{2}\sigma^2\right)\Delta t + \sigma\sqrt{\Delta t}Z\right\}. \end{aligned}$$

We can use the command `random('norm',0,1)` in MATLAB to generate a random normal variable. Figure 4.1 shows five simulated sample paths under Black-Scholes model.

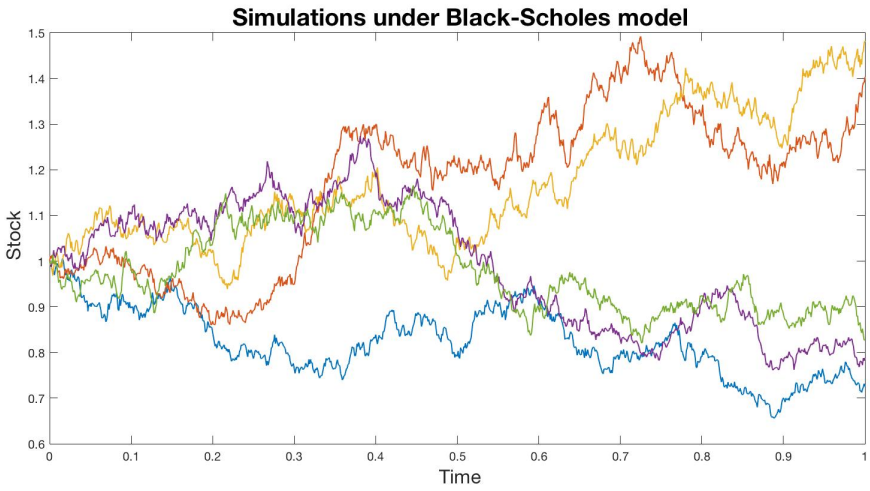


**Fig. 4.1:** Simulations of stock price process under Black-Scholes model. $S_0 = 1, r = 0.01, q = 0.02, \sigma = 0.3, T = 1, dt = 0.001, M = 5$.

### 4.1.2 Simulations under Jump-diffusion models

A jump-diffusion process is nothing else than a Brownian motion with drift to which a jump process modeled by a compound Poisson process is added. In other words, we have

$$X_t^{\text{JD}} = \gamma^* t + \sigma W_t + \sum_{i=1}^{N_t} Y_i,$$

where $N_t \sim \text{Poisson}(\lambda t)$ and the jump size $Y_i$ has density function $f_J$. We have seen the two special cases where the distribution $f_J$ is normal $\mathcal{N}(\alpha, \delta^2)$ in the Merton model and double exponential $\text{DoubleExp}(p, \eta_1, \eta_2)$ in the Kou model.

Therefore, we have that

$$\Delta X_t^{\text{JD}} = \gamma^* \Delta t + \sigma\sqrt{\Delta t}Z + J(\Delta t),$$

where $J(\Delta t)$ is the sum of all jumps between $t$ and $t + \Delta t$, i.e.

$$J(\Delta t) = \sum_{i=1}^{N_{\Delta t}} Y_i.$$

We can use the command MATLAB `random('poiss',`$\lambda\Delta t$`)` to simulate the variable $N_{\Delta t}$.

### Merton model

In his model, Merton supposed that the jump size is normally distributed with mean $\alpha$ and standard deviation $\delta$, i.e. $Y_i \sim \mathcal{N}(\alpha, \delta)$. Then, recall that the risk-neutral drift is given by

$$\gamma^* = r - q - \frac{1}{2}\sigma^2 - \lambda\left(e^{\alpha+\frac{1}{2}\delta^2} - 1\right).$$

Thus we have

$$S_{t+\Delta t} = S_t \exp\left\{\gamma^*\Delta t + \sigma\sqrt{\Delta t}Z + J(\Delta t)\right\},$$

where $J(\Delta t) \sim \mathcal{N}(N_{\Delta_t}\alpha, N_{\Delta t}\delta)$ and $N_{\Delta t} \sim$ Poisson$(\lambda\Delta t)$.

Finally, we obtain the results of five simulated sample paths in figure 4.2.

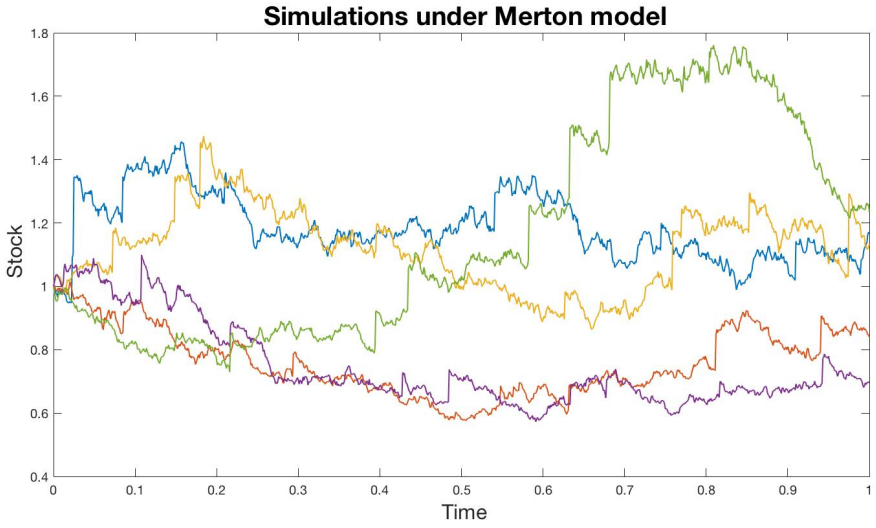


**Fig. 4.2:** Simulations of stock price process under Merton model.
$S_0 = 1, r = 0.06, q = 0.02, \lambda = 10, \alpha = 0.1, \delta = 0.05, \sigma = 0.3,$
$T = 1, dt = 0.001, M = 5.$

### Kou model

This model is very similar to the Merton's one, but Kou proposed to use a double exponential distribution for the jump size, i.e. $Y_i \sim \text{DoubleExp}(p, \eta_1, \eta_2)$. Thus the difficulty is to simulate double exponential random variables. Note that the sum of $K$ independent exponential random variables of parameter $\eta$ has a gamma distribution with parameters $K$ and $\eta$. In other words, if $X_1, \ldots, X_K \sim \text{Exp}(\eta)$, then $Y = \sum_{i=1}^{K} X_i \sim \Gamma(K, \eta)$ and

$$f_Y(y) = y^{K-1} \frac{\eta^K e^{-\eta y}}{K-1}.$$

Hence, to simulate the jumps $J(\Delta t)$, we begin by simulating a binomial random variable $K$ that counts the number of positive jumps in $[t, t+\Delta t]$,

$$K \sim \text{Binomial}(N_{\Delta t}, p), \qquad \text{with } N_{\Delta t} \sim \text{Poisson}(\lambda \Delta t).$$

Then, we simulate the positive and negative jumps

$$\begin{aligned} J^+ &\sim \text{Gamma}(K, \eta_1), \\ J^- &\sim \text{Gamma}(N_{\Delta t} - K, \eta_2). \end{aligned}$$

This reads in MATLAB as `random('gam',`$K, 1/\eta_i$`)` because of the convention of the parameters (shape/scale versus shape/rate).

Therefore the sum of jumps in the time interval $[t, t+\Delta t]$ is given by

$$J(\Delta t) = J^+ - J^-.$$

At the end, we have the same representation of the stock price as before

$$S_{t+\Delta t} = S_t \exp\left\{\gamma^* \Delta t + \sigma\sqrt{\Delta t} Z + J(\Delta t)\right\},$$

with

$$\gamma^* = r - q - \frac{1}{2}\sigma^2 - \lambda\left(\frac{p \cdot \eta_1}{\eta_1 + 1} + \frac{(1-p)\cdot \eta_2}{\eta_2 + 1} - 1\right).$$

The simulation of sample paths under Kou model are illustrated in figure 4.3

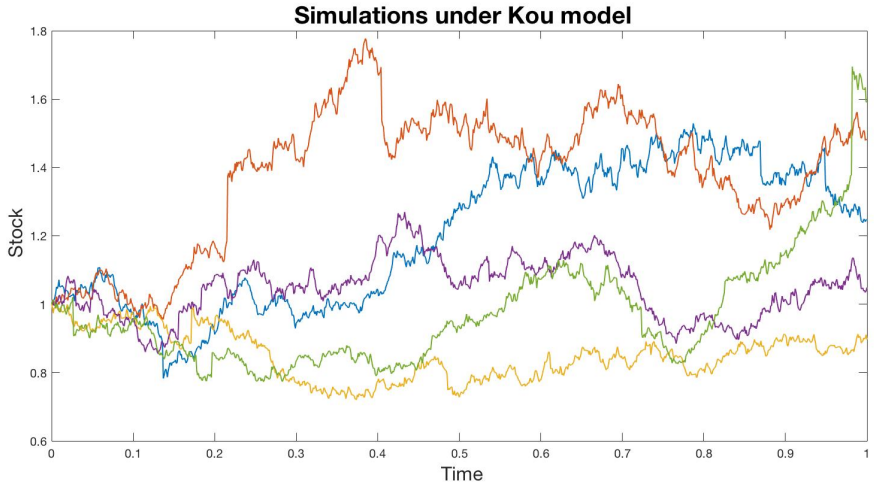


**Fig. 4.3:** Simulations of stock price process under Kou model.
$S_0 = 1, r = 0.06, q = 0.02, \lambda = 10, p = 0.55, \eta_1 = \eta_2 = 25, \sigma = 0.3,$
$T = 1, dt = 0.001, M = 5.$

### 4.1.3 Simulations under Pure jump models

Recall that a pure jump process, as Normal Inverse Gaussian (NIG) process or Variance Gamma (VG) process, can be seen as a Brownian subordination

$$X_t^{\text{PJ}} = \theta T_t + \sigma W_{T_t},$$

where $T = \{T_t, t \geq 0\}$ is a random time process, called the *subordinator*. The goal is then to simulate this subordinator and substitute it to the time of a Brownian motion with drift. In the Normal Inverse Gaussian model, this time subordinator will be an Inverse Gaussian process, and in the Variance Gamma model, it will be a Gamma process.

#### Normal Inverse Gaussian model

First of all, recall that the Lévy process in the Normal Inverse Gaussian model is given by

$$X_t^{\text{PJ}} = \beta\delta^2 T_t + \delta W_{T_t},$$

with $T_t \sim \text{IG}\left(t, \delta\sqrt{\alpha^2 - \beta^2}\right)$. Hence we have to construct a Normal Inverse Gaussian (NIG) process. To do that, we simulate an Inverse Gaussian (IG) process and set it as time parameter of the Brownian motion. In fact, we have that

$$\Delta X_t^{\text{PJ}} = \beta\delta^2 \Delta T_t + \delta\sqrt{\Delta T_t} Z,$$

where $\Delta T_t \sim \text{IG}\left(\Delta t, \delta\sqrt{\alpha^2 - \beta^2}\right)$ and $Z \sim \mathcal{N}(0, 1)$.

Finally, we have the stock price sample path

$$S_{t+\Delta t} = S_t \exp\left\{\gamma^* \Delta t + \Delta X_t^{\text{PJ}}\right\},$$

with $\gamma^* = r - q - \delta\left(\sqrt{\alpha^2 - \beta^2} - \sqrt{\alpha^2 - (\beta+1)^2}\right)$. Be careful with the convention of the MATLAB command `random('inversegaussian',`$\mu, \lambda$`)`, where $\mu = \frac{a}{b}$ is the mean and $\lambda = a^2$ is the shape parameter. We can see the result of five sample path in figure 4.4.

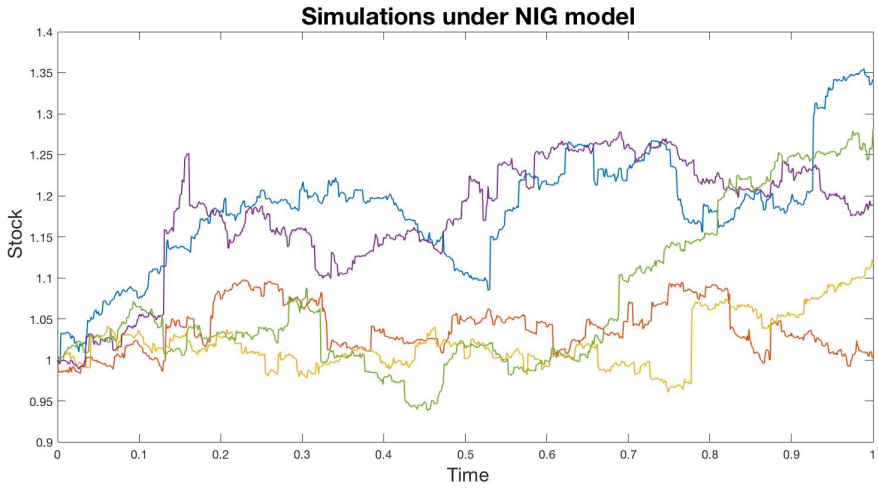


**Fig. 4.4:** Simulations of a stock price process under NIG model.
$S_0 = 1, r = 0.06, q = 0.02, \alpha = 50, \beta = 3, \delta = 1,$
$T = 1, dt = 0.001, M = 5.$

### Variance Gamma model

Following the same procedure as before, we just have to change the time subordinator process by taking a Gamma process. Then we have the time-changed Brownian motion

$$X_t^{\text{PJ}} = \theta T_t + \sigma W_{T_t},$$

with $T_t \sim \text{Gamma}\left(\frac{t}{\nu}, \frac{1}{\nu}\right)$. Therefore, we get

$$\Delta X_t^{\text{PJ}} = \theta \Delta T_t + \sigma\sqrt{\Delta T_t}\, Z,$$

where $\Delta T_t \sim \text{Gamma}\left(\frac{\Delta t}{\nu}, \frac{1}{\nu}\right)$ and $Z \sim \mathcal{N}(0,1)$. Thus we get

$$S_{t+\Delta t} = S_t \exp\left\{\gamma^* \Delta t + \Delta X_t^{\text{PJ}}\right\},$$

with $\gamma^* = r - q + \frac{1}{\nu}\ln\left(1 - \theta\nu - \frac{\sigma^2\nu}{2}\right)$. The figure 4.5 illustrates the result of five simulations under this last model.

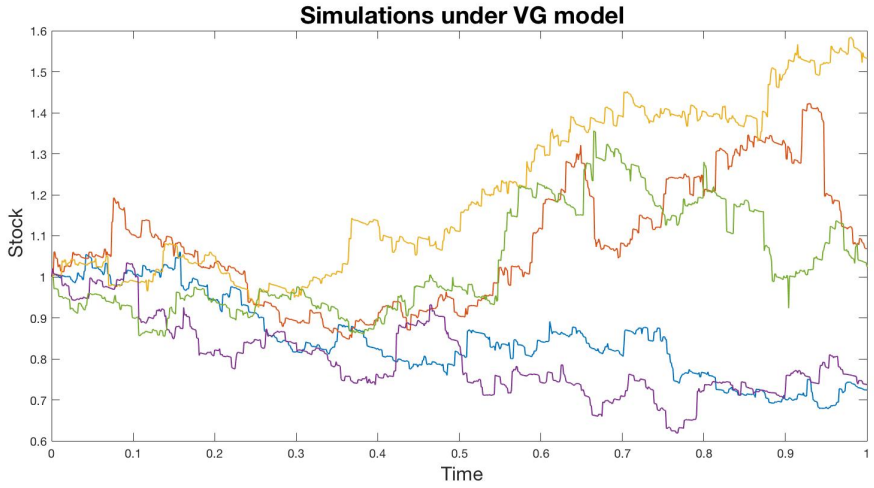


**Fig. 4.5:** Simulations of a stock price process under VG model. $S_0 = 1, r = 0.06, q = 0.02, \theta = 0.5, \sigma = 0.3, \nu = 0.01,$ $T = 1, dt = 0.001, M = 5.$

### 4.1.4 Pricing FX-TARN with Monte Carlo

Note that for the pricing of the FX TARN it suffices to take $\Delta t$ equal to the difference of two consecutive fixing dates, i.e. the length of a period (e.g. Daily/Weekly/Monthly). It is not necessary to simulate the points between these dates because the cash flows depend only on the observations on the fixing dates.

From the simulations above, and equations (1.1) and (1.2), it is easy to compute the payoff on each fixing date $t_n, (n = 1, \dots, N)$, with respect to the realization $S_{t_n}$. It is also necessary to update the variable $A(t_n)$ that takes into account the accumulated gain, and record if the target $U$ is breached.

Finally, we have for each simulated scenario $\mathbf{S}_m, (m = 1, \dots, M)$, the present value from equation (1.3)

$$P(\mathbf{S}_m) = \sum_{n=1}^{\tilde{N}} e^{-r_d(t_n - t_0)} C^{\text{tot}}(S(t_n), A(t_{n-1})),$$

where we have taken $B_d(t_0, t_n)^{-1} = e^{-r_d(t_n - t_0)}$, with $r_d$ the domestic risk-free rate. Recall that $\tilde{N}$ is the knockout index and there is no cash flow beyond $t_{\tilde{N}}$. Hence, the value of the FX-TARN obtained with the Monte-Carlo method is given by

$$\hat{P}(\mathbf{S}) = \frac{1}{M} \sum_{m=1}^{M} P(\mathbf{S}_m).$$

## 4.2 Finite Difference Method

This section is devoted to the Finite Difference (FD) method for different models. We will see how to solve numerically the PDE in the Black-Scholes model and the PIDE in the jump-diffusion and pure jump models. The central tool of Lévy processes in FD methods is the Lévy measure $\nu$ used to characterize the jumps in the integral part of the PIDE. In the case of Black-Scholes, we have seen that this measure is null.

### 4.2.1 Black-Scholes world

A Finite Difference method to price Target Accrual Redemption Note (TARN) under (generalized) Black-Scholes model was proposed by Luo and Shevchenko (2015) [LS15]. To summarize, their approach, consider the value of the FX-TARN $V(S,t,A)$, where $S$ is the spot rate and $A$ is the accumulated amount until time $t$. Since the accumulation $A$ has no effect in the diffusion between two fixing dates, the Black-Scholes option pricing PDE is still valid

$$\frac{\partial V}{\partial t} + \frac{1}{2}\sigma^2(S,t)S^2\frac{\partial^2 V}{\partial S^2} + (r_d(t) - r_f(t))\,S\frac{\partial V}{\partial S} - r_d(t)V = 0, \tag{4.1}$$

with $r_d$ and $r_f$ respectively the domestic and foreign risk free rates.

At the end of the product's life, there is no more coming cash flow. Therefore at time $T$, the value of the option is null. Hence we can consider the terminal condition to be

$$V(S,T,A) = 0, \qquad \forall S, A \in \mathbb{R}_+.$$

However, just before the last fixing date, at $T^- = t_N^-$, the value is equal to the last payment

$$\begin{aligned} &V(S,t_N^-,A) = C^{\text{pos}}(S,A) + C^{\text{neg}}(S,A) = C^{\text{tot}}(S,A), \quad \forall S \in \mathbb{R}_+, 0 \le A \le U, \\ &V(S,t_N^-,A) = 0, \qquad\qquad\qquad\qquad\qquad\qquad\qquad\quad \forall S \in \mathbb{R}_+, A \ge U, \end{aligned}$$

where $C^{\text{pos}}$ and $C^{\text{neg}}$ are respectively the positive and the negative cash flows at time $t_N$, given by equations (1.1) and (1.2), and $C^{\text{tot}}$ is the total cash flow. Note that the accumulated amount $A(t)$ is a discontinuous piecewise constant process. Moreover, this is a cadlag process. Then we have that $A(t_n^-) = A(t_{n-1})$ and $A(t_n^+) = A(t_n)$ for $n = 1, \dots, N$.

The total cash flow on the $n^{\text{th}}$ fixing date $t_n$ induces a jump in the value of the product. In other words, at $t_n^-$, the value is given by

$$\begin{aligned} V(S, t_n^-, A) &= V(S, t_n, A + \tilde{C}_n^{\text{pos}}(S, A)) + C^{\text{tot}}(S, A), \quad \forall S \in \mathbb{R}_+, 0 \leq A \leq U, \\ V(S, t_n^-, A) &= 0, \qquad\qquad\qquad\qquad\qquad\qquad\qquad\quad \forall S \in \mathbb{R}_+, A \geq U. \end{aligned} \tag{4.2}$$

In fact, the value of the product is null since after the knock out event, there is no future cash flow. Then the condition $A(t_{n-1}) \geq U$ means that the knockout event has already occurred.

Finally, we can get the today's FX-TARN price by taking $V_0 = V(S(t_0), t_0, 0)$.

### Finite difference scheme and Cubic spline interpolation

First of all, consider the time interval between two successive fixing dates $[t_n, t_{n+1}]$ on which the diffusion by Finite Difference method is done. A uniform discretization gives us the time grid $t_k = t_n + k\Delta t, k = 0, 1, \ldots, N_t$. Then a discretization in the spot price variable $S$ is given by a grid $0 < S_{\min} = S_1 < \cdots < S_M = S_{\max}$.

In order to get this final solution, the idea of Luo and Shevchenko is to introduce an auxiliary finite grid $0 = A_1 < A_2 < \cdots < A_{N_a} = U$ to track the accumulated amount, where $U$ denotes the target. Then the goal is to perform $N_a$ finite difference solutions between all fixing dates, for each value $A_j$ of accumulated amount, which corresponds to a different "scenario". Note that we do not have to care about the value of the product for $A \geq U$, because $V(S, t, A) = 0$ for $A \geq U$.

For the fixing date $t_{n+1}$, if we associate the node $A_j$ to the accumulated amount $A(t_n)$, the equation (4.2) can be written as

$$V(S_m, t_{n+1}^-, A_j) = V(S_m, t_{n+1}, A_j^+) + C^{\text{tot}}(S_m, A_j),$$

with $A_j^+ = A_j + \tilde{C}^{\text{pos}}(S_m)$, for $m = 1, \ldots, M$. This quantity is used as initial condition at the beginning of each finite difference scheme.

Since only the value $V(S_m, t_{n+1}, A_j)$ is known after a diffusion step, we evaluate $V(S_m, t_{n+1}, A_j^+)$ by cubic spline interpolation. Hence, we can extract $N_a$ values $V(S_m, t_{n+1}, A_j^+), j = 1, \ldots, N_a$, by interpolating $V(S_m, t_{n+1}, A_j)$ with respect to $A_j$. Notice that if $A_j^+ \geq U$, then $V(S_m, t_{n+1}, A_j^+) = 0$ and no interpolation is needed.

To perform the finite difference step, it is common to write equation (4.1) in terms of log asset price $x = \log(S)$ and time to maturity $\tau = T - t$. However, here we

do not consider the Finite Different scheme until the maturity $T$. Then we will use $\tau = t_{n+1} - t$ for $t \in (t_n, t_{n+1})$. This gives us the following PDE

$$\frac{\partial V}{\partial \tau} - \frac{1}{2}\sigma^2 \frac{\partial^2 V}{\partial x^2} - \left(r_d - r_f - \frac{1}{2}\sigma^2\right) \frac{\partial V}{\partial x} + r_d V = 0. \tag{4.3}$$

The advantage of this representation is that in a Black-Scholes world with constant parameters, all the coefficient are constant. Therefore the finite difference grid in $x$ is given by $\log(S_{\min}) = x_0 < x_1 < \cdots < x_M = \log(S_{\max})$.

Let us denote the option price at time $\tau_k = t_{n+1} - t_k$, and grid point $x_i$ and grid scenario $A_j$ as $V_{i,j}^k$, for $k = 0, 1, \ldots, N_t$ and $i = 0, \ldots, M$. Hence, for an uniform grid, $\Delta x_i = x_i - x_{i-1} = \Delta x$, we get the finite difference approximation with second order accuracy

$$\begin{aligned}
\frac{\partial V}{\partial x}(x_i, \tau_k, A_j) &= \mathcal{D}_{\Delta x} V_{ij}^k + \mathcal{O}(\Delta x^2), \\
\frac{\partial^2 V}{\partial x^2}(x_i, \tau_n, A_j) &= \mathcal{D}_{\Delta x}^2 V_{ij}^k + \mathcal{O}(\Delta x^2),
\end{aligned}$$

where

$$\begin{aligned}
\mathcal{D}_{\Delta x} V_{ij}^k &= \frac{V_{i+1,j}^k - V_{i-1,j}^k}{2\Delta x}, \\
\mathcal{D}_{\Delta x}^2 V_{ij}^k &= \frac{V_{i+1,j}^k - 2V_{ij}^k + V_{i-1,j}^k}{\Delta x^2}.
\end{aligned}$$

Then with the finite difference operator $F_{ij}^k$ defined as

$$F_{ij}^k \equiv -\frac{1}{2}\sigma^2 \mathcal{D}_{\Delta x}^2 V_{ij}^k - \left(r_d - r_f - \frac{1}{2}\sigma^2\right) \mathcal{D}_{\Delta x} V_{ij}^k + r_d V_{ij}^k,$$

the $\theta$-scheme can be expressed as

$$\frac{V_{ij}^{k+1} - V_{ij}^k}{\Delta t} + \theta F_{ij}^{k+1} + (1-\theta) F_{ij}^k = 0, \qquad \begin{cases} j = 1, \ldots, N_a, \\ i = 1, \ldots, M-1 \\ k = 0, \ldots, N_t - 1 \end{cases}$$

with $\theta \in [0, 1]$. The special cases $\theta = 0, \theta = 0.5$ and $\theta = 1$ correspond respectively to the fully explicit, Crank-Nicholson and fully implicit scheme.

### Boundary Conditions

Recall that the fixing dates in time to maturity notation can be written as

$$\begin{aligned}\tau_0 &= T - t_N = 0,\\ \tau_1 &= T - t_{N-1},\\ &\vdots\\ \tau_N &= T - t_0 = T.\end{aligned}$$

First of all, we explain the boundary conditions for an FX-TARN Accumulator, where the positive payoff on fixing date $\tau_n$ is given by

$$\tilde{C}^{\text{pos}}(S, \tau_n) = \text{Call}(S, \tau_n, K),$$

and the negative payoff by

$$\tilde{C}^{\text{neg}}(S, \tau_n) = -g \cdot \text{Put}(S, \tau_n, K).$$

Therefore, if the product is still alive ($A < U$), the positive and negative cash flows $C^{\text{pos}}$ and $C^{\text{neg}}$ are piecewise linear functions in $S$.

Then, note that for $\tau \in (\tau_0, \tau_1)$ the value of the product depends only on the last total cash flow $C^{\text{tot}}(S(\tau_0), A)$, at maturity $\tau_0$. This total cash flow can be as usual decomposed as

$$C^{\text{tot}}(S(\tau_0), A) = C^{\text{pos}}(S(\tau_0), A) + C^{\text{neg}}(S(\tau_0), A).$$

Recall that the famous Black-Scholes formula for the European option price allows us to use the fact that

$$\begin{aligned}\lim_{x\to\infty} \text{Call}(x, \tau, K) &= e^{x - r_f\tau} - Ke^{-r_d\tau},\\ \lim_{x\to-\infty} \text{Call}(x, \tau, K) &= 0,\\ \lim_{x\to\infty} \text{Put}(x, \tau, K) &= 0,\\ \lim_{x\to-\infty} \text{Put}(x, \tau, K) &= Ke^{-r_d\tau} - e^{x - r_f\tau}.\end{aligned}$$

Thus, if we choose $x_{\max}$ big enough and $x_{\min}$ small enough, we get the Dirichlet boundary conditions for European options

$$\begin{aligned}
\text{Call}(x_{\max}, \tau, K) &= \left(e^{x_{\max}+(r_d-r_f)\tau} - K\right) e^{-r_d\tau} \\
&\equiv \tilde{C}^{\text{pos}}(e^{x_{\max}+(r_d-r_f)\tau}, \tau)e^{-r_d\tau}, \\
\text{Put}(x_{\min}, \tau, K) &= \left(K - e^{x_{\min}+(r_d-r_f)\tau}\right) e^{-r_d\tau} \\
&\equiv -\frac{1}{g}\tilde{C}^{\text{neg}}(e^{x_{\min}+(r_d-r_f)\tau}, \tau)e^{-r_d\tau}.
\end{aligned}$$

Since $e^{x_{\max}+(r_d-r_f)\tau} - K > 0$ and $e^{x_{\min}+(r_d-r_f)\tau} - K < 0$, we have necessarily a positive expected cash flow in $x_{\max}$ and a negative expected cash flow in $x_{\min}$. Thus, it is reasonable to set the boundary conditions for $V$ as

$$\begin{aligned}
V(x_{\max}, \tau, A) &= C^{\text{pos}}\left(e^{x_{\max}+(r_d-r_f)\tau}, A\right) e^{-r_d\tau}, \\
V(x_{\min}, \tau, A) &= C^{\text{neg}}\left(e^{x_{\min}+(r_d-r_f)\tau}, A\right) e^{-r_d\tau}.
\end{aligned}$$

The case where $\tau \in (\tau_n, \tau_{n+1})$ requires more attention. In fact, with a good choice of $x_{\max}$, we have that $e^{x_{\max}+(r_d-r_f)(\tau-\tau_n)} - K \geq U$ and this leads to a knockout on the following fixing date. Therefore, we have

$$\begin{aligned}
V(x_{\max}, \tau_{n+1}^-, A) &= V(x_{\max}, \tau_{n+1}, A^+) + C^{\text{pos}}\left(e^{x_{\max}}, \tau_{n+1}\right) \\
&= C^{\text{pos}}(e^{x_{\max}}, \tau_{n+1}),
\end{aligned}$$

and a reasonable boundary condition at $\tau \in (\tau_n, \tau_{n+1})$ is

$$V(x_{\max}, \tau, A) = C^{\text{pos}}\left(e^{x+(r_d-r_f)(\tau-\tau_n)}, A\right) e^{-r_d(\tau-\tau_n)},$$

where the discounting is done only until the next fixing date $\tau_n$. On the other side, we have that $e^{x_{\min}+(r_d-r_f)\tau} - K < 0$ and negative cash flows do not affect the accumulated gain. Then, we have to take in account all the future expected negative cash flows to determine the boundary condition in $x_{\min}$. Thus,

$$\begin{aligned}
V(x_{\min}, \tau_{n+1}^-, A) &= V(x_{\min}, \tau_{n+1}, A^+) + C^{\text{neg}}\left(e^{x_{\min}}, A\right) \\
&= V(x_{\min}, \tau_{n+1}, A) + C^{\text{neg}}\left(e^{x_{\min}}, A\right),
\end{aligned}$$

and a reasonable boundary condition at any $\tau \in (\tau_n, \tau_{n+1})$ is

$$V(x_{\min}, \tau, A) = \sum_{j=0}^{n} C^{\text{neg}}\left(e^{x_{\min}+(r_d-r_f)(\tau-\tau_j)}\right) e^{-r_d(\tau-\tau_j)},$$

where each cash flow is discounted to its respective fixing date.

The case of the FX-TARN Decumulator is the same by inverting the roles of $x_{\min}$ and $x_{\max}$ with payoff functions

$$\tilde{C}^{\text{pos}}(S,\tau_n) = \text{Put}(S,\tau_n,K), \tilde{C}^{\text{neg}}(S,\tau_n) = -g\cdot\text{Call}(S,\tau_n,K),$$

Hence, we can generalize the Dirichlet boundary conditions with the equations

$$\begin{aligned} V(x_{\max},\tau,A) = {} & C^{\text{pos}}\left(e^{x_{\max}+(r_d-r_f)(\tau-\tau_n)},A\right)e^{-r_d(\tau-\tau_n)} \\ & + \sum_{j=0}^{n} C^{\text{neg}}\left(e^{x_{\max}+(r_d-r_f)(\tau-\tau_j)},A\right)e^{-r_d(\tau-\tau_j)}, \end{aligned}$$

and

$$\begin{aligned} V(x_{\min},\tau,A) = {} & C^{\text{pos}}\left(e^{x_{\min}+(r_d-r_f)(\tau-\tau_n)},A\right)e^{-r_d(\tau-\tau_n)} \\ & + \sum_{j=0}^{n} C^{\text{neg}}\left(e^{x_{\min}+(r_d-r_f)(\tau-\tau_j)},A\right)e^{-r_d(\tau-\tau_j)}, \end{aligned}$$

for $\tau_n, n = 0,1,\ldots,N$.

### 4.2.2 Jump-diffusion models

To go beyond the Black-Scholes world, we can generalize this method to the jump-diffusion models. As proposed by Cont and Voltchkova (2005) [CV05], we can solve numerically the Partial Integro Differential equation (PIDE) evolving under Lévy processes. The PIDE is given by

$$\begin{aligned} & \frac{\partial V}{\partial\tau}(x,\tau,A) - \frac{1}{2}\sigma^2\frac{\partial^2 V}{\partial x^2}(x,\tau,A) - \left(r_d - r_f - \frac{1}{2}\sigma^2\right)\frac{\partial V}{\partial x}(x,\tau,A) + r_d V(x,\tau,A) \\ & \quad - \int_{-\infty}^{\infty}\left[V(x+y,\tau,A) - V(x,\tau,A) - (e^y-1)\frac{\partial V}{\partial x}(x,\tau,A)\right]\nu(dy) = 0, \end{aligned}$$

where $\nu(\cdot)$ is the Lévy measure of the process $X = \{X_t, t\geq 0\}$ that characterizes the log asset price. Recall that in the Merton and Kou models, the Lévy density is, respectively, given by

$$\begin{aligned} \nu^{\text{Mer}}(dy) &= \frac{\lambda}{\sqrt{2\pi}\delta}e^{-\frac{(y-\alpha)^2}{2\delta^2}}dy, \\ \nu^{\text{Kou}}(dy) &= \lambda\left(p\cdot\eta_1 e^{-\eta_1 y}\mathbf{1}_{y\geq 0} + (1-p)\cdot\eta_2 e^{\eta_2 y}\mathbf{1}_{y<0}\right)dy. \end{aligned}$$

Therefore, some integral terms can be analytically computed as

$$\begin{aligned}
\int_{-\infty}^{\infty} \nu^*(dy) &= \lambda, \qquad \text{with } \nu^* = \nu^{\text{Mer}} \text{ or } \nu^{\text{Kou}}, \\
\int_{-\infty}^{\infty} (e^y - 1)\nu^{\text{Mer}}(dy) &= \lambda \left( e^{\alpha + \frac{1}{2}\delta^2} - 1 \right) \equiv c, \\
\int_{-\infty}^{\infty} (e^y - 1)\nu^{\text{Kou}}(dy) &= \lambda \left( \frac{p\eta_1}{\eta_1 - 1} + \frac{(1-p)\eta_2}{\eta_2 + 1} - 1 \right) \equiv c.
\end{aligned}$$

Hence, we can rewrite the PIDE in the form

$$\begin{aligned}
\frac{\partial V}{\partial \tau}(x,\tau,A) - \frac{1}{2}\sigma^2 \frac{\partial^2 V}{\partial x^2}(x,\tau,A) - \left( r_d - r_f - \frac{1}{2}\sigma^2 - c \right) \frac{\partial V}{\partial x}(x,\tau,A) + (r_d + \lambda) V(x,\tau,A) \\
- \int_{-\infty}^{\infty} V(x+y,\tau,A)\nu(dy) = 0,
\end{aligned}$$

Note that in the log asset price form, the last integral term $\int_{-\infty}^{\infty} V(x+y,\tau,A)\nu(dy)$ has a convolution structure that allows us to compute it by Fast Fourier Transform (FFT). This is not the case in the asset price PIDE.

### Localization to a bounded domain

To solve this numerical problem, we first truncate the space domain to a bounded interval $x \in (x_{\min}, x_{\max})$ as usually. The boundary conditions are the same as in the Black-Scholes case. Hence the truncated Cauchy problem reads

$$\begin{cases}
\dfrac{\partial V}{\partial \tau} - \dfrac{1}{2}\sigma^2 \dfrac{\partial^2 V}{\partial x^2} - \left( r_d - r_f - \dfrac{1}{2}\sigma^2 - c \right) \dfrac{\partial V}{\partial x} + (r_d + \lambda) V \\
\qquad\qquad - \displaystyle\int_{-\infty}^{\infty} V(x+y,\tau,A)\nu(dy) = 0, & x \in (x_{\min}, x_{\max}), \\
V(x,\tau,A) = \Psi(x,\tau,A), & x \notin (x_{\min}, x_{\max}),
\end{cases}$$

where

$$\begin{aligned}
\Psi(x,\tau,A) = & C^{\text{pos}} \left( e^{x + (r_d - r_f)(\tau - \tau_n)}, A \right) e^{-r_d(\tau - \tau_n)} \\
& + \sum_{j=0}^{n} C^{\text{neg}} \left( e^{x + (r_d - r_f)(\tau - \tau_j)}, A \right) e^{-r_d(\tau - \tau_j)}.
\end{aligned}$$

Note that since the extended function $\Psi$ is linear, we can show that the integral term is zero. Thus, $V(x,\tau,A)$ evaluated on the extended grid is always a solution of the PIDE, because $\Psi$ is nothing else than the boundary conditions extended beyond $x_{\min}$ and $x_{\max}$.

Observe that the integral term $\int_{-\infty}^{\infty} V(x+y,\tau,A)\nu(dy)$ still involves the values of $V(x,t,A)$ outside of the truncated domain. Hence the boundary conditions have to be imposed for all $x \notin (x_{\min}, x_{\max})$ and not only at the two boundary points $x_{\min}$ and $x_{\max}$.

### Truncation of the integral

For computational purposes, we need to truncate the integral term,

$$J = \int_{-\infty}^{\infty} V(x+y,\tau,A)\nu(dy),$$

as

$$J_{B_l,B_r} = \int_{-B_l}^{B_r} V(x+y,\tau,A)\nu(dy).$$

In practice, it is more convenient to use a variable truncation on

$$[-(x-x_{\min})-B_l, (x_{\max}-x)+B_r] \supset [-B_l, B_r].$$

Therefore, we get

$$J \approx \int_{-(x-x_{\min})-B_l}^{(x_{\max}-x)+B_r} V(x+y,\tau,A)\nu(dy).$$

If the Lévy measure $\nu$ has density $\nu(dy) = k(y)dy$, which is the case in Merton or Kou model, we have

$$J \approx \int_{x_{\min}-B_l}^{x_{\max}+B_r} V(z,\tau,A)k(z-x)dz.$$

Hence, the fully truncated problem can be written as

$$\begin{cases} \dfrac{\partial V}{\partial \tau} - \dfrac{1}{2}\sigma^2\dfrac{\partial^2 V}{\partial x^2} - \left(r_d - r_f - \dfrac{1}{2}\sigma^2 - c\right)\dfrac{\partial V}{\partial x} + (r_d+\lambda)V \\ \qquad\qquad - \displaystyle\int_{x_{\min}-B_l}^{x_{\max}+B_r} V(z,\tau,A)k(z-x)dz = 0, \qquad x \in (x_{\min}, x_{\max}), \\ V(x,\tau,A) = \Psi(x,\tau,A), \qquad\qquad x \in [x_{\min}-B_l, x_{\min}] \cup [x_{\max}, x_{\max}+B_r]. \end{cases}$$

### Finite difference approximation

The major change from the simple case of a PDE is to extend the spatial grid to be able to compute the integral part outer of the original grid. In other words, consider the following original and extended spatial grid

$$\begin{aligned} x_i &= x_{\min} + i\Delta x, \qquad \text{for } i \in I = \{1, M-1\}, \\ x_i &= x_{\min} + i\Delta x, \qquad \text{for } i \in \tilde{I} = \{-K_l, \ldots, M + K_r\}. \end{aligned}$$

One way to compute the integral term is to use the trapezoidal rule using the extended computational grid $j \in \tilde{I}$. This means that for a continuous function $f : \mathbb{R} \to \mathbb{R}$ and an internal grid point $x_i$, denoting $k_i = k(x_i)$, we have

$$\int_{x_{\min}-B_l}^{x_{\max}+B_r} f(z)k(z - x_i) \approx \sum_{l=-K_l}^{M+K_r} \Delta x f(x_l) k(\underbrace{x_l - x_i}_{x_{l-i}}) = \sum_{l=-K_l}^{M+K_r} \Delta x f(x_l) k_{l-i}.$$

Hence our integral can be approximated by

$$\int_{x_{\min}-B_l}^{x_{\max}+B_r} V(z, \tau_n, A_j)k(z - x)dz \approx \Delta x \sum_{l=-K_l}^{M+K_r} V_l^n k_{l-i}.$$

This development brings us to the *Forward Euler* finite difference approximation

$$\begin{cases} \dfrac{V_i^{k+1} - V_i^k}{\Delta t} - \dfrac{1}{2}\sigma^2 \dfrac{V_{i+1}^k - 2V_i^k + V_{i-1}^k}{\Delta x^2} - \left(r_d - r_f - \dfrac{1}{2}\sigma^2 - c\right) \dfrac{V_{i+1}^k - V_{i-1}^k}{2\Delta x} \\ \qquad\qquad +(r_d + \lambda)V_i^k - \Delta x \displaystyle\sum_{l=-K_l}^{M+K_r} V_l^k k_{l-i} = 0, \qquad i \in I, \\ V_i^k = \Psi(x_i, \tau_k, A), \qquad\qquad i \in \tilde{I} \backslash I, \end{cases}$$

where we have suppressed the subindex $j$ for notational convenience.

With the following vectorial notation

$$\begin{aligned} \mathbf{V}^k &= \{V_i^k, i \in I\}\text{: vector of unknowns on internal nodes,} \\ \tilde{\mathbf{V}}^k &= \{V_i^k, i \in \tilde{I}\}\text{: vector of nodal values on the extended grid,} \end{aligned}$$

we can write the Forward Euler finite difference in the algebraic form as

$$\begin{cases} \dfrac{\mathbf{V}^{k+1} - \mathbf{V}^k}{\Delta t} + A\mathbf{V}^k - J\tilde{\mathbf{V}}^k = \mathbf{F}^k, \quad k = 0, \ldots, N_t - 1, \\ \tilde{\mathbf{V}}_I^{k+1} = \mathbf{V}^{k+1}, \qquad \tilde{\mathbf{V}}_{\tilde{I}\backslash I}^{k+1} = \boldsymbol{\Psi}_{\tilde{I}\backslash I}^{k+1}, \quad k = 0, \ldots, N_t - 1, \end{cases}$$

with the matrix $A \in \mathbb{R}^{(M-1)\times(M-1)}$ and right hand side vector $\mathbf{F}^n \in \mathbb{R}^{M-1}$

$$A = \begin{bmatrix} \alpha & \gamma & & \\ \delta & \alpha & \gamma & \\ & \delta & \ddots & \ddots \\ & & \ddots & \end{bmatrix} \qquad \text{with} \begin{cases} \alpha = \frac{\sigma^2}{\Delta x^2} + r_d + \lambda, \\ \gamma = -\frac{\sigma^2}{2\Delta x^2} - \frac{1}{2\Delta x}\left(r_d - r_f - \frac{\sigma^2}{2} - c\right), \\ \delta = -\frac{\sigma^2}{2\Delta x^2} + \frac{1}{2\Delta x}\left(r_d - r_f - \frac{\sigma^2}{2} - c\right), \end{cases}$$

and

$$\mathbf{F}^k = \begin{bmatrix} -\delta\Psi(x_0, \tau_n) \\ 0 \\ \vdots \\ 0 \\ -\gamma\Psi(x_M, \tau_n) \end{bmatrix}.$$

The matrix $J = \{J_{il}\} = \{k_{l-i}\}$ is a rectangular, Toepliz matrix, $J \in \mathbb{R}^{(M-1)\times(\tilde{M}+1)}$, with $\tilde{M} = M + K_l + K_r$ the number of intervals in the extended grid.

$$J = \Delta x \begin{bmatrix} k_{-K_l-1} & k_{-K_l} & \cdots & \cdots & \cdots & \cdots & k_{M+K_r-1} \\ k_{-K_l-2} & k_{-K_l-1} & k_{-K_l} & \cdots & \cdots & \cdots & k_{M+K_r-2} \\ \vdots & \ddots & \ddots & \ddots & \ddots & \ddots & \vdots \\ k_{-K_l-M+1} & \cdots & \cdots & k_{-K_l-1} & k_{-K_l} & \cdots & k_{K_r+1} \end{bmatrix}.$$

Finally it is common to use an Explicit-Implicit scheme to reduce instability. The idea is to treat implicitly the convection-diffusion term and explicitly the integral term.

$$\begin{cases} \dfrac{\mathbf{V}^{k+1} - \mathbf{V}^k}{\Delta t} + A\mathbf{V}^{k+1} - J\tilde{\mathbf{V}}^k = \mathbf{F}^k, & k = 0, \dots, N_t - 1, \\ \tilde{\mathbf{V}}_I^{k+1} = \mathbf{V}^{k+1}, \qquad \tilde{\mathbf{V}}_{\tilde{I}\setminus I}^{k+1} = \mathbf{\Psi}_{\tilde{I}\setminus I}^{k+1}, & k = 0, \dots, N_t - 1, \end{cases}$$

At each iteration of this explicit-implicit scheme, we have to compute the integral term $\mathbf{F}_J^k = J\tilde{\mathbf{V}}^n$, in $\mathcal{O}(M \times \tilde{M})$ operations, and then solve the tridiagonal linear system

$$(I + \Delta t A)\mathbf{U}^{k+1} = \mathbf{U}^k + \Delta t\left(\mathbf{F}_J^k + \mathbf{F}^{k+1}\right),$$

in $\mathcal{O}(M)$ operations. However we can reduce the total number of operations to $\mathcal{O}(M\log(M))$ by computing the integral term by FFT.

### Computation of the integral term by FFT

The idea is to enlarge the matrix $J$ to make it circulant. Let us first define a circulant matrix. Consider an arbitrary vector $\alpha = (\alpha_1, \ldots, \alpha_N) \in \mathbb{R}^N$. Then a circulant matrix $J_c(\alpha)$ is

$$J_c(\alpha) = \begin{bmatrix} \alpha_1 & \cdots & \alpha_{N-1} & \alpha_N \\ \alpha_N & \alpha_1 & \cdots & \alpha_{N-1} \\ \vdots & \ddots & \ddots & \vdots \\ \alpha_2 & \cdots & \alpha_N & \alpha_1 \end{bmatrix}.$$

Then the matrix vector product $w = J_c(\alpha)v$ can be computed in $\mathcal{O}(N \log(N))$ operations using the following algorithm

$$\begin{aligned} \hat{\alpha} &= \text{fft}(\alpha), \\ \hat{v} &= \text{fft}(v), \\ \hat{w} &= \text{conj}(\hat{\alpha}) . * \hat{v}, \\ w &= \text{ifft}(\hat{w}). \end{aligned}$$

In our case, let $M_T = 2M + K_l + K_r - 1$ and define the vector

$$\mathbf{k} = (k_{-K_l-M+1}, \ldots, k_{-1}, k_0, k_1, \ldots, k_{M+K_r-1}) \in \mathbb{R}^{M_T},$$

and the circulant matrix $J_c(\mathbf{k}) \in \mathbb{R}^{M_T \times M_T}$.

Moreover, given $\tilde{\mathbf{V}}^k \in \tilde{\mathbb{M}}$, extend it by zero as

$$\tilde{\mathbf{V}}^k_{\text{ext}} = (\underbrace{0, \ldots, 0}_{M-2}, \tilde{\mathbf{U}}^k) \in \mathbb{R}^{M_T}.$$

At the end, we have that

$$J\tilde{\mathbf{V}}^k = \left( J_c(\mathbf{k}) \tilde{\mathbf{V}}^k_{\text{ext}} \right)_{1:M-1},$$

and we have computed the integral term in $\mathcal{O}(M_T \log(M_T))$.

**Fixed point iterations for implicit scheme**

In order to avoid all stability constrains, we have to solve the numerical problem with an implicit scheme. However, the resolution of the linear system of equations, which can be written as

$$B\mathbf{V}^{k+1} = \tilde{\mathbf{F}}^{k+1},$$

is very expensive ($\mathcal{O}(M^3)$) by $\mathcal{LU}$ factorization.

Then a possible remedy is to use fixed-point iterations. In other words, at time step $\tau_{k+1}$, denote $\mathbf{V}_{(j)}^{k+1}$ the $j$-th fixed point iteration and compute $\mathbf{V}_{(j+1)}^{k+1}$ as

$$(I + \Delta t A)\mathbf{V}_{(j+1)}^{k+1} = -\Delta t J \tilde{\mathbf{V}}_{(j)}^{k+1} + \mathbf{V}^k + \Delta t \mathbf{F}^{k+1}.$$

The fixed point iterations can be started from $\mathbf{V}_{(0)}^{k+1} = \mathbf{V}^k$ and stopped as soon as $\| \mathbf{V}_{(j+1)}^{k+1} - \mathbf{V}_{(j)}^{k+1} \| < tol$ for a prescribed tolerance.

Therefore, at each iteration, we have to solve a tridiagonal system, which costs $\mathcal{O}(M)$, and compute $J\tilde{\mathbf{V}}_{(j)}^{k+1}$, which costs $\mathcal{O}(M_T \log(M_T))$ if we use FFT. At the end, if the FX-TARN is composed of $N$ fixing dates, the total computational cost of the FD method is $\mathcal{O}(N N_a M_T \log(M_T))$, where $N_a$ is the number of grid points in the accumulated variable $A$ discretization.

### 4.2.3 Pure jump models

In the case of pure jump models, the Lévy measure has the property that $\nu(\mathbb{R}) = \infty$, which means that the process has infinite activity, i.e. there are infinitely many small jumps. In other words, the Lévy density $\nu(dy) = k(y)dy$ explodes at the origin, as we can see on the Figure 4.6. Unfortunately, it does not allow us to apply the preceding procedure by splitting the integral term in three parts

$$\int_{-\infty}^{\infty} \left[ V(x+y,\tau,A) - V(x,\tau,A) - (e^y - 1)\frac{\partial V}{\partial x}(x,\tau,A) \right] \nu(dy) =$$
$$\int_{-\infty}^{\infty} V(x+y,\tau,A)k(y)dy - \int_{-\infty}^{\infty} V(x,\tau,A)k(y)dy - \int_{-\infty}^{\infty} (e^y - 1)\frac{\partial V}{\partial x}(x,\tau,A)k(y)dy,$$

as each of them is unbounded.

The idea is thus to come down to a non-singular case by approximating the process $X = \{X_t, t \geq 0\}$, by an appropriate finite activity process $X^\epsilon = \{X_t^\epsilon, t \geq 0\}$.

Cont and Voltchkova propose a possible strategy consisting in cutting out the small jumps, i.e. the singular part of $k(y)$ and approximating them with a Wiener process. Let us now define the truncated density

$$k_\epsilon(y) = \begin{cases} k(y), & \text{for } |y| \geq \epsilon \\ \frac{k(\epsilon)-k(-\epsilon)}{2\epsilon} y + \frac{k(\epsilon)+k(-\epsilon)}{2}, & |y| < \epsilon, \end{cases}$$

so that $k_\epsilon(y)$ corresponds to a finite activity Lévy process with intensity $\lambda(\epsilon) = \int k_\epsilon(y)dy < \infty$. This truncated density is illustrated on the Figure 4.6.

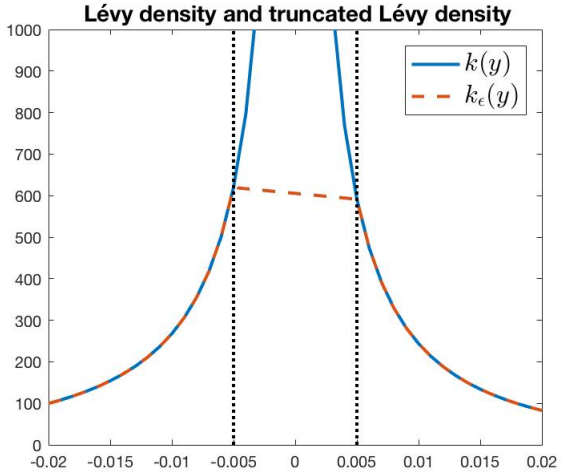


**Fig. 4.6:** Pure jump Lévy density (in blue) and its truncated density (in red) with $\epsilon = 0.005$.

We set now $\tilde{k}(y) = k(y) - k_\epsilon(y)$, which is non zero only for $|y| \leq \epsilon$, and split the integral terms as

$$\int_{-\infty}^{\infty} \left[ V(x+y,\tau,A) - V(x,\tau,A) - (e^y - 1)\frac{\partial V}{\partial x}(x,\tau,A) \right] k(y)dy = I_1 + I_2,$$

with

$$I_1 = \int_{-\infty}^{\infty} \left[ V(x+y,\tau,A) - V(x,\tau,A) - (e^y - 1)\frac{\partial V}{\partial x}(x,\tau,A) \right] k_\epsilon(y)dy$$
$$I_2 = \int_{-\epsilon}^{\epsilon} \left[ V(x+y,\tau,A) - V(x,\tau,A) - (e^y - 1)\frac{\partial V}{\partial x}(x,\tau,A) \right] \tilde{k}(y)dy.$$

The first term corresponds to the finite activity Lévy process $X^\epsilon$ and can be treated as the previous case.

The second integral requires a bit more work. By summing and subtracting the term $y\frac{\partial V}{\partial x}$, we have

$$I_2 = \int_{-\epsilon}^{\epsilon} \Bigg[ \underbrace{V(x+y,\tau,A) - V(x,\tau,A) - y\frac{\partial V}{\partial x}(x,\tau,A)}_{\frac{y^2}{2}\frac{\partial^2 V}{\partial x^2}+\mathcal{O}(y^3)} - \underbrace{(e^y - 1 - y)}_{\frac{y^2}{2}+\mathcal{O}(y^3)} \frac{\partial V}{\partial x}(x,\tau,A) \Bigg] \tilde{k}(y)dy$$
$$= \left(\frac{\partial^2 V}{\partial x^2} - \frac{\partial V}{\partial x}\right)\frac{\sigma^2(\epsilon)}{2} + \int_{-\epsilon}^{\epsilon} \mathcal{O}(y^3)\tilde{k}(y)dy,$$

with

$$\sigma^2(\epsilon) = \int_{-\epsilon}^{\epsilon} y^2 \tilde{k}(y)dy.$$

Therefore, we can treat the infinite activity case with a finite activity process $X^\epsilon$ characterized by the Lévy triplet $(\gamma^*, \sigma(\epsilon), k_\epsilon(y))$. Hence, up to $\mathcal{O}(\epsilon^3)$ terms, the option price $V(x,t,A)$ satisfies the modified PIDE

$$\frac{\partial V}{\partial \tau}(x,\tau,A) - \frac{1}{2}\sigma^2(\epsilon)\frac{\partial^2 V}{\partial x^2}(x,\tau,A) - \left(r_d - r_f - \frac{1}{2}\sigma^2(\epsilon) - c(\epsilon)\right)\frac{\partial V}{\partial x} +$$
$$(r_d + \lambda(\epsilon))V(x,\tau,A) - \int_{-\infty}^{\infty} V(x+y,\tau,A)k_\epsilon(y)dy = 0,$$

with

$$\lambda(\epsilon) \equiv \int_{-\infty}^{\infty} k_\epsilon(y)dy,$$
$$c(\epsilon) \equiv \int_{-\infty}^{\infty} \left(y^2 - 1\right) k_\epsilon(y)dy,$$
$$\sigma^2(\epsilon) \equiv \int_{-\infty}^{\infty} y^2 k_\epsilon(y)dy.$$

For more details about the consistency, stability and convergence of finite difference schemes for exponential Lévy models, see [CV05].

## 4.3 The Convolution Method

The idea of this method is to replace the finite difference scheme by the convolution method proposed by Lord et al. (2008) [Lor+08], based on the *Fast Fourier Transform* (FFT). The main advantage of this method is that we don't need to discretize time between fixing dates. Thus, the total computational cost of the method is reduced to $\mathcal{O}(N_{\text{fix-dates}} N_a M \log(M))$, where $M$ and $N_a$ are respectively the number of grid

points used to discretize the stock price $S$ and the accumulated amount variable $A$.

### 4.3.1 Description of the method

Consider $V(S(t_n), t_n, A)$ the value of our FX-TARN at the $n^{\text{th}}$ fixing date. Therefore, we can write, under risk-neutral measure $\mathbb{Q}$,

$$\begin{aligned} V(S(t_n), t_n, A) &= \mathbb{E}^{\mathbb{Q}}\left[e^{-r_d \Delta t} V(S(t_{n+1}), t_{n+1}, A | S(t_n)\right] \\ &= e^{-r_d \Delta t} \int_{-\infty}^{\infty} V(y, t_{n+1}, A) f(y|S(t_n)) dy, \end{aligned}$$

where $f(y|S(t_n))$ represents the transition density from $S(t_n)$ at $t_n$ to $y$ at $t_{n+1}$, and $\Delta t$ is the period between two consecutive fixing dates. Since we use exponential Lévy processes to characterize the stock price $S(t_n) = e^{X(t_n)}$, the stock price process has independent increments and we can write

$$f(y|x) = f(y - x),$$

where $x = \log(S(t_n))$ and $y = \log(S(t_{n+1}))$.

By changing variables $z = y - x$, the value $V$ can be expressed as

$$V(x, t_n, A) = e^{-r_d \Delta_t} \int_{-\infty}^{\infty} V(x + z, t_{n+1}^-, A) f(z) dz, \tag{4.4}$$

which is a cross-correlation of the option value at time $t_{n+1}^-$ and the density $f(z)$. We can equivalently see this as a convolution of $V(\cdot, t_{n+1}^-, A)$ and the conjugate of $f(z)$.

Let us now define the Fourier transform.

**Definition 4.1 (*Fourier Transform*)**

*Given $h \in L^1(\mathbb{R})$, i.e. $h$ is an integrable function, we denote by $\hat{h}$ the* ***Fourier transform*** *of $h$, defined by*

$$\hat{h}(u) := \mathcal{F}\{h(t)\}(u) = \int_{-\infty}^{\infty} e^{iut} h(t) dt.$$

*Moreover, if $\hat{h} \in L^1(\mathbb{R})$, the* ***inverse Fourier transform*** *is given by*

$$h(t) := \mathcal{F}^{-1}\{\hat{h}(u)\}(t) = \frac{1}{2\pi} \int_{-\infty}^{\infty} e^{-iut} \hat{h}(u) du.$$

Note that if $f$ is the density function of the Lévy process, the Fourier transform of $f$ corresponds exactly to the characteristic function $\Phi$ of the process $X = \{X_t, t \geq 0\}$,

$$\Phi(u) = \mathbb{E}\left[e^{iuX_t}\right] = \int_{-\infty}^{\infty} e^{iux} f(x)dx = \hat{f}(u).$$

This is the main key of the method. The advantage is that the characteristic function of our Lévy processes are available in closed form. This is not necessarily the case of the density function. Therefore, intuitively, we can pass to the "frequencies" world with *Fourier transform* to compute the price of our option, and then use the *inverse Fourier transform* to come back in the "real" world.

Technically, if we damp the option value by a factor $\exp(\alpha x)$ and take the Fourier transform of equation (4.4), we get

$$\begin{aligned} e^{r_d \Delta t}\mathcal{F}\{v(x, t_n, A)\}(u) &= \int_{-\infty}^{\infty} e^{iux} e^{\alpha x} \int_{-\infty}^{\infty} V(x + z, t_{n+1}^-, A) f(z)dzdx \\ &= \int_{-\infty}^{\infty} \int_{-\infty}^{\infty} e^{iu(x+z)} v(x + z, t_{n+1}^-, A) e^{-iz(u-i\alpha)} f(z)dzdx, \end{aligned}$$

where $v(x, t, A) = e^{\alpha x} V(x, t, A)$ is the damped value option. Changing the order of integration, we obtain

$$\begin{aligned} e^{r_d \Delta t}\mathcal{F}\{v(x, t_n, A)\}(u) &= \int_{-\infty}^{\infty} \int_{-\infty}^{\infty} e^{iuy} v(y, t_{n+1}^-, A)dy \; e^{-i(u-i\alpha)z} f(z)dz \\ &= \int_{-\infty}^{\infty} e^{iuy} v(y, t_{n+1}^-, A)dy \int_{-\infty}^{\infty} e^{-i(u-i\alpha)z} f(z)dz \\ &= \mathcal{F}\{v(x, t_{n+1}^-, A)\}(u)\Phi(-(u - i\alpha)). \end{aligned}$$

The difference with the approach of Carr and Madan (1999) [CM99] is that we take the transform with respect to the log-spot price instead the log-strike price.

### 4.3.2 Implementation of the method

The goal is now to compute the convolution

$$v(x) = \frac{1}{2\pi} \int_{-\infty}^{\infty} e^{-iux} \hat{v}(u)\Phi(-(u - i\alpha))du, \tag{4.5}$$

where $\hat{v}(u)$ is the Fourier transform of $v$:

$$\hat{v}(u) = \int_{-\infty}^{\infty} e^{iuy} v(y)dy. \tag{4.6}$$

For notational convenience, we dropped the discounting factor out of the equation. We can approximate both integrals by a discrete sum, that allows us to use FFT to compute them. Thus we have to construct uniform grids for $u, x$ and $y$:

$$\begin{aligned} u_j &= u_0 + j\Delta u, \\ x_j &= x_0 + j\Delta x, \\ y_j &= y_0 + j\Delta y, \end{aligned}$$

for $j = 0, \dots, M-1$. We can take the same mesh size for the $x$- and $y$-grids, i.e. $\Delta x = \Delta y$. However, the Nyquist relation must be satisfied, i.e.

$$\Delta u \cdot \Delta y = \frac{2\pi}{M}.$$

The discretization of equations (4.5), with a general Newton-Côtes rule to approximate the equations (4.6), gives us

$$v(x_p) \approx \frac{\Delta u \Delta y}{2\pi} \sum_{j=0}^{M-1} e^{-iu_j x_p} \Phi(-(u_j - i\alpha)) \sum_{n=0}^{M-1} w_n e^{iu_j y_n} v(y_n),$$

for $p = 0, \dots, M-1$.

Here, we will use the trapezoidal rule with the weights $w_n$:

$$w_0 = w_{M-1} = \frac{1}{2}, \qquad w_n = 1, \quad \text{for } n = 1, \dots, M-2.$$

Including the grids discretization in our approximation, we have

$$v(x_p) \approx \frac{e^{-iu_0(x_0 + p\Delta y)}}{2\pi} \Delta u \sum_{j=0}^{M-1} w_j e^{-ijp2\pi/M} e^{ij(y_0 - x_0)\Delta u} \Phi(-(u_j - i\alpha)) \hat{v}(u_j),$$

where the Fourier transform of $v$ is approximated by

$$\hat{v}(u_j) \approx e^{iu_0 y_0} \Delta y \sum_{n=0}^{M-1} e^{ijn2\pi/M} e^{inu_0 \Delta y} w_n v(y_n).$$

Let us now define the *Discrete Fourier Transform* (DFT) and its inverse.

**Definition 4.2 (*Discrete Fourier Transform*)**

*The **Discrete Fourier Transform** (DFT) of $x$ is a vector $\hat{x} \in \mathbb{R}^M$ defined by*

$$\mathcal{D}_j\{x_n\} := \hat{x}_j = \sum_{n=0}^{M-1} e^{ijn2\pi/M} x_n.$$

*Its inverse is given by*

$$\mathcal{D}_n^{-1}\{\hat{x}_j\} := x_n = \frac{1}{M} \sum_{j=0}^{M-1} e^{-ijn2\pi/N} x_j.$$

*Be careful with the* MATLAB *conventions where $\mathcal{D} \equiv$ `ifft` and $\mathcal{D}^{-1} \equiv$ `fft`.*

If we set $u_0 = -M/2\Delta u$, we have that

$$\begin{aligned} e^{inu_0\Delta y} &= e^{in\pi} \\ &= \cos(n\pi) + i\sin(n\pi) \\ &= (-1)^n. \end{aligned}$$

Finally, we obtain the result

$$v(x_p) \approx e^{iu_0(y_0-x_0)}(-1)^p \mathcal{D}_p^{-1}\left\{e^{ij(y_0-x_0)\Delta u}\Phi(-(u_j - i\alpha))\mathcal{D}_j\left\{(-1)^n w_n v(y_n)\right\}\right\}.$$

Thus, we have just to undamp the quantity $v(x, t_n, A)$ and discount the result to get the value $V(x, t_n, A)$ of the financial product.

### 4.3.3 Criticism

Note that there is some undesired margin effects due to the discontinuity in the function of cash flows $C^{\text{tot}}(S(t_n), A(t_{n-1}))$. In fact, when we use the Fourier transform, the value function $V(x, t, A)$ becomes periodic and a gap appears between the negative cash flow in $x_{\min}$, in the case of an Accumulator, and the positive cash flow in $x_{\max}$. We can observe this effect clearly in the Figure 4.7.

As explained by Lord et al., the damping factor is needed to ensure that $V(x, t, A)$ is $L^1$-integrable. For example, we need a damping factor $\alpha > 0$ for a Call option and $\alpha < 0$ for a Put option. In our case, since there are at the same time a Call option payoff and a Put option payoff, there is no optimal value for $\alpha$. We have to keep this in mind, but we will see, with $\alpha = 0$, that this inconvenient does not have

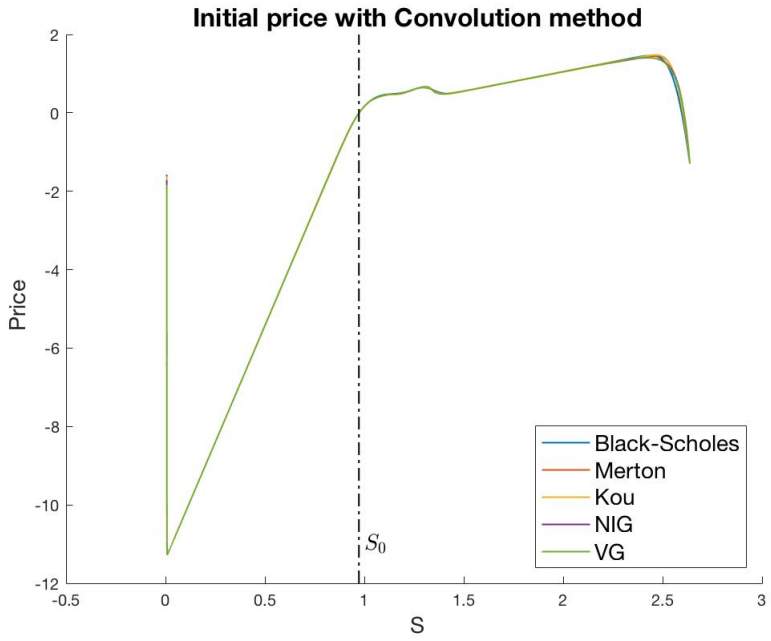


**Fig. 4.7:** Initial price with Convolution method for a simple FX-TARN with 6 fixing dates over 1 year. Remark the margin effect due to the gap between positive payoff and negative payoff.

any consequence on the results around $S_0 = e^{x_0}$, far away from $S_{\min} = e^{x_{\min}}$ and $S_{\max} = e^{x_{\max}}$.

## 4.4 Summary

To conclude this chapter, we can summarize the whole algorithm of the two last methods.

1. Apply the zero final condition at $T = t_N$ for all the $N_a$ solutions to equation (4.1) corresponding to $A_j, 1 \leq j \leq N_a$.

2. Apply the jump condition to obtain $A_j^+ = A_j + \tilde{C}_n^{\text{pos}}$, where $\tilde{C}_n^{\text{pos}}$ is the positive gain on the fixing date $t_n$.

3. Perform the cubic spline interpolation from points $V(S_m, t_n, A_j), j = 1, \ldots, N_a$, to new points $V(S_m, t_n, A_j^+)$ for each spot grid point $S_m$.

4. Add the total cash flow $C_n^{\text{tot}}$ respecting the knock-out condition imposed by the accumulated amount. This leads to the value $V(S_m, t_n^-, A_j)$ expressed by equation (4.2).

5. Perform the **finite difference** or the **convolution method** for each $N_a$ solutions $V(S_m, t_n^-, A_j), j = 1, \ldots, N_a$, corresponding to the $N_a$ grid points in the auxiliary variable $A$. This gives us the value $V(S_m, t_{n-1}, A_j)$ for $m = 1, \ldots, M$.

6. Repeat steps 2 to 5 until $n = 0$ to get the today's value $V(S_m, t_0, A_j)$. Note that only the value for $A_0 = 0$ interests us, since at the beginning no amount is accumulated. Then the fair price of the FX-TARN is given by $V(S(t_0), t_0, 0)$.

# 5 Calibration

> *If you want to know the value of a security, use the price of another security that is as similar to it as possible. All the rest is modelling.*
>
> — **Emanuel Derman**
> (1946)

In order to be able to price a FX-TARN, we have to calibrate our models to the market option prices. The aim of the calibration is to estimate the unknown parameters of the model which reproduce the same prices as in the market. This is analogous to the implied volatility in the Black-Scholes framework. For this purpose, we will use European vanilla option prices calculated from the implied volatility given by BLOOMBERG.

Firstly, in Section 5.1, we will present the calibration inputs and how we can compute the European vanilla option price. Secondly, in Section 5.2, we will explain the procedure that we used to calibrate our models. In Section 5.3, we will discuss the results of the calibrations of our models. The Section 5.4 concludes this chapter with the analysis of the resulting calibrated models.

## 5.1 Calibration inputs

All the data we have used in this chapter come from the provider BLOOMBERG. We have recovered the implicit volatility quotes with respect to the delta Call or delta Put and tenor for the exchange rate USD/CHF on the 23 May 2017. The delta notations are listed in the Table 5.1 with the corresponding theoretical delta.

For the calibration, we have only used the volatility quotes for maturities 1W, 2W, 3W, 1M, 2M, 3M, 4M, 6M, 9M and 1Y. At the end, that represents 110 implied volatilities including ATM ($\Delta = \pm 0.50$) quote.

The Figure 5.1 shows us the CHF and USD risk-free rate curves used in our calibration.

| Notation | Delta | Notation | Delta |
|---|---|---|---|
| 5D Put | -0.05 | 5D Call | 0.05 |
| 10D Put | -0.10 | 10D Call | 0.10 |
| 15D Put | -0.15 | 15D Call | 0.15 |
| 25D Put | -0.25 | 25D Call | 0.25 |
| 35D Put | -0.35 | 35D Call | 0.35 |

**Tab. 5.1:** Notation convention of delta Call and delta Put.

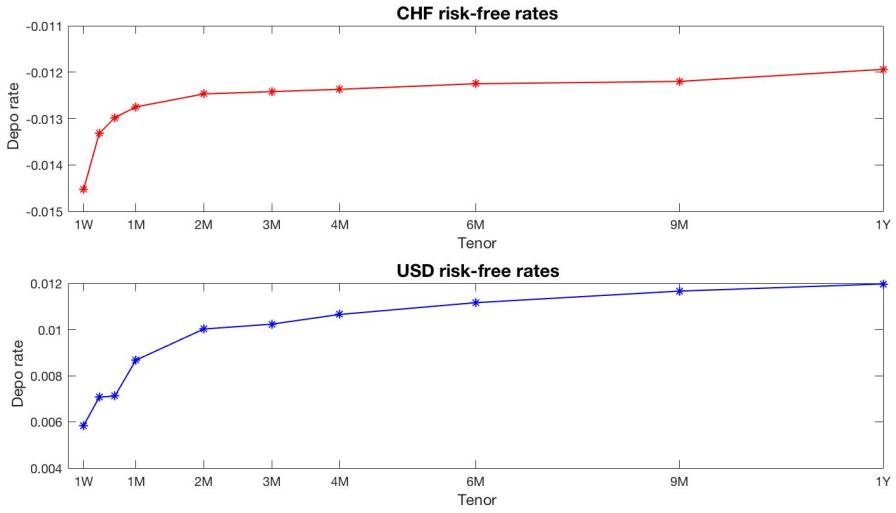


**Fig. 5.1:** Risk-free rates from BLOOMBERG used for the calibration.

Since the implied volatilities are quoted with respect to the delta, to compute the European vanilla option price, we have to recover the corresponding strike. In the Black-Scholes framework, we have the following relationship between the delta $\Delta$ and the strike $K$:

$$K = S_0 e^{(r_d - r_f)T} \exp\left(-\beta\sigma\sqrt{T}\Phi^{-1}\left(e^{-r_f T}|\Delta|\right) + \frac{1}{2}\sigma^2 T\right),$$

where $\beta = 1$ for a Call option and $\beta = -1$ for a Put option and $\Phi$ is the standard Gaussian cumulative probability function. The initial spot price $S_0 = 0.9730$ is naturally given by the term sheet of the FX-TARN.

From here, we can use the Black-Scholes formula to compute the European vanilla option prices:

$$V(K,T) = \beta\left(S_0 e^{-r_f T}\Phi(\beta d_+) - K e^{-r_d T}\Phi(\beta d_-)\right),$$

with

$$d_\pm = \frac{\log\left(\frac{S_0 e^{(r_d - r_f)T}}{K}\right) \pm \frac{1}{2}\sigma^2 T}{\sigma\sqrt{T}}.$$

The delta less than 50 means that the market quotes are priced with respect to out of the money (OTM) options. Therefore, we have computed the OTM European option prices under Black-Scholes model illustrated in Figure 5.2. On the left hand side, we have the OTM Put options and on the right hand side, we have the OTM Call options.


**Fig. 5.2:** European option prices; on the left hand side, the OTM Put options, and on the right hand side, the OTM Call options.

## 5.2 Calibration method

To calibrate our models, we seek to minimize the root-mean-square error (RMSE) of the differences between the model prices and the observed prices:

$$\text{RMSE}(\Theta) = \sqrt{\sum_{i=1}^{N} \frac{1}{N} \left| V(\Theta; K_i, T_i) - V^{\text{obs}}(K_i, T_i) \right|^2},$$

where $\Theta$ is the parameter vector of the model.

For example, the RMSE of the Black-Scholes model with 1Y ATM constant volatility, $\sigma = 0.07908$, is equal to $8.95 \cdot 10^{-4}$, which is not very precise. Effectively, we can observe in the Figure 5.3 that the model prices don't fit good with the market prices. We will see that the jump models perform better than the Black-Scholes model.

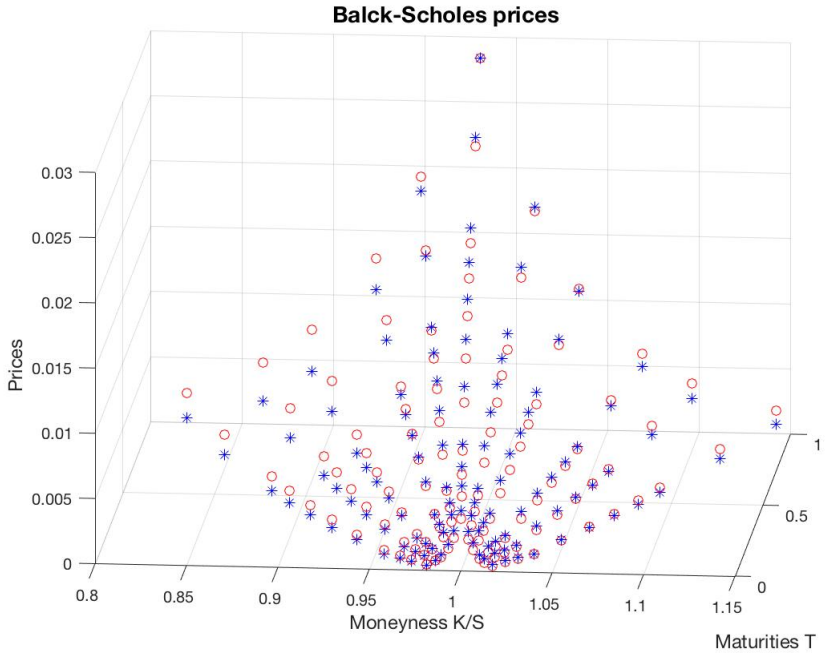


**Fig. 5.3:** Black-Scholes prices (in blue) in comparison with the market prices (in red).

The calibrated parameters $\hat{\Theta}$ of the model with jumps satisfy

$$\hat{\Theta} = \arg\min_{\Theta} \text{RMSE}(\Theta).$$

We can use the MATLAB command `fmincon` which allows us to find the minimum of a constrained nonlinear multi-variable function. Note that the method used to price the European options under jump models is the convolution method with $N_x = 1'000$ and damping factor $\alpha = -\beta$, where $\beta = 1$ for a Call option and $\beta = -1$ for a Put option. This method is in fact the fastest method to apply the minimizing function.

## 5.3 Results of calibrations

The resulting calibrated parameters and RMSE for each jump model are summarized in the the Table 5.2 in comparison with the Black-Scholes model. We can see that all models perform better that the Black-Scholes model. The models that fit the best the market prices are the jump-diffusion models because they have more parameters and give more freedom in the calibration.

| Models | Calibrated parameters $\hat{\Theta}$ | RMSE |
|---|---|---|
| Black-Scholes($\sigma$) | $[0.07908]$ | $8.98 \cdot 10^{-4}$ |
| Merton($\sigma, \lambda, \alpha, \delta$) | $[0.0649, 0.1303, -0.0584, 0.1603]$ | $2.77 \cdot 10^{-4}$ |
| Kou($\sigma, \lambda, p, \eta_1, \eta_2$) | $[0.0665, 0.1305, 0.0751, 3.3154, 9.0490]$ | $2.49 \cdot 10^{-4}$ |
| NIG($\alpha, \beta, \delta$) | $[18.8492, -3.9282, 0.1250]$ | $4.79 \cdot 10^{-4}$ |
| VG($\theta, \sigma, \nu$) | $[-0.0324, 0.0810, 0.2451]$ | $5.73 \cdot 10^{-4}$ |

**Tab. 5.2:** Calibrated parameters $\hat{\Theta}$ and RMSE for each models.

We can see in Figure 5.4 that all the model prices are closer to the market prices than the results obtained with Black-Scholes. This means that the FX-TARN price computed with a jump model will be more relevant with respect to the market than the FX-TARN price under Black-Scholes.

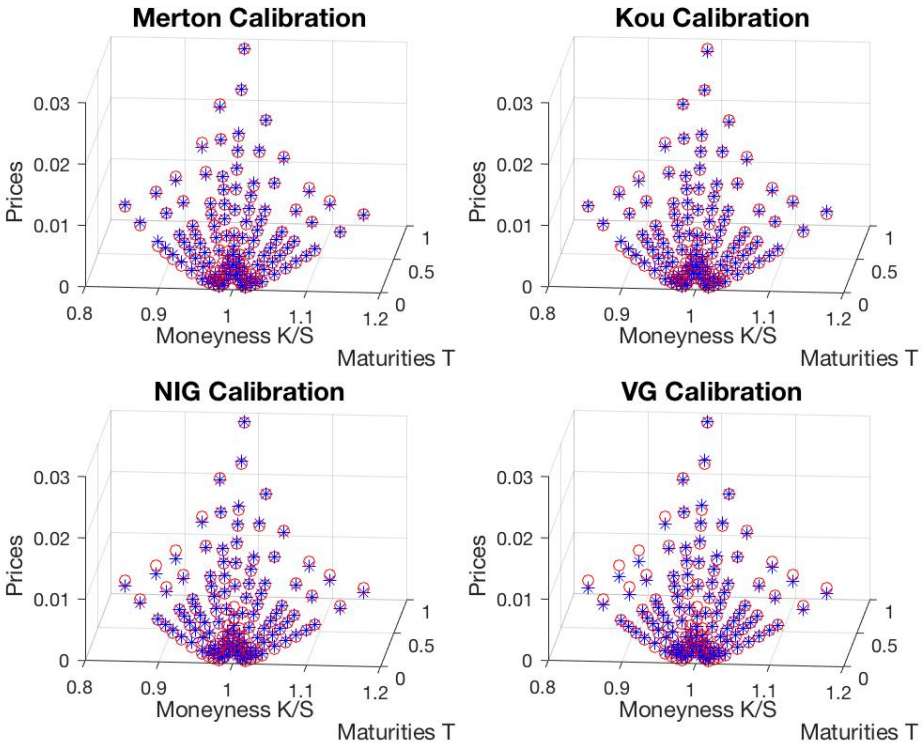


**Fig. 5.4:** Jump models calibration; model prices in blue and market prices in red.

## 5.4 Analysis of the calibration

As we have chosen to calibrate our models for the whole structure of the implied volatility, i.e. for all tenors at the same time, the fitting with the market prices can not be perfect. We will now investigate how the Lévy models with jumps reflect the

information contained in the smile of the volatility surface. Figure 5.5 shows the original volatility surface that we used to calibrate our models.

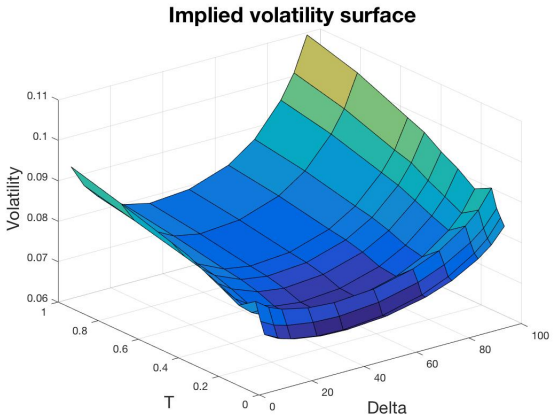


**Fig. 5.5:** Original volatility surface.

By repricing all the options with the Lévy models with jumps, it is possible to compute the volatility surface corresponding the a specific model. Figure 5.6 illustrates the implied volatility surfaces of the Lévy models with jumps.

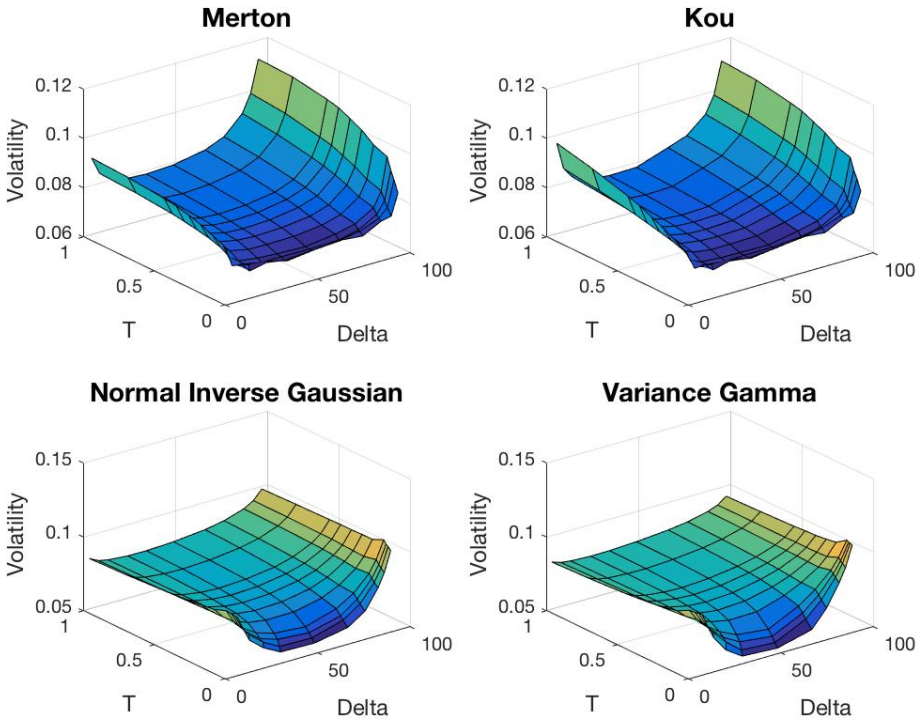


**Fig. 5.6:** Jump models implied volatility surfaces.

As we can see, the jump-diffusion models replicate almost the original volatility surface, which means that the Merton and Kou models can express all the information contained in the volatility smile. On the other side, the smile structure in pure jump models for long term is lost. Thus the pure jumps model can not replicate perfectly the market prices for long maturity.

Another way to check the accuracy of the calibration of a model is to price an option out of the sample used for the calibration. In our case, we can price the European options for the tenor 18M and 2Y with the calibrated models on 1W to 1Y, and compare them to the market prices. The results are given in Figures 5.7 and 5.8.

We can conclude that the Merton and Kou models are clearly more accurate than the NIG and VG models with respect to the market. Indeed, we can see that the NIG and VG do not perform very well deep out of the money for long maturity date. Even if the tenor 18M and 2Y are not part of the sample used for calibration, the Merton and Kou models fit really good with the market prices beyond 1Y maturity. All this confirm the choice to use jump diffusion models in the pricing of FX-TARN products.

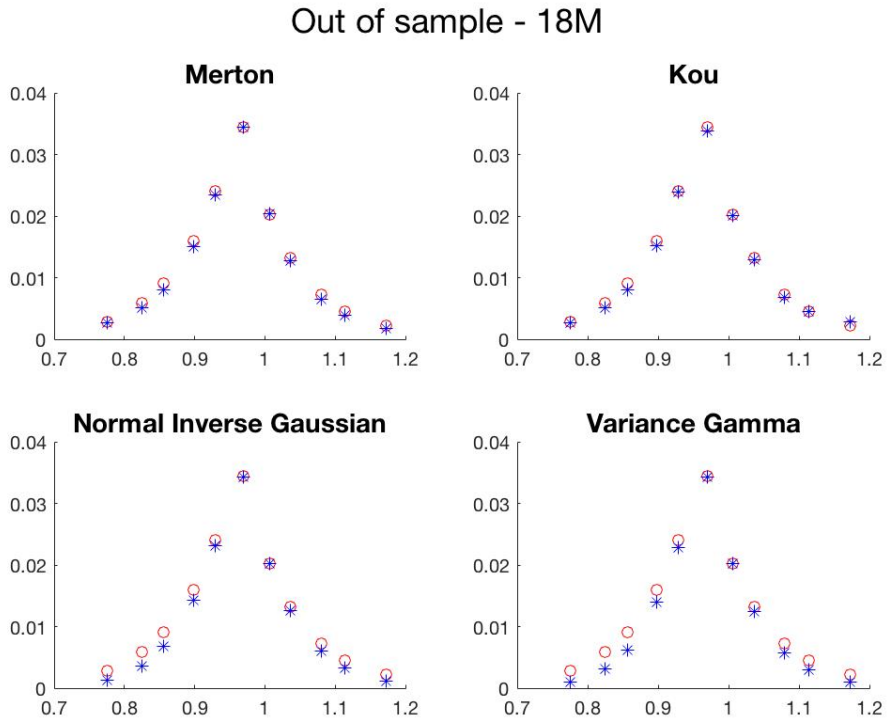


**Fig. 5.7:** Out of sample 18M options priced with jump models.

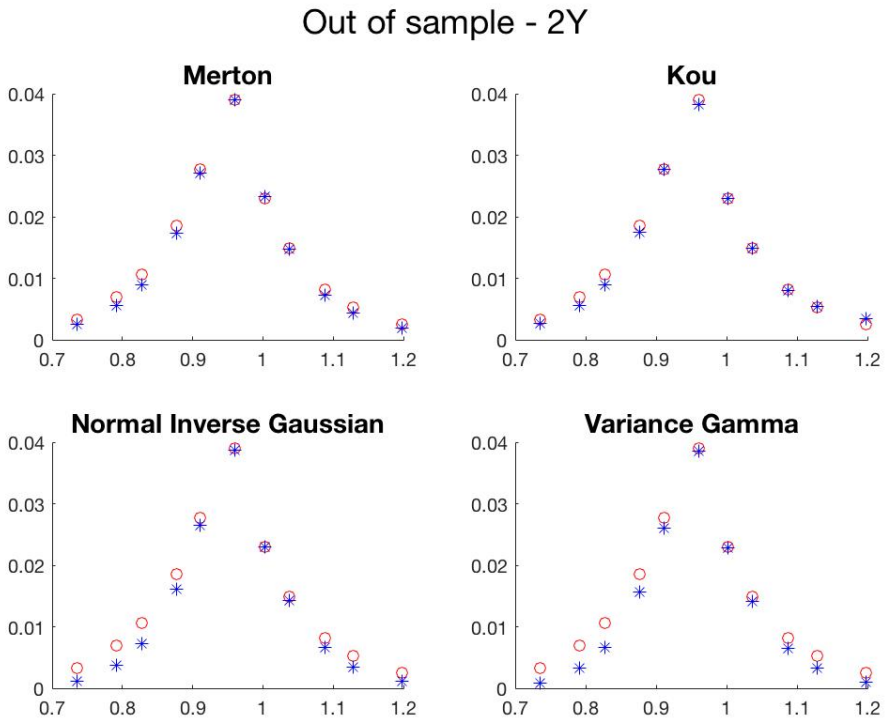


**Fig. 5.8:** Out of sample 2Y options priced with jump models.

# 6 Numerical Results

> *In the end, a theory is accepted not because it is confirmed by conventional empirical tests, but because researchers persuade one another that the theory is correct and relevant.*
>
> **— Fisher Black**
> (1938-1995)

Having calibrated our models, now we are able to price the FX-TARN with the different methods we have studied. This chapter presents the results of experiments on simplified FX-TARN, described in Section 6.1. Then, in Section 6.2, we will expose all the results in the three different cases of redemption, i.e. No gain, Part gain and Full gain. Next, in Section 6.3, we will study the speed, the accuracy and the convergence of the Finite Difference and Convolution methods. Finally, to conclude this chapter with Section 6.4, we will price the term sheet example that we have presented in the introduction.

## 6.1 Experimental setup

The programming was done in MATLAB and run on a MacBook Pro with 2 GHz Intel Core i5 processor and 8 Go RAM. Hence, all computational times in this chapter are expressed in seconds and represent the time to the pricing engine to give the FX-TARN price for a specific model and a specific method. To be more accurate in the analysis of the results and don't waste time in computation, we have chosen to price a simplified FX-TARN.

Consider the same FX-TARN as in our term sheet example with only 6 fixing dates over one year and constant strike $K = 0.942$ and accrual amount per fixing date $N_f = 1$. Recall the underlying foreign exchange rate is the USD/CHF on 23 May 2017 with $S_0 = 0.9730$. The deposit rates of USD and CHF are respectively given by $r_f = 1.197\%$ and $r_d = -1.237\%$ at 1Y maturity. Finally, the target level is settled at $0.4$. We will treat the three different types of knock-out condition, i.e. No gain, Part gain and Full gain.

The error of the methods will be presented as the absolute value of the difference between the calculated value and a reference value, $|V(S_0, t_0, 0) - V_{\text{ref}}(S_0, t_0, 0)|$. We choose the reference value to be the value computed with a very fine discretization in convolution method, i.e. $N_x = 2 \cdot 10^4, N_a = 2 \cdot 10^3$. This choice is motivated by the fact that the other methods are too expensive in computational cost for a similar accuracy. In particular, the computations of prices under jump-diffusion models in Monte Carlo are very slow since we have to simulate a lot of random variables that modeled the jumps in addition to the diffusion path. However, we can compare the results of $10^8$ simulations versus the reference values under Black-Scholes, NIG and VG models, (cf. Tables 6.1, 6.2 and 6.2).

| No gain | $V_{\text{ref}}$ | $V_{\text{MC}}$ | SE |
|---|---|---|---|
| Black-Scholes | 0.15877 | 0.15876 | $1.33 \cdot 10^{-5}$ |
| NIG | 0.16166 | 0.16165 | $1.28 \cdot 10^{-5}$ |
| VG | 0.16246 | 0.16248 | $1.29 \cdot 10^{-5}$ |

**Tab. 6.1:** No gain TARN reference value in comparison with $10^8$ Monte Carlo simulations.

| Part gain | $V_{\text{ref}}$ | $V_{\text{MC}}$ | SE |
|---|---|---|---|
| Black-Scholes | 0.16863 | 0.16861 | $1.46 \cdot 10^{-5}$ |
| NIG | 0.17093 | 0.17094 | $1.41 \cdot 10^{-5}$ |
| VG | 0.17181 | 0.17180 | $1.42 \cdot 10^{-5}$ |

**Tab. 6.2:** Part gain TARN reference value in comparison with $10^8$ Monte Carlo simulations.

| Full gain | $V_{\text{ref}}$ | $V_{\text{MC}}$ | SE |
|---|---|---|---|
| Black-Scholes | 0.17763 | 0.17763 | $1.62 \cdot 10^{-5}$ |
| NIG | 0.17929 | 0.17927 | $1.57 \cdot 10^{-5}$ |
| VG | 0.18024 | 0.18026 | $1.57 \cdot 10^{-5}$ |

**Tab. 6.3:** Full gain TARN reference value in comparison with $10^8$ Monte Carlo simulations.

We can see that the reference value is very closed to the Monte Carlo value and the standard error of $1.28 \cdot 10^{-5}$ to $1.62 \cdot 10^{-5}$ confirm that our choice is not so bad. Then, we can hope that the reference value for the Merton and Kou models are closed to the true value as well.

## 6.2 Results

In this section, we define the settings of the experiments and present the numerical results. We will discuss the results properties in the following section.

### 6.2.1 Settings

Concerning the Finite difference method, we fixed

$$\begin{aligned} x_{\min} &= -5, \qquad x_{\max} = 1, \\ q_{\min} &= x_{\min} - B_l = -7, \\ q_{\max} &= x_{\max} + B_r = 3, \\ \epsilon &= 0.05. \end{aligned}$$

$x_{\min}$ and $x_{\max}$ were chosen such that $S_{\min} = e^{x_{\min}}$ and $S_{\max} = e^{x_{\max}}$ are far from $S_0$. Then $q_{\min}$ and $q_{\max}$ were chosen such that the Lévy density centered in $x_{\min}$ and $x_{\max}$ is closed to zero on $q_{\min}$ and $q_{\max}$ as we can see in figure 6.1. This is necessary to treat correctly the integral term in the PIDE. The choice of the parameter $\epsilon$ was a bit more complicated since the error of the method is given by

$$error \sim \epsilon + C(\epsilon)\Delta x^2 + \Delta t,$$

and $C(\epsilon) \to \infty$ when $\epsilon \to 0$. Some tests on $\epsilon$ encouraged us to choose the value 0.05.

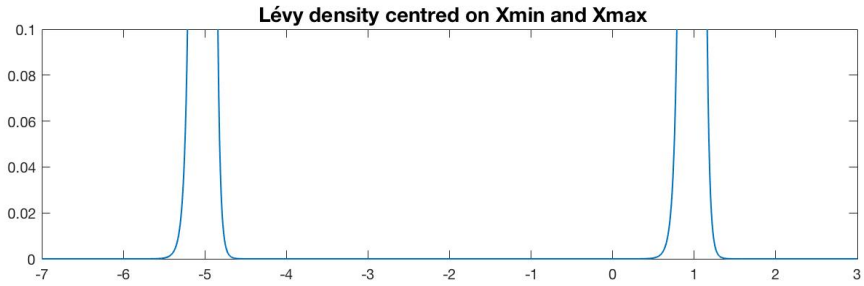


**Fig. 6.1:** Lévy density centered on $x_{\min}$ and $x_{\max}$ to justify the choice of $q_{\min}$ and $q_{\max}$.

For the Convolution method, we took the same values for $x_{\min}$ and $x_{\max}$ as the Finite Difference method.

Finally, the discretization parameters per scenario are summarized in Table 6.4.

| Scenarios | Monte Carlo | Finite Difference | Convolution |
|---|---|---|---|
| I | $M = 10^2$ | $N_x = 250, N_a = 25, N_t = 5$ | $N_x = 250, N_a = 25$ |
| II | $M = 10^3$ | $N_x = 500, N_a = 50, N_t = 10$ | $N_x = 500, N_a = 50$ |
| III | $M = 10^4$ | $N_x = 1000, N_a = 100, N_t = 20$ | $N_x = 1000, N_a = 100$ |
| IV | $M = 10^5$ | $N_x = 2000, N_a = 200, N_t = 40$ | $N_x = 2000, N_a = 200$ |
| V | $M = 10^6$ | $N_x = 4000, N_a = 400, N_t = 80$ | $N_x = 4000, N_a = 400$ |

**Tab. 6.4:** Number of simulations per Monte Carlo scenario and grids discretization for the FD and Conv methods.

### 6.2.2 Results tables

All the numerical results are listed in Tables 6.6 to 6.8 at the end of the chapter.

## 6.3 Speed, Accuracy and Convergence analysis

This section is devoted to the analysis of the results. We will first briefly discuss the Monte Carlo method before studying the performance of the Finite Difference method and Convolution method.

### 6.3.1 Monte Carlo method analysis

First of all, let's see the decay of the standard error with respect to the number of simulation $M$ illustrated in Figure 6.2. As expected, the error decays with the rate $1/\sqrt{M}$. This method gives good results from $M = 10^6$ but it is very expensive in computational time, especially for the jump diffusion models where we have to simulate jumps independently of the Brownian path. In this case, we can see in the results tables that the CPU time explodes for the Merton and Kou models. Therefore, it is not a good choice to use Monte Carlo method for pricing options when other numerical methods are available.

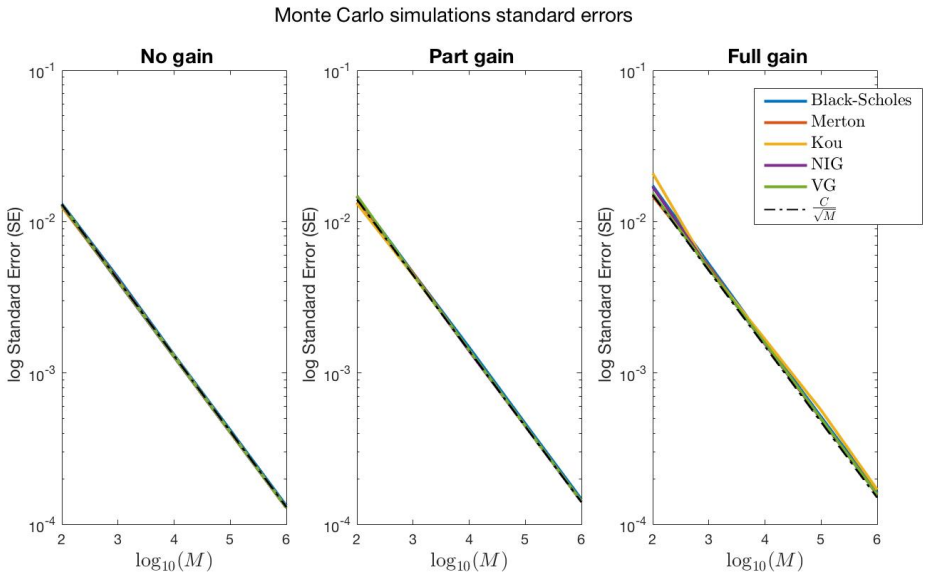


**Fig. 6.2:** Monte Carlo standard error analysis.

### 6.3.2 Convergence analysis

Let's now check the convergence of the Finite Difference method and the Convolution method. In Figure 6.3 and 6.4, we plot the convergence error of the two methods.

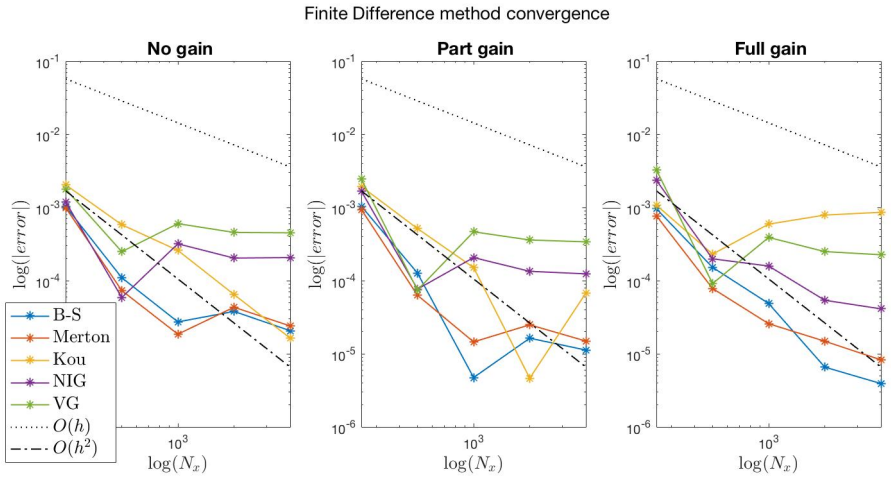


**Fig. 6.3:** Convergence of the Finite Difference method.

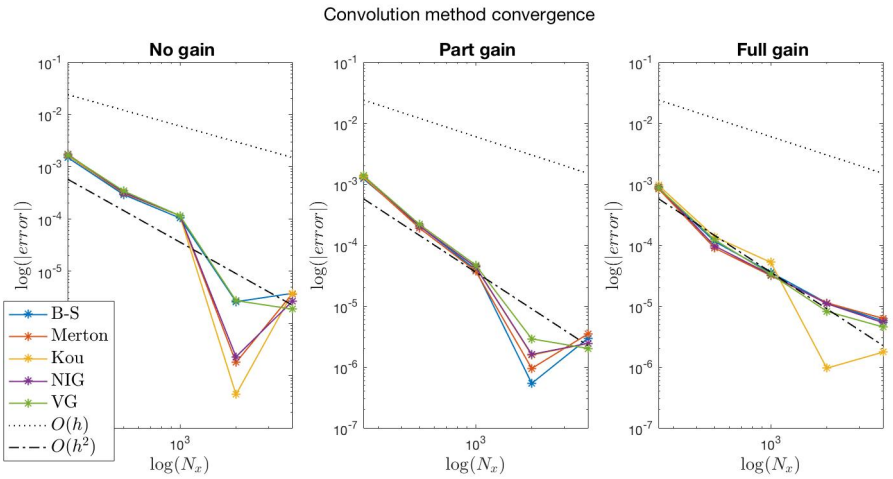


**Fig. 6.4:** Convergence of the Convolution method.

We can see that the Convolution method has a convergence order 2 while the Finite Difference method has difficulties to converge for pure jump models. This is certainly due to the truncation in the Lévy density. Therefore, the method converges to this truncation error. Here, since the Convolution method uses the characteristic function in its closed form without modification or approximation, we have fewer losses in the accuracy.

### 6.3.3 Speed and accuracy analysis

It can be interesting to compare the speed and accuracy of both numerical methods to make a good choice for pricing engine. At the top of the Figure 6.5, we can see the accuracy of the methods with respect to the computational time. And at the bottom, the running time in function of the grid points number $N_x$.

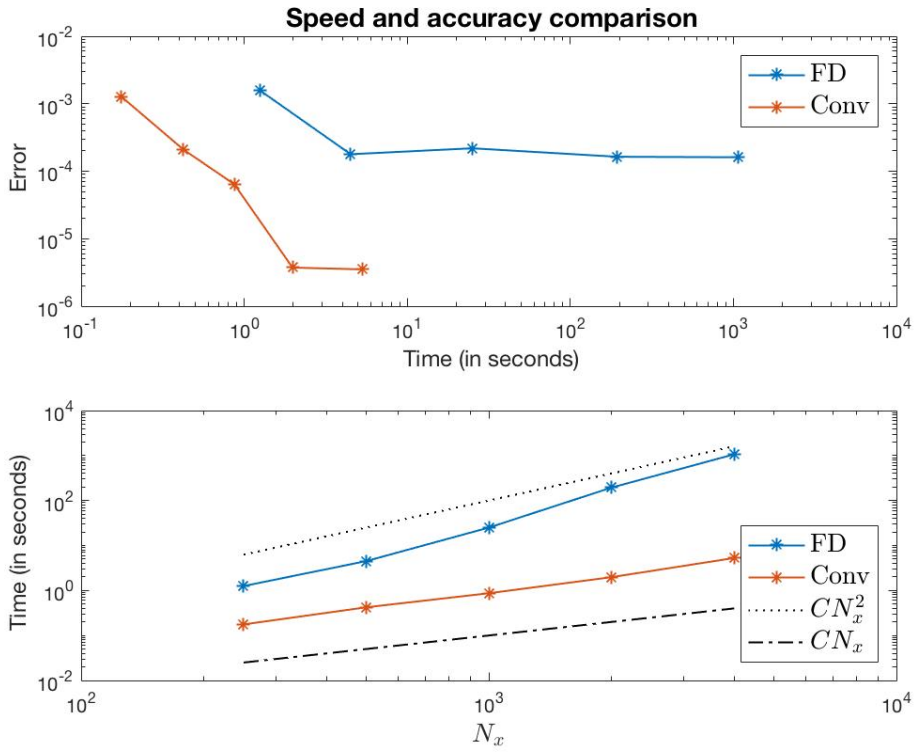


**Fig. 6.5:** Speed and accuracy comparison between the FD method and the Conv method. At the top: Error in function of computational time. At the bottom: Running time with respect to $N_x$.

In addition to being much faster than Finite Difference method, the Convolution method is more precise. In fact, cost of the Convolution method grows linearly with respect to the number of grid points $N_x$, while the Finite Difference method grows up quadratically. Finally, for the same accuracy, the Convolution method can be from 13 to 15 times faster than the Finite Difference method.

The gain in accuracy from $N_x = 2000$ to $N_x = 4000$ in the Convolution method is not very important. Thus it seems to be a good compromise to choose the Convolution method with $N_x = 2000$ to price our FX-TARN option.

## 6.4 Value of the term sheet example

We arrive to the goal of the project that is to price a real case of FX-TARN. We will then compute three different prices which are

- A bid price, obtained from the calibration on the bid volatility quotes,
- A mid price, obtained from the calibration on the mid volatility quotes,
- An ask price, obtained from the calibration on the ask volatility quotes.

We use, as discussed before, the Convolution method, with $N_x = 2000$ and $N_a = 200$, to price the FX-TARN of the term sheet example. The prices are given in Table 6.5.

| **FX-TARN** | Bid | Mid | Ask | RMSE |
|---|---|---|---|---|
| Black-Scholes | CHF $-21'204$ | CHF $-23'197$ | CHF $-25'202$ | 10.2e-04 |
| Merton | CHF $-17'713$ | CHF $-19'960$ | CHF $-22'104$ | 3.05e-04 |
| Kou | CHF $-18'348$ | CHF $-21'193$ | CHF $-23'812$ | 2.79e-04 |
| NIG | CHF $-17'409$ | CHF $-19'252$ | CHF $-20'983$ | 4.97e-04 |
| VG | CHF $-17'692$ | CHF $-19'506$ | CHF $-21'160$ | 5.88e-04 |

**Tab. 6.5:** Prices of the FX-TARN for all the models. The RMSE is the deviation of the calibrated model prices with respect to the market prices. Each price is computed in 19 seconds.

The negative value means that the client will receive a premium when signing the contract. The price given by a trader to the client will depend on his book and the risk premium he would like to take. The most representative price with respect to the market is the prices given by the Kou model because its RMSE, which quantify the deviation between the European options model prices and the market prices, is the smallest. Then, a fair premium for the client would be around CHF 18'300.-, where the risk premium is already included in the volatility price. Then, the risk premium of the trader would be around CHF 5'500.-, which is the difference with the ask price.

| **No Gain** | **Monte Carlo** | | | **Finite Difference** | | | **Convolution** | | |
|---|---|---|---|---|---|---|---|---|---|
| Black-Scholes ($V_{\text{ref}} = 0.15877$) | Value | Std Error | Time | Value | Error | Time | Value | Error | Time |
| Scenario I | 0.14932 | 1.31e-02 | 0.01 | 0.15774 | 1.03e-03 | 1.11 | 0.15728 | 1.50e-03 | 0.19 |
| Scenario II | 0.15863 | 4.27e-03 | 0.02 | 0.15866 | 1.10e-04 | 4.94 | 0.15848 | 2.91e-04 | 0.36 |
| Scenario III | 0.15676 | 1.32e-03 | 0.10 | 0.15875 | 2.73e-05 | 28.8 | 0.15867 | 1.04e-04 | 0.80 |
| Scenario IV | 0.15870 | 4.20e-04 | 0.50 | 0.15881 | 3.80e-05 | 192 | 0.15878 | 2.60e-06 | 1.71 |
| Scenario V | 0.15859 | 1.33e-04 | 4.77 | 0.15879 | 2.07e-05 | 1244 | 0.15878 | 3.76e-06 | 4.85 |
| Merton ($V_{\text{ref}} = 0.15929$) | Value | Std Error | Time | Value | Error | Time | Value | Error | Time |
| Scenario I | 0.16950 | 1.29e-02 | 0.06 | 0.15829 | 9.94e-04 | 0.98 | 0.15765 | 1.64e-03 | 0.16 |
| Scenario II | 0.16485 | 4.13e-03 | 0.28 | 0.15921 | 7.32e-05 | 4.64 | 0.15898 | 3.08e-04 | 0.34 |
| Scenario III | 0.15834 | 1.29e-03 | 1.89 | 0.15927 | 1.85e-05 | 27.3 | 0.15917 | 1.14e-08 | 0.79 |
| Scenario IV | 0.15968 | 4.07e-04 | 16.3 | 0.15933 | 4.33e-05 | 187 | 0.15929 | 1.79e-07 | 1.87 |
| Scenario V | 0.15920 | 1.29e-04 | 184 | 0.15931 | 2.40e-05 | 1094 | 0.15929 | 3.67e-06 | 5.59 |
| Kou ($V_{\text{ref}} = 0.15792$) | Value | Std Error | Time | Value | Error | Time | Value | Error | Time |
| Scenario I | 0.14190 | 1.24e-02 | 0.11 | 0.15588 | 2.04e-03 | 0.94 | 0.15624 | 1.68e-03 | 0.18 |
| Scenario II | 0.15042 | 4.06e-03 | 0.77 | 0.15733 | 5.81e-04 | 4.42 | 0.15760 | 3.14e-04 | 0.35 |
| Scenario III | 0.15837 | 1.30e-03 | 6.05 | 0.15766 | 2.59e-04 | 22.1 | 0.15780 | 1.14e-04 | 0.75 |
| Scenario IV | 0.15823 | 4.08e-04 | 60.2 | 0.15785 | 6.46e-05 | 183 | 0.15792 | 4.37e-08 | 1.83 |
| Scenario V | 0.15789 | 1.29e-04 | 689 | 0.15790 | 1.64e-05 | 1077 | 0.15792 | 3.74e-06 | 6.25 |
| NIG ($V_{\text{ref}} = 0.16166$) | Value | Std Error | Time | Value | Error | Time | Value | Error | Time |
| Scenario I | 0.13656 | 1.28e-02 | 0.02 | 0.16285 | 1.19e-03 | 1.25 | 0.15992 | 1.73e-03 | 0.16 |
| Scenario II | 0.15641 | 4.01e-03 | 0.04 | 0.16160 | 5.88e-05 | 5.00 | 0.16134 | 3.19e-04 | 0.40 |
| Scenario III | 0.16377 | 1.27e-03 | 0.11 | 0.16134 | 3.19e-04 | 22.2 | 0.16154 | 1.16e-04 | 0.74 |
| Scenario IV | 0.16166 | 4.04e-04 | 0.60 | 0.16145 | 2.03e-04 | 184 | 0.16166 | 2.30e-07 | 1.80 |
| Scenario V | 0.16179 | 1.28e-04 | 6.29 | 0.16145 | 2.07e-04 | 1078 | 0.16166 | 2.63e-06 | 5.87 |
| VG ($V_{\text{ref}} = 0.16246$) | Value | Std Error | Time | Value | Error | Time | Value | Error | Time |
| Scenario I | 0.16907 | 1.29e-03 | 0.01 | 0.16426 | 1.79e-03 | 1.26 | 0.16077 | 1.69e-03 | 0.15 |
| Scenario II | 0.15588 | 4.05e-04 | 0.02 | 0.16222 | 2.49e-04 | 5.43 | 0.16212 | 3.41e-04 | 0.33 |
| Scenario III | 0.16314 | 1.28e-04 | 0.18 | 0.16186 | 6.01e-04 | 22.3 | 0.16235 | 1.15e-04 | 0.77 |
| Scenario IV | 0.16235 | 4.06e-04 | 0.61 | 0.16201 | 4.56e-04 | 184 | 0.16246 | 2.73e-06 | 1.86 |
| Scenario V | 0.16227 | 1.29e-04 | 6.04 | 0.16201 | 4.50e-04 | 1050 | 0.16247 | 1.88e-06 | 5.21 |

**Tab. 6.6:** Results of No Gain TARN. The error in FD and Conv methods are given by $|V(S_0, t_0, 0) - V_{\text{ref}}(V(S_0, t_0, 0)|$ and the CPU Times are expressed in seconds.

| **Part Gain** | **Monte Carlo** | | | **Finite Difference** | | | **Convolution** | | |
|---|---|---|---|---|---|---|---|---|---|
| Black-Scholes ($V_{\text{ref}} = 0.16863$) | Value | Std Error | Time | Value | Error | Time | Value | Error | Time |
| Scenario I | 0.16856 | 1.47e-02 | 0.01 | 0.16759 | 1.04e-03 | 1.14 | 0.16740 | 1.22e-03 | 0.17 |
| Scenario II | 0.16711 | 4.59e-03 | 0.03 | 0.16850 | 1.27e-04 | 5.18 | 0.16842 | 2.06e-04 | 0.32 |
| Scenario III | 0.17228 | 1.48e-03 | 0.11 | 0.16862 | 4.73e-05 | 23.0 | 0.16859 | 3.97e-05 | 0.74 |
| Scenario IV | 0.16863 | 4.62e-04 | 0.53 | 0.16864 | 1.63e-05 | 200 | 0.16863 | 5.39e-07 | 2.11 |
| Scenario V | 0.16841 | 1.46e-04 | 5.05 | 0.16864 | 1.12e-05 | 1197 | 0.16863 | 2.95e-06 | 4.85 |
| Merton ($V_{\text{ref}} = 0.16854$) | Value | Std Error | Time | Value | Error | Time | Value | Error | Time |
| Scenario I | 0.18279 | 1.34e-02 | 0.05 | 0.16760 | 9.40e-04 | 0.95 | 0.16726 | 1.28e-03 | 0.14 |
| Scenario II | 0.17194 | 4.57e-03 | 0.20 | 0.16848 | 6.31e-05 | 3.88 | 0.16835 | 1.90e-04 | 0.35 |
| Scenario III | 0.16990 | 1.41e-03 | 1.72 | 0.16856 | 1.45e-05 | 23.7 | 0.16850 | 3.77e-05 | 0.94 |
| Scenario IV | 0.16865 | 4.48e-04 | 18.2 | 0.16857 | 2.49e-05 | 194 | 0.16854 | 9.47e-07 | 2.06 |
| Scenario V | 0.16870 | 1.42e-04 | 164 | 0.16856 | 1.49e-05 | 1019 | 0.16854 | 3.48e-06 | 5.34 |
| Kou ($V_{\text{ref}} = 0.16688$) | Value | Std Error | Time | Value | Error | Time | Value | Error | Time |
| Scenario I | 0.16444 | 1.32e-02 | 0.09 | 0.16495 | 1.93e-03 | 1.19 | 0.16557 | 1.31e-03 | 0.18 |
| Scenario II | 0.16616 | 4.43e-03 | 0.67 | 0.16637 | 5.15e-04 | 4.07 | 0.16668 | 2.05e-04 | 0.40 |
| Scenario III | 0.16508 | 1.42e-03 | 6.97 | 0.16673 | 1.51e-04 | 24.2 | 0.16684 | 4.35e-05 | 0.82 |
| Scenario IV | 0.16675 | 4.46e-04 | 70.5 | 0.16689 | 4.63e-06 | 198 | 0.16688 | 1.57e-06 | 2.14 |
| Scenario V | 0.16676 | 1.41e-04 | 604 | 0.16695 | 6.77e-05 | 992 | 0.16688 | 2.43e-06 | 5.12 |
| NIG ($V_{\text{ref}} = 0.17093$) | Value | Std Error | Time | Value | Error | Time | Value | Error | Time |
| Scenario I | 0.20942 | 1.47e-02 | 0.01 | 0.17261 | 1.67e-03 | 1.43 | 0.16956 | 1.37e-03 | 0.18 |
| Scenario II | 0.17137 | 4.50e-03 | 0.04 | 0.17101 | 7.66e-05 | 4.23 | 0.17073 | 2.04e-04 | 0.45 |
| Scenario III | 0.17025 | 1.40e-03 | 0.10 | 0.17072 | 2.07e-04 | 24.7 | 0.17089 | 4.39e-05 | 0.86 |
| Scenario IV | 0.17054 | 4.45e-04 | 0.67 | 0.17080 | 1.34e-04 | 196 | 0.17093 | 1.61e-06 | 2.18 |
| Scenario V | 0.17094 | 1.41e-04 | 5.43 | 0.17081 | 1.24e-04 | 1064 | 0.17093 | 2.44e-06 | 5.73 |
| VG ($V_{\text{ref}} = 0.17181$) | Value | Std Error | Time | Value | Error | Time | Value | Error | Time |
| Scenario I | 0.18370 | 1.48e-02 | 0.01 | 0.17424 | 2.43e-03 | 1.97 | 0.17043 | 1.38e-03 | 0.22 |
| Scenario II | 0.17527 | 4.48e-03 | 0.01 | 0.17173 | 7.43e-05 | 4.43 | 0.17159 | 2.18e-04 | 0.35 |
| Scenario III | 0.17162 | 1.42e-03 | 0.09 | 0.17134 | 4.65e-04 | 24.2 | 0.17176 | 4.71e-05 | 0.90 |
| Scenario IV | 0.17091 | 4.47e-04 | 0.67 | 0.17145 | 3.59e-04 | 200 | 0.17181 | 2.89e-06 | 2.29 |
| Scenario V | 0.17182 | 1.42e-04 | 6.40 | 0.17147 | 3.39e-04 | 1086 | 0.17181 | 2.01e-06 | 5.30 |

**Tab. 6.7:** Results of Part Gain TARN. The error in FD and Conv methods are given by $|V(S_0, t_0, 0) - V_{\text{ref}}(V(S_0, t_0, 0)|$ and the CPU Times are expressed in seconds.

| **Full Gain** | **Monte Carlo** | | | **Finite Difference** | | | **Convolution** | | |
|---|---|---|---|---|---|---|---|---|---|
| Black-Scholes ($V_{\text{ref}} = 0.17763$) | Value | Std Error | Time | Value | Error | Time | Value | Error | Time |
| Scenario I | 0.17144 | 1.73e-02 | 0.01 | 0.17667 | 9.61e-04 | 1.31 | 0.17678 | 8.23e-01 | 0.19 |
| Scenario II | 0.17773 | 5.25e-03 | 0.02 | 0.17748 | 1.52e-04 | 4.89 | 0.17751 | 1.15e-04 | 0.31 |
| Scenario III | 0.17749 | 1.62e-03 | 0.07 | 0.17758 | 4.87e-05 | 26.9 | 0.17759 | 3.56e-05 | 0.71 |
| Scenario IV | 0.17670 | 5.13e-04 | 0.54 | 0.17763 | 6.57e-06 | 193 | 0.17764 | 1.13e-05 | 1.75 |
| Scenario V | 0.17756 | 1.62e-04 | 4.50 | 0.17763 | 3.92e-06 | 1116 | 0.17763 | 5.73e-06 | 4.59 |
| Merton ($V_{\text{ref}} = 0.17687$) | Value | Std Error | Time | Value | Error | Time | Value | Error | Time |
| Scenario I | 0.16647 | 1.47e-02 | 0.03 | 0.17610 | 7.69e-04 | 1.10 | 0.17603 | 8.39e-04 | 0.17 |
| Scenario II | 0.18610 | 5.05e-03 | 0.21 | 0.17679 | 7.82e-05 | 4.02 | 0.17678 | 8.95e-05 | 0.33 |
| Scenario III | 0.17616 | 1.58e-03 | 2.08 | 0.17684 | 2.58e-05 | 26.3 | 0.17683 | 3.15e-05 | 1.26 |
| Scenario IV | 0.17605 | 4.97e-04 | 16.5 | 0.17688 | 1.48e-05 | 199 | 0.17688 | 1.13e-05 | 1.91 |
| Scenario V | 0.17701 | 1.58e-04 | 161 | 0.17687 | 8.27e-05 | 989 | 0.17687 | 6.26e-06 | 5.24 |
| Kou ($V_{\text{ref}} = 0.17534$) | Value | Std Error | Time | Value | Error | Time | Value | Error | Time |
| Scenario I | 0.21626 | 2.09e-02 | 0.10 | 0.17427 | 1.07e-03 | 1.09 | 0.17439 | 9.56e-04 | 0.19 |
| Scenario II | 0.17653 | 4.86e-03 | 0.64 | 0.17557 | 2.30e-04 | 4.01 | 0.17521 | 1.37e-04 | 0.35 |
| Scenario III | 0.17956 | 1.67e-03 | 7.64 | 0.17593 | 5.92e-04 | 27.0 | 0.17529 | 5.21e-05 | 1.25 |
| Scenario IV | 0.17655 | 5.67e-04 | 68.4 | 0.17613 | 7.87e-04 | 196 | 0.17534 | 9.55e-07 | 2.27 |
| Scenario V | 0.17645 | 1.69e-04 | 589 | 0.17620 | 8.59e-04 | 989 | 0.17534 | 1.75e-06 | 4.96 |
| NIG ($V_{\text{ref}} = 0.17929$) | Value | Std Error | Time | Value | Error | Time | Value | Error | Time |
| Scenario I | 0.20382 | 1.69e-02 | 0.01 | 0.18164 | 2.35e-03 | 1.54 | 0.17840 | 8.93e-04 | 0.20 |
| Scenario II | 0.17687 | 4.91e-03 | 0.03 | 0.17949 | 1.99e-04 | 4.07 | 0.17920 | 9.68e-05 | 0.35 |
| Scenario III | 0.17872 | 1.55e-03 | 0.11 | 0.17913 | 1.58e-04 | 26.9 | 0.17926 | 3.27e-05 | 0.81 |
| Scenario IV | 0.17910 | 4.95e-04 | 0.61 | 0.17924 | 5.39e-05 | 203 | 0.17930 | 1.09e-05 | 2.06 |
| Scenario V | 0.17923 | 1.57e-04 | 6.38 | 0.17925 | 4.12e-05 | 989 | 0.17930 | 5.35e-06 | 5.20 |
| VG ($V_{\text{ref}} = 0.18024$) | Value | Std Error | Time | Value | Error | Time | Value | Error | Time |
| Scenario I | 0.18783 | 1.53e-02 | 0.01 | 0.18350 | 3.26e-03 | 1.53 | 0.17937 | 8.65e-04 | 0.16 |
| Scenario II | 0.17395 | 4.86e-03 | 0.03 | 0.18033 | 9.11e-05 | 4.21 | 0.18011 | 1.22e-04 | 0.35 |
| Scenario III | 0.18189 | 1.58e-03 | 0.11 | 0.17985 | 3.89e-04 | 25.5 | 0.18020 | 3.34e-05 | 0.89 |
| Scenario IV | 0.17998 | 4.97e-04 | 0.66 | 0.17999 | 2.49e-04 | 201 | 0.18024 | 8.18e-06 | 1.84 |
| Scenario V | 0.18017 | 1.57e-04 | 5.60 | 0.18001 | 2.26e-04 | 990 | 0.18024 | 4.54e-06 | 5.11 |

**Tab. 6.8:** Results of Full Gain TARN. The error in FD and Conv methods are given by $|V(S_0, t_0, 0) - V_{\text{ref}}(V(S_0, t_0, 0)|$ and the CPU Times are expressed in seconds.

# 7 Conclusion

> *Derivatives are financial weapons of mass destruction.*
>
> — **Warren Buffett**
> (1930)

This chapter closes this thesis with a brief review of the main findings in Section 7.1 and an overview of possible further works in Section 7.2.

## 7.1 Review of main findings

Firstly, we studied the exponential Lévy processes and their characteristics used in option pricing. Then, we implemented three different methods in order to evaluate an FX-TARN. The Finite Difference method uses the Lévy density of the process while the Convolution method is based on its characteristic function. Since the characteristic function is available in a closed form, we have seen that the Convolution method performs better than the Finite Difference or Monte Carlo methods and gives us remarkably fast and accurate results. Indeed, we have seen that the Convolution method can be nearly 15 times faster than the Finite Difference method for the same accuracy.

To finally price the FX-TARN option, we calibrated our models to the market prices and have remarked that the Kou model with five parameters fitted very well. The other models were not too bad and can give us different alternatives in relation to our needs.

The conclusion of this work is that we have been able to find a fast and accurate method very flexible in function of our model to price exotic options such as FX-TARN. Indeed, if we would change the model, it suffices to change the characteristic function in the implementation of the method. The Convolution method could be also applied to other exotic options with path dependency by changing the intermediate step where the cubic interpolation is used to treat the jump condition on fixing dates.

## 7.2 Further works

First of all, we can spend more time on the convergence analysis of the different methods. In particular, in the Finite Difference method, the choice of the truncation parameter $\epsilon$ in the infinite activity processes could be more optimal. Therefore, it would be needed to compare the convergence analysis of the method for several value of $\epsilon$ to find the optimum.

Then to go beyond the jump-diffusion and pure jump models, it could be interesting to study the hybrid models combining jumps and stochastic volatilities. The most popular of this kind of model is proposed by Bates (1996). In this model, an independent jump component is added to the Heston stochastic volatility model:

$$\begin{aligned} dX_t &= \mu dt + \sqrt{V_t} dW_t^X + dZ_t, & S_t &= S_0 e^{X_t}, \\ dV_t &= \xi(\eta - V_t)\, dt + \theta \sqrt{V_t} dW_t^V, & d\left\langle W^V, W^X \right\rangle_t &= \rho dt, \end{aligned}$$

where $Z = \{Z_t, t \geq 0\}$ is a compound Poisson process with Gaussian jumps. This process is not a Lévy process but its characteristic function is still known in closed form. Therefore, the pricing and the calibration is similar to our approach.

Finally, we didn't talk about the risk management of the FX-TARN in this thesis. Thus, we could study the Greeks (sensitivities of the option). This can give us an idea about the hedging of this kind of option.

# Bibliography


[Bac00] Louis Bachelier. *Théorie de la spéculation*. Gauthier-Villars, 1900 (cit. on p. 12).

[Bar97a] Ole E Barndorff-Nielsen. „Normal inverse Gaussian distributions and stochastic volatility modelling“. In: *Scandinavian Journal of statistics* 24.1 (1997), pp. 1–13 (cit. on p. 31).

[Bar97b] Ole E Barndorff-Nielsen. „Processes of normal inverse Gaussian type“. In: *Finance and stochastics* 2.1 (1997), pp. 41–68 (cit. on pp. 23, 29).

[Bat96] David S Bates. „Jumps and stochastic volatility: Exchange rate processes implicit in Deutschemark options“. In: *Review of financial studies* 9.1 (1996), pp. 69–107 (cit. on p. 86).

[BS73] Fischer Black and Myron Scholes. „The pricing of options and corporate liabilities“. In: *Journal of political economy* 81.3 (1973), pp. 637–654 (cit. on p. 23).

[CM99] Peter Carr and Dilip Madan. „Option valuation using the fast Fourier transform“. In: *Journal of computational finance* 2.4 (1999), pp. 61–73 (cit. on p. 62).

[CV05] Rama Cont and Ekaterina Voltchkova. „A finite difference scheme for option pricing in jump diffusion and exponential Lévy models“. In: *SIAM Journal on Numerical Analysis* 43.4 (2005), pp. 1596–1626 (cit. on pp. 52, 59, 60).

[EP98] Ernst Eberlein and Karsten Prause. „The Generalized Hyperbolic Model: Financial Derivatives and Risk Measures“. In: (1998) (cit. on p. 29).

[G+94] Hans U Gerber, Elias SW Shiu, et al. „Option pricing by Esscher transforms“. In: *Transactions of the Society of Actuaries* 46.99 (1994), p. 140 (cit. on p. 19).

[Gem02] Hélyette Geman. „Pure jump Lévy processes for asset price modelling“. In: *Journal of Banking & Finance* 26.7 (2002), pp. 1297–1316 (cit. on p. 30).

[Hes93] Steven L Heston. „A closed-form solution for options with stochastic volatility with applications to bond and currency options“. In: *Review of financial studies* 6.2 (1993), pp. 327–343 (cit. on p. 86).

[Kou02] Steven G Kou. „A jump-diffusion model for option pricing“. In: *Management science* 48.8 (2002), pp. 1086–1101 (cit. on pp. 23, 27, 43).

[Kyp06] Andreas Kyprianou. *Introductory lectures on fluctuations of Lévy processes with applications*. Springer Science & Business Media, 2006 (cit. on p. 16).

[Lor+08] Roger Lord, Fang Fang, Frank Bervoets, and Cornelis W Oosterlee. „A fast and accurate FFT-based method for pricing early-exercise options under Lévy processes“. In: *SIAM Journal on Scientific Computing* 30.4 (2008), pp. 1678–1705 (cit. on pp. v, vii, 2, 60, 64).

[LS15] Xiaolin Luo and Pavel V Shevchenko. „Pricing TARNs Using a Finite Difference Method“. In: *The Journal of Derivatives* 23.1 (2015), pp. 62–72 (cit. on pp. v, vii, 1, 2, 47, 48).

[MCC98] Dilip B Madan, Peter P Carr, and Eric C Chang. „The variance gamma process and option pricing“. In: *European finance review* 2.1 (1998), pp. 79–105 (cit. on pp. 23, 29, 32, 34).

[Mer76] Robert C Merton. „Option pricing when underlying stock returns are discontinuous“. In: *Journal of financial economics* 3.1-2 (1976), pp. 125–144 (cit. on pp. 23, 26, 29, 42).

[Miy11] Yoshio Miyahara. *Option pricing in incomplete markets: Modeling based on geometric Lévy processes and minimal entropy martingale measures*. Vol. 3. World Scientific, 2011 (cit. on p. 21).

[Nob15] Fabio Nobile. *Lecture notes in Computational Finance, Part II*. 2015 (cit. on p. 2).

[Sam65] Paul A Samuelson. „Rational theory of warrant pricing“. In: *IMR; Industrial Management Review (pre-1986)* 6.2 (1965), p. 13 (cit. on p. 23).

[Sat99] Ken-iti Sato. *Lévy processes and infinitely divisible distributions*. Cambridge university press, 1999 (cit. on p. 18).

[TC03] Peter Tankov and Rama Cont. *Financial modelling with jump processes*. CRC press, 2003 (cit. on p. 16).

# List of Figures


1.1 Positive cash flow that produces jump on a fixing date for different type of knock-out. . . . . 6

2.1 Examples of Lévy processes: a linear drift with Lévy triplet $(2, 0, 0)$, a Wiener process with Lévy triplet $(2, 1, 0)$, a compound Poisson process with Lévy triplet $(0, 0, \lambda \cdot f_J)$, where $\lambda = 5$, and $f_J \sim \mathcal{N}(0, 1)$ and finally a jump-diffusion process with Lévy triplet $(2, 1, \lambda \cdot f_J)$. . . . . 17

2.2 The density of Lévy measure in the Merton model (left) and the Variance Gamma model (right). . . . . 19

4.1 Simulations of stock price process under Black-Scholes model. $S_0 = 1, r = 0.01, q = 0.02, \sigma = 0.3, T = 1, dt = 0.001, M = 5$. . . . . 41

4.2 Simulations of stock price process under Merton model. $S_0 = 1, r = 0.06, q = 0.02, \lambda = 10, \alpha = 0.1, \delta = 0.05, \sigma = 0.3, T = 1, dt = 0.001, M = 5$. . . . . 42

4.3 Simulations of stock price process under Kou model. $S_0 = 1, r = 0.06, q = 0.02, \lambda = 10, p = 0.55, \eta_1 = \eta_2 = 25, \sigma = 0.3, T = 1, dt = 0.001, M = 5$. . . . . 44

4.4 Simulations of a stock price process under NIG model. $S_0 = 1, r = 0.06, q = 0.02, \alpha = 50, \beta = 3, \delta = 1, T = 1, dt = 0.001, M = 5$. . . . . 45

4.5 Simulations of a stock price process under VG model. $S_0 = 1, r = 0.06, q = 0.02, \theta = 0.5, \sigma = 0.3, \nu = 0.01, T = 1, dt = 0.001, M = 5$. . . . 46

4.6 Pure jump Lévy density (in blue) and its truncated density (in red) with $\epsilon = 0.005$. . . . . 59

4.7 Initial price with Convolution method for a simple FX-TARN with 6 fixing dates over 1 year. Remark the margin effect due to the gap between positive payoff and negative payoff. . . . . 65

5.1 Risk-free rates from BLOOMBERG used for the calibration. . . . . 68

5.2 European option prices; on the left hand side, the OTM Put options, and on the right hand side, the OTM Call options. . . . . 69

5.3 Black-Scholes prices (in blue) in comparison with the market prices (in red). . . . . 70

5.4 Jump models calibration; model prices in blue and market prices in red. 71

5.5 Original volatility surface. . . . . 72

5.6 Jump models implied volatility surfaces. . . . . 72
5.7 Out of sample 18M options priced with jump models. . . . . 73
5.8 Out of sample 2Y options priced with jump models. . . . . 74

6.1 Lévy density centered on $x_{\min}$ and $x_{\max}$ to justify the choice of $q_{\min}$ and $q_{\max}$. . . . . 77
6.2 Monte Carlo standard error analysis. . . . . 78
6.3 Convergence of the Finite Difference method. . . . . 79
6.4 Convergence of the Convolution method. . . . . 79
6.5 Speed and accuracy comparison between the FD method and the Conv method. At the top: Error in function of computational time. At the bottom: Running time with respect to $N_x$. . . . . 80

# List of Tables


1.1 FX-TARN Term Sheet example. . . . . 8

3.1 Lévy processes $X_t$ for several models. . . . . 37
3.2 Risk-neutral drifts $\gamma^*$ for several models. . . . . 37
3.3 Lévy measure $\nu(dx)$ for several models. . . . . 37
3.4 Characteristic exponent $\Psi(u)$ for several models. . . . . 37

5.1 Notation convention of delta Call and delta Put. . . . . 68
5.2 Calibrated parameters $\hat{\Theta}$ and RMSE for each models. . . . . 71

6.1 No gain TARN reference value in comparison with $10^8$ Monte Carlo simulations. . . . . 76
6.2 Part gain TARN reference value in comparison with $10^8$ Monte Carlo simulations. . . . . 76
6.3 Full gain TARN reference value in comparison with $10^8$ Monte Carlo simulations. . . . . 76
6.4 Number of simulations per Monte Carlo scenario and grids discretization for the FD and Conv methods. . . . . 77
6.5 Prices of the FX-TARN for all the models. The RMSE is the deviation of the calibrated model prices with respect to the market prices. Each price is computed in 19 seconds. . . . . 81
6.6 Results of No Gain TARN. The error in FD and Conv methods are given by $|V(S_0,t_0,0) - V_{\text{ref}}(V(S_0,t_0,0)|$ and the CPU Times are expressed in seconds. . . . . 82
6.7 Results of Part Gain TARN. The error in FD and Conv methods are given by $|V(S_0,t_0,0) - V_{\text{ref}}(V(S_0,t_0,0)|$ and the CPU Times are expressed in seconds. . . . . 83
6.8 Results of Full Gain TARN. The error in FD and Conv methods are given by $|V(S_0,t_0,0) - V_{\text{ref}}(V(S_0,t_0,0)|$ and the CPU Times are expressed in seconds. . . . . 84

# Colophon

This thesis was typeset with LaTeX 2$_\varepsilon$. It uses the *Clean Thesis* style developed by Ricardo Langner. The design of the *Clean Thesis* style is inspired by user guide documents from Apple Inc.

Download the *Clean Thesis* style at http://cleanthesis.der-ric.de/.

# Declaration

I hereby declare that the thesis with title

*Pricing FX-TARN Under Lévy Processes Using Numerical Methods*

has been composed by myself autonomously and that no means other than those declared were used. In every single case, I have marked parts that were taken out of published or unpublished work, either verbatim or in a paraphrased manner, as such through a quotation. This thesis has not been handed in or published before in the same or similar form.

*Lausanne, June 22, 2017*

Valentin Bandelier